sinta S2 Sinta Score

e-ISSN 2503-5010
p-ISSN 2087-0965

Accredited by Ristekdikti: Nomor 158/E/KPT/2021

JURNAL RISET TEKNOLOGI PENCEGAHAN PENCEMARAN INDUSTRI

Research Journal of Industrial Pollution Prevention Technology

Vol. 14, No. 2, November 2023

JURNAL RISET Teknologi Pencegahan Pencemaran Industri	Vol.14	No. 2	Page 1 - 53	Semarang, November 2023	ISSN No. 2087-0965

Kementerian Perindustrian REPUBLIK INDONESIA

Published by :
BADAN STANDARDISASI DAN KEBIJAKAN JASA INDUSTRI
BALAI BESAR STANDARDISASI DAN PELAYANAN JASA PENCEGAHAN PENCEMARAN INDUSTRI

Jurnal Riset

Teknologi Pencegahan Pencemaran Industri

Volume 14 No. 2, November 2023

FOCUS AND SCOPE

Jurnal Riset Teknologi Pencegahan Pencemaran Industri (Research Journal of Industrial Pollution Prevention Technology) seeks to promote and disseminate original research as well as review, related to following area:

Environmental Technology : within the area of air pollution technology, wastewater treatment technology, and management of solid waste and harzardous toxic substance.

Process Technology and Simulation : technology and/or simulation in industrial production process aims to minimize waste and environmental degradation.

Design Engineering : device engineering to improve process efficiency, measurement accuracy and to detect pollutant.

Material Fabrication : environmental friendly material fabrication as subtitution material for industry.

Energy Conservation : process engineering/ technology/ conservation of resources for energy generation.

Ir. Nilawati
National Research and Innovation Agency

Moch. Syarif Romadhon, S.Si., M.Sc.
National Research and Innovation Agency

Bekti Marlena, S.T., M.Si.
Center for Standardization and Industrial Pollution Prevention Services

Rame, S.Si., M.Si.
Center for Standardization and Industrial Pollution Prevention Services

Novarina I. Handayani, S.Si., M.Si.
Center for Standardization and Industrial Pollution Prevention Services

Ir. Nasuka, M.M.
Center for Standardization and Industrial Pollution Prevention Services

Januar Arif Fatkhurrahman S.T., M.T.
Center for Standardization and Industrial Pollution Prevention Services

Rustiana Yuliasni, S.T., M.Sc.
National Research and Innovation Agency

Silvy Djayanti, S.T., M.Si.
National Research and Innovation Agency

Hanny Vistanty, S.T., M.T.
National Research and Innovation Agency

Nanik Indah Setianingsih, S.TP., M.Ling.
National Research and Innovation Agency

Evana Yuanita, S.T., M.T.
Center for Standardization and Services of Chemical, Pharmaceutical and Packaging Industries

Ella Kusumastuti, S.Si., M.Si.
Universitas Negeri Semarang

Jurnal Riset
Teknologi Pencegahan Pencemaran Industri
Volume 14 No. 2, November 2023

IMPRINT

JRTPPI published by Center for Standardization and Industrial Pollution Prevention Services (BBSPJPPI) – Agency for Standardization and Industrial Services (BSKJI), Ministry of Industry. JRTPPI is published online twice in every year.
ISSN print edition : 2087-0965
ISSN electronic edition : 2503-5010
Electronic edition available on :
ejournal.kemenperin.go.id/jrtppi

INDEXING

JRTPPI has been covered by these following indexing services :
Crossref, Indonesian Scientific Journal Database (ISJD), Mendeley, Infobase Index, Indonesian Publication Index (IPI), Bielefeld Academic Search Engine (BASE), Google Scholar, Directory of Research Journals Indexing (DRJI).

MAILING ADDRESS

Center for Standardization and Industrial Pollution Prevention Services.
Jl. Ki Mangunsarkoro No. 6 Semarang, Central Java, 50136 Indonesia.
Telp. +62 24 8316315
Fax. +62 24 8414811
e-mail: jurnalrisettppi@kemenperin.go.id
Working hour : Monday - Friday
07.30 – 16.00 GMT+7

Jurnal Riset
Teknologi Pencegahan Pencemaran Industri
Volume 14 No. 2, November 2023

PREFACE

Thanks to Allah, the Most Gracious and Most Merciful, the Journal of Industrial Pollution Prevention Technology (JRTPPI) has published its 14th volume, second edition. This journal contains scientific articles, particularly in the fields of environmental technology, process technology and simulation, design engineering, material fabrication, and energy conservation. We would like to express our sincere appreciation to the head of the Center for Standardization and Industrial Pollution Prevention Services, Ministry of Industry, for their continuous support of JRTPPI. We also extend our gratitude to the authors, editorial board, and reviewers who have actively participated in maintaining the consistency of quality and timely publication.

This edition consists of five full-text English scientific articles. This is part of the editorial board's commitment to improving the authors' performance in delivering the results of their research and making it easily accessible to a broader audience to increase the number of citations. This policy is also aimed at realizing our goal of JRTPPI being a globally indexed international journal.

The articles in this edition include modification of steel surface with addition of cocoa fruit pod extract inhibitor using electrodeposition method, water hyacinth potential in the pollution impact reduction of coffee agroindustry wastewater, removal of ammonium and phosphate from synthetic wastewater of complex fertilizer industry through struvite crystallization process, application of green retrofitting ready mix concrete plant in indonesia to increase financial benefits and reduce environmental issues: a case study, and easy preparation of zinc molybdate photocatalyst ($ZnMoO_4$) and its application for degradation of methylene blue. These five manuscripts were accepted and published in this edition from researchers and lecturers in Indonesia. The submission, review, and editing process for these manuscripts ranged from 1 to 6 months.

Hopefully, these scientific articles will provide new knowledge and experiences for readers in academia, researcher, industry, community and society at large. We realize that nothing is perfect until all parties have continuously improved.

Semarang, November 2023

Chief Editor

Jurnal Riset
Teknologi Pencegahan Pencemaran Industri
Volume 14 No. 2, November 2023

TABLE OF CONTENT

Jurnal Riset
Teknologi Pencegahan Pencemaran Industri
Volume 14 No. 2, November 2023

ABSTRACT

Published on November 10, 2023

Rakiman[1], Sukatik[2], Maimuzar[1], Silva Azaria Mahaputri[3], Yuli Yetri*[1]

([1]Department of Mechanical Engineering, Politeknik Negeri Padang, [2]Department of Civil Engineering, Politeknik Negeri Padang, [3]Department of Physics, Faculty of Mathematics and Natural Sciences, Universitas Andalas)

Modification of Steel Surface with Addition of Cocoa Fruit Pod Extract Inhibitor Using Electrodeposition Method

Jurnal Riset Teknologi Pencegahan Pencemaran Industri, November 2023, Vol. 14, No. 2, p. 1-9, 5 ill, 6 tab, 35 ref

The steel surface modification has been carried out with the addition of an inhibitor of cocoa fruit pod extract with varying concentrations of 0.5%, 1%, 1.5%, 2.0% and 2.5%. The aim is to add inhibitors to improve the appearance, and to slow down the corrosion rate. The electrodeposition method was used to form a thin film on the surface at a voltage of 3 volts for 3 minutes. Surface characterization using optical microscopy and scanning electron microscopy (SEM). X-Ray Diffraction (XRD) is used to determine the phase that occurs. The corrosion rate was calculated using the weight loss and potentiostate methods. The results of the characterization of the steel surface with the addition of 1% fruit pod extract inhibitor at the electrodeposition showed that the surface was smoother and more even and there was no porosity. XRD analysis showed that the electrodeposition results under the same conditions contained two elemental phases, namely Cu and Fe with different intensity values. The highest intensity is located at the peak of the second position of 2-Theta 44,84860 which is the peak of the Fe crystal. The lowest intensity is located at the third peak of 259.89 at the position of 2-Theta 98.9141 which is the peak of Cu. The high intensity indicates that the particle has good crystallinity. Cocoa fruit pod inhibitor is able to slow down the corrosion rate and smooth the metal surface by electrodeposition method.

(Author)

Keywords: Electrodeposition, Inhibitor, Intensity, Tafel

Elida Novita[1], Sri Wahyuningsih[1], Mastuki Andika[1], Hendra Andiananta Pradana[1]

([1]Department of Agriculture Engineering, Faculty of Agricultural Technology, University of Jember, Jawa Timur 68121 Indonesia)

Water Hyacinth Potential in The Pollution Impact Reduction of Coffee Agroindustry Wastewater

Jurnal Riset Teknologi Pencegahan Pencemaran Industri, November 2023, Vol. 14, No. 2, p. 10-22, 6 ill, 4 tab, 37 ref

Coffee processing wastewater originating from the coffee agroindustry has the potential to reduce environmental quality. Water hyacinth is one of the biological agents capable of reducing pollutants in wastewater through a rhizofiltration mechanism in the phytoremediation process. The pollutant-reducing ability of water hyacinth is limited, so the replacement of water hyacinth is one of the alternatives for optimizing the phytoremediation method. This research aimed to compare the replacement time of water hyacinth to the decreased parameters, namely turbidity, Biochemicals Oxygen Demand (BOD), Chemicals Oxygen Demand (COD), ammonia, and phosphate in the treatment of coffee processing wastewater using the phytoremediation method. The research stages consisted of water hyacinth acclimatization, determination of hydraulic resistance time, water hyacinth replacement time, and analysis of wastewater pollutant reduction. The density of water hyacinth used is 30 grams / L, and the incubation time is 14 days. The results showed that replacing water hyacinth improved the quality of coffee processing wastewater. The most water hyacinth replacement was on the seventh day. The percentage of turbidity parameters, Biochemicals Oxygen Demand (BOD), Chemicals Oxygen Demand (COD), ammonia (NH_3-N), and phosphate (PO_4-P) in the treatment of coffee processing wastewater with replacement of water hyacinth sequentially is 92.02%; 81.10%; 81.05%; 76.03% and 72.40%.

(Author)

Keywords: Agroindustry, Phytoremediation, Water Quality

Muhammad Zulfikar Luthfi*[1], Tjandra Setiadi[2], Dennis Farina Nury[3], Choerudin[4]

([1]Politeknik ATI Padang, [2]Pusat Studi Lingkungan Hidup, Institut Teknologi Bandung, [3]Institut Teknologi Sumatera.)

Removal of Ammonium and Phosphate from Synthetic Wastewater of Complex Fertilizer Industry Through Struvite Crystallization Process

Jurnal Riset Teknologi Pencegahan Pencemaran Industri, November 2023, Vol. 14, No. 2, p. 23-32, 7 ill, 3 tab, 24 ref

The complex fertilizer industry produces wastewater that contributes to water pollution because it contains high organic nitrogen in the form of urea which can be hydrolyzed to ammonium using the urease enzyme and high levels of phosphate and ammonium concentrations. Struvite precipitation is an effective method for removing and recovering ammonium and phosphate from wastewater. This study aimed to determine the effect of aeration and the enzyme urease in removing ammonium and phosphate in complex fertilizer synthetic wastewater through struvite precipitation. Struvite precipitation was carried out in a batch reactor with a working volume of 0.5 L with variations in aeration rate, aeration time, and the addition of urease enzyme from Jack bean peas (*Canavalia ensiformis*). Residual ammonium and phosphate levels were analyzed, and struvite crystal formation (MAP) was determined using Scanning Electron Microscope (SEM) and X-ray diffraction (XRD). The results showed that the aeration reactor could form struvite crystals and transform the ammonium and phosphate content in the synthetic wastewater of complex fertilizers. The removal of ammonium with a molar ratio of $[Mg^{2+}] : [NH_4^+] : [PO_4^{3-}]$ 1:2:1 reached 61-77% at high aeration rates because much ammonia was released into the air. The phosphate removal reached 99%. The urease enzyme was proven to hydrolyze urea into ammonium, increase the pH value, and affect the shape of the resulting struvite crystals. The precipitate product obtained was struvite crystals, which SEM-EDX and XRD analysis confirmed.

(Author)

Keywords: Aeration, Complex Fertilizer Waste, Magnesium Ammonium Phosphate, Struvite, Urease Enzyme

Mohammad Kholis Ardiansyah[1], Albert Eddy Husin[1*], Mawardi Amin[1]

([1]Department of Civil Engineering, Faculty of Engineering, Universitas Mercu Buana, Jakarta 11650 , Indonesia.)

Application of Green Retrofitting Ready Mix Concrete Plant in Indonesia to Increase Financial Benefits and Reduce Environmental Issues: A Case Study

Jurnal Riset Teknologi Pencegahan Pencemaran Industri, November 2023, Vol. 14, No. 2, p. 33-44, 6 ill, 7 tab, 31 ref

Currently, the Indonesian government continues to encourage the realization of sustainable development. The green concept is a sustainable development trend in the construction material industry. The concrete industry plays a vital role as a supplier of concrete materials in construction, so its availability is essential. The role of concrete industry itself has a negative impact on the environment. Stakeholders increase the cost of green retrofitting so that the industry or building becomes eco-friendly. The research method was carried out using a process case study, namely, how to implement green retrofitting cost performance in the concrete industry using Value Engineering and Life Cycle Cost Analysis. Theoretically, the research results provide additional knowledge for academics; practitioners can provide problem-solving to get an overview of the implementation of the green concept in the industry regarding the flow of implementation and the benefits of savings in an environmentally friendly production process. The application of value engineering in the green retrofitting of the concrete industry has increased the cost performance of green retrofitting by 8.66% with a return of 3 years and 8 months and increased the functions and benefits of an eco-friendly and sustainable concrete industry.

(Author)

Keywords: FAST, Green Retrofitting, Life Cycle Cost Analysis, Ready-Mix Concrete, Value Engineering

Ridla Bakri*[1], Rika Firmansyah[1], Yoki Yulizar[1]

([1]Department of Chemistry, Universitas Indonesia)

Easy Preparation of Zinc Molybdate Photocatalyst (ZnMoO4) and Its Application for Degradation of Methylene Blue

Jurnal Riset Teknologi Pencegahan Pencemaran Industri, November 2023, Vol. 14, No. 2, p. 45-53, 6 ill, 1 tab, 32 ref

Using photocatalyst is one way to overcome the problem of dye waste in water. Hazardous chemicals are commonly used in the manufacture of photocatalysts. In this research, $ZnMoO_4$ was prepared through an environmentally friendly and cost-effective synthesis. $ZnMoO_4$ was synthesized using peppermint leaf extract. The alkaloid content of the leaf extract was hydrolysed to form hydroxy ions. Subsequently, the hydroxyl ions were subjected to a hydrothermal process, resulting in the formation of $ZnMoO_4$. The functional groups, crystalline structure and morphology of $ZnMoO_4$ were characterised using fourier transform infrared (FTIR), X-ray diffraction (XRD), field emission scanning electron microscopy (FE-SEM), and transmission electron microscopy (TEM). The band gap energy was investigated through UV-Vis diffuse reflectance spectroscopy (UV-Vis DRS). The photocatalytic activity of $ZnMoO_4$ was tested against the organic pollutant methylene blue under visible light irradiation and its degradation products were analysed with a UV-Vis spectrophotometer at a wavelength of 664 nm. After 80 minutes of irradiation, the photocatalytic process of $ZnMoO_4$ degraded 99% of methylene blue. The excellent photodegradation performance suggests that the transition activity of electron currents from the valence band to the conduction band on $ZnMoO_4$ is occurring effectively.

(Author)

Keywords: Methylene Blue, Organic Pollutant, Photocatalyst, Zinc Molybdate

Vol. 14 No. 2 (2023) 1-9

Jurnal Riset
Teknologi Pencegahan Pencemaran Industri

Journal homepage : https://www.jrtppi.id

Kementerian Perindustrian
REPUBLIK INDONESIA

Modification of Steel Surface with Addition of Cocoa Fruit Pod Extract Inhibitor Using Electrodeposition Method

Rakiman[1], Sukatik[2], Maimuzar[1], Silva Azaria Mahaputri[3], Yuli Yetri*[1]

[1] Department of Mechanical Engineering, Politeknik Negeri Padang.

[2] Department of Civil Engineering, Politeknik Negeri Padang.

[3] Department of Physics, Faculty of Mathematics and Natural Sciences, Universitas Andalas.

ARTICLE INFO

Article history:
Received October 20, 2022
Received in revised form February 8, 2023
Accepted May 15, 2023
Available online November 10, 2023

Keywords :
Electrodeposition
Inhibitor
Intensity
Tafel

ABSTRACT

The steel surface modification has been carried out with the addition of an inhibitor of cocoa fruit pod extract with varying concentrations of 0.5%, 1%, 1.5%, 2.0% and 2.5%. The aim is to add inhibitors to improve the appearance, and to slow down the corrosion rate. The electrodeposition method was used to form a thin film on the surface at a voltage of 3 volts for 3 minutes. Surface characterization using optical microscopy and scanning electron microscopy (SEM). X-Ray Diffraction (XRD) is used to determine the phase that occurs. The corrosion rate was calculated using the weight loss and potentiostate methods. The results of the characterization of the steel surface with the addition of 1% fruit pod extract inhibitor at the electrodeposition showed that the surface was smoother and more even and there was no porosity. XRD analysis showed that the electrodeposition results under the same conditions contained two elemental phases, namely Cu and Fe with different intensity values. The highest intensity is located at the peak of the second position of 2-Theta 44,84860 which is the peak of the Fe crystal. The lowest intensity is located at the third peak of 259.89 at the position of 2-Theta 98.9141 which is the peak of Cu. The high intensity indicates that the particle has good crystallinity. Cocoa fruit pod inhibitor is able to slow down the corrosion rate and smooth the metal surface by electrodeposition method.

1. INTRODUCTION

The increasing use of steel in infrastructure construction, autos, shipboards, railroad, arms, and equipment, and in line with current technological developments (Afandi, Arief, & Amiadji, 2015; AL-Senani, AL-Saeedi, & AL-Mufarij, 2016). Steel is widely used because this material is easy to obtain, manufacture, and high-strength (Yetri & Jamarun, 2015). However, the weakness is that steel is easily corroded, decreasing the material's mechanical properties. Corrosion causes substantial economic losses (Wang et al., 2016). These losses reach trillions of rupiah per year or an estimated almost 3.5% of the country's Gross National Product (GNP).

There are several methods to prevent the decline in the function of steel due to corrosion, including others minimize the weak areas on the steel surface, keeping the steel clean, providing an oil layer, and can also be by insulating the steel surface (Rodríguez Torres, Valladares Cisneros, & González Rodríguez, 2016), adding inhibitors, and by coating the surface with an impenetrable layer such as paint (Victoria, Prasad, & Manivannan, 2015). The surface coating method by synthesizing a lamella on the surface of a metal is widely used because this coating method

*Correspondence author.
E-mail : yuliyetri@pnp.ac.id (Yuli Yetri)

doi : https://10.21771/jrtppi.2023.v14.no.2.p1-9

Accreditation number : (Ristekdikti) 158/E/KPT/2021

can isolate the surface of the metal from the surroundings, control the microenvironment on the surface of a metal, beautify the appearance or decorative (Bayuseno, 2009). The steel surface coating process can use a thin layer of Cu because Cu is relatively cheap and non-toxic, and the Cu synthesis process is relatively easy (Oktaviani, 2014).

There are several ways to synthesize thin films, such as electrodeposition, sol-gel, sputtering, and anodic oxidation methods. This electrodeposition method is more commonly used in the industrial sector (Tissos, Dahlan, & Yetri, 2018) because it has advantages compared to other methods, namely the implementation is quite simple, the substrate can be coated entirely on the top surface, and the average probability of deposition is high (Dahlan, 2009).

In addition to coating with a thin layer, the inhibitor application is still the best solution to protect metals from corrosion (Nugroho, 2015). The use of corrosion inhibitors has made significant progress in technological development since 1950 and 1960 and is expected to increase by 4.1% per year to 2.5 billion USD by 2017 (Dariva & Galio, 2014). The use of inhibitors as an effort to prevent corrosion has a weakness if the inhibitors used are inorganic inhibitors which are chemicals that are harmful to the organism, are relatively expensive, and can damage the environment (Umoren & Solomon, 2017; Yetri & Jamarun, 2015, 2016; Yetri, Jamarun, Nakai, & Niinomi, 2015). Inhibitors contain organic matter and as a solution to solve this problem, many studies have used natural ingredients as inhibitors, mainly plant extracts, be it leaves, stems, fruit, seeds, bark, or plant roots. For example, henna leaves (Chaudhari & Vashi, 2016; Zulkifli, Yusof, Isa, Yabuki, & Nik, 2017), gambier leaves (Murti, Handani, & Yetri, 2016), lime leaves (Hassan, Khadom, & Kurshed, 2016), spoon leaves (Mobin & Rizvi, 2017), elephant grass leaves (Ituen, James, Akaranta, & Sun, 2016), banana peels (Ismail & M Tajuddin, 2015), peony skins (Honarvar Nazari, Shihab, Cao, Havens, & Shi, 2017), mangosteen rinds (Turnip, Handani, & Mulyadi, 2015), peels of cocoa (Purnomo, 2015; Yetri, Emriadi, Jamarun, & Gunawarman, 2016; Yetri & Jamarun, 2015), aloe vera (Gupta & Jain, 2014), and there are still many studies using extracts of natural ingredients that can be used as inhibitors.

Indonesia is the world's third largest cocoa producer, with total production reaching 1 million tonnes (Badan Pusat Statistik, 2022). Cocoa pod is an abundant natural resource. 70-75% of its production is cocoa pod waste (Yetri & Jamarun, 2015) which has yet to be processed optimally (Yetri, 2021). The choice fell on cocoa pod skin as a research topic because this pod shell contains catechin and epi catechin compounds which can form a thin layer on the steel surface.

So, it is possible in this study to combine the electrodeposition method with adding inhibitors from cocoa pod waste. Because the availability of cocoa pod skin is relatively abundant, it is easy to extract the tannin compounds, and it is not harmful to the environment. So that is why cocoa fruit pod extract is used for corrosion inhibitors. Previous studies have added nickel to form a thin layer on the surface using the electrodeposition method to enhance its appearance and have not analyzed its mechanical properties (Tissos et al., 2018). In this study, an inhibitor of cocoa pod extract will be added to the electrolyte solution in coating steel substrates with Cu using the electrodeposition method. Utilization of this waste is expected to maximize the use of cocoa pod waste which has been left to waste, thus damaging the beauty of the environment.

2. METHODS

Cocoa pods are taken from residents' plantations in Lubuk Minturun, Padang. Cu lamella was manufactured using the electrodeposition method at the Laboratory of Materials, Physics Department, Faculty of Mathematics and Natural Sciences, University of Andalas. XRD characterization at Politeknik Negeri Padang, SEM characterization at the Department of Mechanical Engineering, Faculty of Engineering, Andalas University, and corrosion rate testing with potentiodynamic polarization and weight loss methods were done at the Chemistry Department, Andalas University.

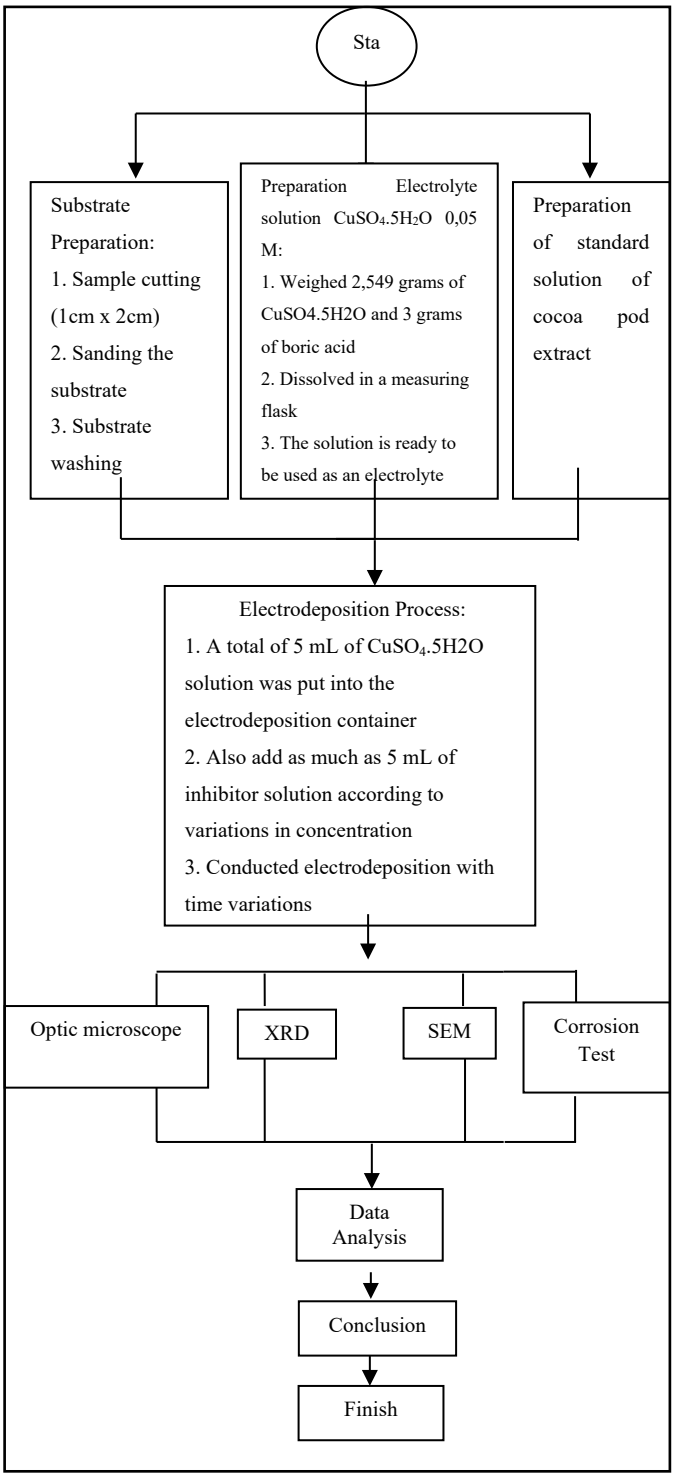

Figure 1. The Research Flowchart

The equipment needed to support the research are OHAUS GALAXYTM 160 digital balance, Power Supply, Ultrasonic bath, Basicmeter, Desiccator, Oven, chemical glassware, tweezers, Disposable syringe, spatula, gloves, mask, Vacuum Rotary Evaporator, distillation equipment, Potentiostat e-Corder 416, optical microscope, X-ray Diffraction (XRD) PanAlytical, Scanning Electron Microscope (SEM) Hitachi S-3400N, Hot Plate Magnetic Stirrer C-MAG HS 7. The materials used in this study included: commercial steel specimens, Merck's $CuSO_4.5H_2O$ as an electrolyte solution, Merck's HCl p.a, Boric Acid (H_3BO_3), Cocoa pods, Methanol 70%, Alcohol p.a 96%, sterile Aquades, sandpaper with various kinds of roughness sizes, and filter paper.

2.1. Preparation of Solution

First, an electrolyte solution is made for the electrodeposition process. CuSO4.5H2O weighed 2.495 grams, and HBO3 weighed as much as 3 grams. Then, the two chemical compounds were dissolved in a 200 mL volumetric flask to obtain an electrolyte solution with a concentration of 0.05 M (Jamaluddin, 2012). Meanwhile, the manufacture of cocoa pod extract, corrosive media, and corrosive media solutions with the addition of an extract of cocoa pod inhibitor was carried out by Yetri Y et al. 2015.

2.2. Electrodeposition Process

The process of electrodeposition and determination of the rate of corrosion using the method of weight loss follows what has been done by Tissos 2018, Silfa 2018, and Jamaluddin, 2012. For more details on the work steps in this study, see the flow chart in Figure 1.

3. RESULT AND DISCUSSION

3.1. Surface Analysis with Optical Microscope

In this study, the interaction between Cu and cocoa pod extract will form a thin layer on the surface to block the attack of corrosive ions so that it will inhibit the rate of corrosion. The Cu layer was synthesized using the electrodeposition method using an electrolyte solution of CuSO4.5H2O with variations in the cocoa pod extract solution concentration as an inhibitor solution of 0.5; 1.0; 1.5; 2.9; and 2.5%. The variation of electrodeposition time is 1; 2; 3; 4, and 5 minutes. The results of sample characterization using an optical microscope can be seen in Figure 2.

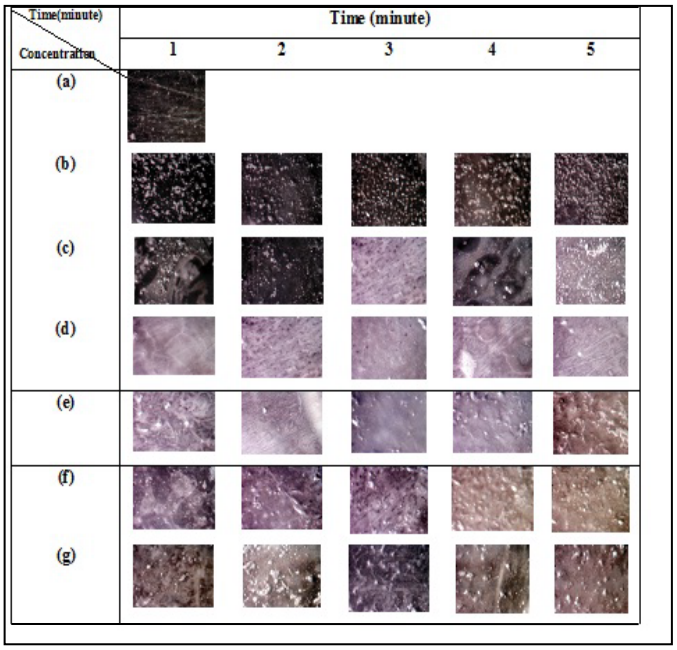

Figure 2. Characterization Results with Optical Microscopy (a) Samples of Steel Before Electrodeposition, and After Electrodeposition (b) Added 0% Inhibitor (c) 0.5% Inhibitor (d) 1% Inhibitor (e) 1.5% Inhibitor (f) 2% Inhibitor (g) 2.5% Inhibitor

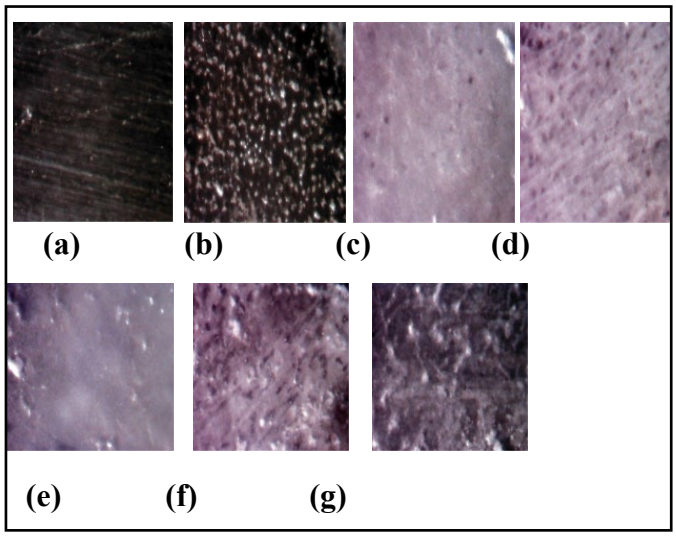

Figure 3. Characterization Results with Optical Microscopy (a) Sample of Steel Before Electrodeposition, and After Electrodeposition (b) Plus 0% inhibitor (c) 0.5% Inhibitor, (d) 1.0% Inhibitor, (e) 1.5% Inhibitor, (f) 3.0 Inhibitor, and (g) 2.5 Inhibitor

Figure 3(a) is a photo of the original steel after grinding and sanding without electrodeposition, which shows only fine lines of the influence of sanding on the surface of the steel. Figure 3b shows the electrodeposition results without adding an inhibitor which was electrodepositioned with an electrodeposition time of 3 minutes. The electrodeposition result is uneven, the particles accumulate, and the grain thickness is coarse. The granules are Cu particles that are starting to form. During the addition of 1% and 1.5% inhibitors (Figures 3c and 3d) with the same electrodeposition time, the deposition results were much smoother and more evenly distributed, there was no accumulation of material in some parts of the deposition results, and the formation of another layer covering the Cu particles.

The results of deposition are reasonable when compared to steel without the addition of inhibitors in Figure 3a. While in Figures 3e, 3f, and 3g, the deposition results are still smooth and even, but other layers are starting to rise to accumulate in some parts. Based on Figure 3, it can be analyzed in general that the increase of concentrations of inhibitor solution 1% and 1.5% was able to improve the deposition results to be more even and smoother, reduce the buildup of particles formed, and produce smaller particles, and produce a layer that protects Cu particles. This layer is produced from the inhibitor of cocoa pod extract added in the electrodeposition process.

3.2. Scanning Electron Microscopy Analysis

Analysis Based on the best results in Figure 3, the surface morphology characterization with SEM was carried out, as shown in Figure 4. Figure 4a shows the surface of the Cu layer on the steel before being electrodepositioned, the deposition results are uneven, and a buildup of particles of non-uniform size is formed. This condition indicates that the Cu coating is imperfect during the electrodeposition process, although macroscopically, the layer looks uniform. In Figure 4b, adding 1% inhibitor shows a smoother, more homogeneous deposition despite a thin gap from the resulting layer. However, the layers are deposited evenly, and particles are not accumulated in some parts. The effects of sanding are not visible on the steel surface.

Furthermore, using a 1.5% inhibitor solution, the characterization results in Figure 4c shows that the deposition results are still evenly distributed, and there is a passive layer that can slow down the corrosion rate on the steel surface. This layer is a barrier against the attack of corrosive ions on the surface of the steel sample (Yetri & Jamarun, 2015). The barrier formed can protect the metal surface (Arista, Dahlan, & Syukri, 2016). Meanwhile, when heating at 600°C in electrodeposition using 1% inhibitor, aggregate buildup occurs in several parts, and the protective layer (barrier) becomes invisible (Tissos et al., 2018). It is shown that heating can damage the layer formed on the steel surface (Rahmawatf, Wahyuningsih, & Handayani, 2008; Sujatno, Salam, Bandriyana, & Dimyati, 2017).

3.3. Characterization by X-Ray Diffraction

XRD analysis was carried out on three samples that were electrodepositioned for 3 minutes, namely the original steel before being electrodepositioned, the steel that was electrodeposited without the addition of an inhibitor, and the steel that was electrodepositioned with the addition of a 1% cocoa pod extract inhibitor are showed in Figure 5. The results showed that the surface was more even, the grain level was finer than the raw cocoa pod extract, and the thickness of the deposition was relatively thin.

The result of XRD characterization is a diffractogram between 2-Theta (2θ) angle and intensity. The 2-Theta angle used is in the range of 20o to 100o. From the data on the intensity and position of the diffraction peaks produced by the X-ray diffractometer and then compared with the Joint Committee on Powder Diffraction Standards (JCPDS) standard data, it is known that the phase of the crystalline element layer on the original steel before electrodeposition.

The XRD characterization data of steel before being electrodepositioned produced three X-ray diffraction peaks, namely peaks at an angle of 2-Theta for the intensity, with their respective values shown in Table 1. By referring to JCPDS, each 2-Theta angle can be identified in phase. At the same time, the XRD data of the Cu layer on the steel that was electrodeposited with the addition of a 1% cocoa pod extract inhibitor showed five X-ray diffraction peaks, namely peaks at an angle of 2-Theta to the intensity with each value shown in Table 2. Each peak has a value of different value intensity towards different 2θ positions. Referring to the data on JCPDS, each 2-Theta angle can be identified in phase (Ismail & M Tajuddin, 2015; Jannah, 2007).

The characterization results show that the electrodepositioned steel with adding a 1% cocoa pod extract inhibitor contains two elemental phases, namely Cu and Fe, with different intensity values, as shown in Table 2. The highest intensity is at the peak of the two positions 2-Theta 44,84860, which is the peak of the Fe crystal. The lowest intensity is located at the third peak of 259.89 at position 2-Theta 98.9141, which is the peak of Cu. The high intensity indicates that the particle has good crystallinity. The data on XRD results of electrodeposition steel with the addition of 1.5% cocoa pod extract inhibitor are shown in Table 3 below.

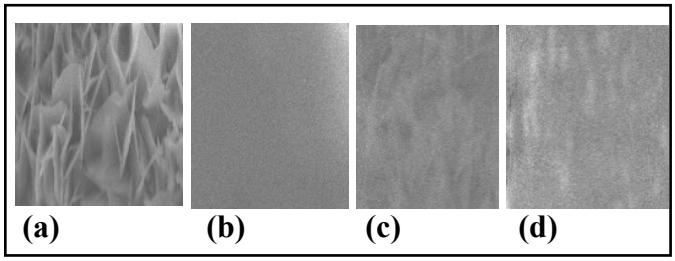

Figure 4. Surface Coating using SEM with 10000x Magnification (a) Sample Before and After Electrodeposition (b) with 1% Inhibitor, (c) 1.5% Inhibitor, and (d) 1% Inhibitor and Heated at 600°C

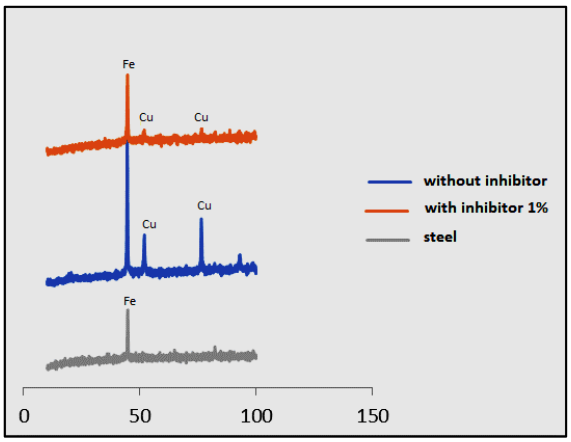

Figure 5. Three X-ray Diffraction Peaks

Table 1. Value of 2θ and Highest Peak Intensity of Steel XRD Curve Before Electrodeposition

Peak	2θ	Intensity	FWHM	D (Aº)
1	44.7434	540.95	0.2362	2.02551
2	64.9524	51.52	0.3542	1.43577
3	82.3163	77.82	0.4723	1.17139

Table 2. Value of 2θ and Highest Peak Intensity of Steel XRD Curve After Electrodeposition with the Addition of 1% Cocoa Pod Extract Inhibitor

Peak	2θ	Intensity	FWHM	D (Aº)
1	43.4831	530.63	0.3149	2.08125
2	44.8486	3891.77	0.3739	2.02100
3	65.0336	402.43	0.3542	1.43418
4	82.3599	630.20	0.3149	1.17088
5	98.9141	259.89	0.6298	1.01450
6	43.4831	530.63	0.3149	2.08125

Table 3. Value of 2θ and Highest Peak Intensity of Steel XRD Curve After Electrodeposition with Addition of 1.5% Cocoa Pod Extract Inhibitor

Peak	2θ	Intensity	FWHM	D (Aº)
1	43,6442	283,89	0,6298	2,07394
2	44,9627	5018,75	0,3739	2,01614
3	65,1290	458,60	0,3936	1,43231
4	82,4614	703,40	0,3936	1,16970
5	98,9576	301,63	0,3936	1,01417

Table 4. Comparison of 2θ Angle of X-Ray Diffraction Peaks of Steel Before and After Electrodeposition with Inhibitor

Peak	2θ		
	Before Electrode position	After Electrodeposition	
		Steel + Inhibitor 1%	Steel + Inhibitor 1.5%
1	44.7434	44.8486	44.9627
2	64.9524	65.0336	65.1290
3	82.3163	82.3599	82.4614

Table 3 shows that the XRD results of electrodeposition steel with the addition of 1.5% cocoa pod extract inhibitor had the five highest X-ray diffraction peaks with different intensity values. The identification results show that the electrodeposition steel with adding 1.5% cocoa pod extract inhibitor contains two phases of crystalline elements, namely Cu and Fe, with different intensity values. The highest intensity is located at the fifth peak, 2-Theta 98.95760, which is 301.63, the peak of the Fe crystal. The lowest intensity is located at the first peak, 2-Theta 43,64420, 283.89, the peak of Cu.

The results of XRD characterization are diffraction patterns which are characteristic peaks of the crystal structure formed in the Cu layer, and the patterns of diffraction of the layer are identified at 2θ angle. The result of XRD characterization for the three samples produced three X-ray diffraction peaks. Apart from that, the diffractogram shows that the phase produced in the steel before electrodeposition is still amorphous, characterized by not many peaks formed and no Cu peaks formed. The comparison of the three peaks in each sample can be seen in Table 4.

From its table, the 2-Theta angle shift is at the first peak, and all peaks experience a shift. The shift reveals a reduction in the interplanar distance of the crystal lattice upon the substitution of Cu atoms (Ong et al., 2014). The first peak is observed, and all steel peaks have diffraction peaks at identical 2-Theta angles. It is shown that adding a cocoa pod inhibitor solution extract in the electrodeposition process of steel samples does not change the crystal structure (Jamaluddin, 2012).

3.4. Corrosion Test Analysis

The polarization curve in the corrosive medium HCl 1 N, which has been extrapolated into Tafel solution, has been published previously. The Tafel curve shows a shift in the value of the corrosion potential to a more positive and negative direction, indicating that the added extract is anodic and cathodic (Honarvar Nazari et al., 2017).

Table 5. Corrosion Parameters of Steel Samples in 1 N HCl Corrosive Media

Concentration of Inhibitor (%V/V)	I corr (mA/cm^2)	-E corr (V)	IE (%)
0	0.0072	0.51	-
1	0.0122	0.59	70.5
1.5	0.0131	0.58	80.1

Table 6. Corrosion Rate of Steel in Corrosive Medium HCl 1N

Steel + Inhibitor	Δm (gram)	A (cm^2)	T (hour)	v ($g/cm^2.hour$)
Steel + 0%	0.0003	2.00	6	$2.50x10^{-5}$
	0.0067	2.10	12	$2.66 x10^{-4}$
	0.0113	2.10	18	$2.99 x10^{-4}$
	0.0182	2.10	24	$3.61 x10^{-4}$
Steel + 0.5%	0.0003	2.42	6	$2.01 x10^{-5}$
	0.0052	2.42	12	$1.79 x10^{-4}$
	0.0083	2.10	18	$2.19 x10^{-4}$
	0.0154	2.10	24	$3.06 x10^{-4}$
Steel + 1.0%	0.0002	2.10	6	$1.59x10^{-5}$
	0.0045	2.42	12	$1.55 x10^{-4}$
	0.0071	2,42	18	$1.88 x10^{-4}$
	0.0102	2,42	24	$2.02 x10^{-4}$
Steel + 1.5%	0.0002	2.42	6	$1.58 x10^{-5}$
	0.0035	2.42	12	$1.20 x10^{-4}$
	0.0067	2.42	18	$1.53 x10^{-4}$
	0.0095	2.42	24	$1.64 x10^{-4}$
Steel + 2.0%	0.0001	2.10	6	$7.94 x10^{-6}$
	0.0026	2.10	12	$1.04 x10^{-4}$
	0,0059	2,42	18	$1,35 x10^{-4}$
	0,0075	2,1	24	$1,49 x10^{-4}$
Steel + 2.5%	0,0001	2,42	6	$6,89 x10^{-6}$
	0,0015	2,1	12	$5,95 x10^{-5}$
	0,0039	2,1	18	$1,03 x10^{-4}$
	0,0069	2,42	24	$1,19 x10^{-4}$

Table 6 shows an increase in mass loss and corrosion rate directly proportional to the time the steel is immersed in a corrosive medium. It means that the longer the time of steel immersion in corrosive media, the greater the corrosion rate (Guo et al., 2017). However, with the same immersion time, the corrosion rate will decrease as the inhibitor concentration of cocoa pod extract is added. Table 6 indicates a decrease in mass loss as the concentration of cocoa pod extract inhibitor increases. In the table, it is clear that the corrosion rate decreases with the increase in the concentration of the inhibitor of the cocoa pod extract. It is because the more cocoa pod extract inhibitors are added, the more cocoa pod extract is adsorbed on the steel surface so that the layer formed on the surface can inhibit the attack of the corrosive rate on the surface of steel so that the rate of corrosion of steel can be inhibited (Wang et al., 2016; Yetri & Jamarun, 2015). This shows that the compounds contained in cocoa pod extract can be used as inhibitors to decrease steel corrosion rate. The inhibition efficiency of steel increases with increasing inhibitor concentration while the corrosion rate decreases (AL-Senani et al., 2016).

4. CONCLUSION

Based on the data and analysis carried out on the study's results, it can be concluded that with a voltage of 3 Volts, the optimum results of morphological electrodeposition were obtained at 3 minutes, and the concentration of inhibitor of the cocoa pod extract was 1%. Then the results of characterizing the electrodepositioned steel surface showed a smoother and more even surface. There was no porosity in the electrodepositioned steel sample with the addition of a 1% concentration of cocoa pod extract inhibitor. Meanwhile, the rate of corrosion test using the weight loss method and potentiodynamic polarization showed that the corrosion rate decreased and the efficiency of inhibition increased along with the rise in the concentration of inhibitor of cocoa pod extract added. Cocoa pod inhibitors can decrease the corrosion rate and smooth the metal surface by electrodeposition.

ACKNOWLEDGMENT

The authors would like to thank Politeknik Negeri Padang (PNP), which has funded this research through PNP DIPA funds with contract number: 187/PL9.15/PG/2022.

REFERENCE

Afandi, Y. K., Arief, I. S., & Amiadji, A. (2015). Analisa Laju Korosi pada pelat baja Karbon dengan Variasi ketebalan coating. Jurnal Teknik ITS, 4(1), G1–G5.

AL-Senani, G. M., AL-Saeedi, S., & AL-Mufarij, R. (2016). Coriandrum sativum leaves extract (CSL) as an eco-friendly green inhibitor for corrosion of

carbon steel in acidic media. J. Mater. Environ. Sci, 7(7), 2240–2251.

Arista, A., Dahlan, D., & Syukri, S. (2016). Sintesis Lapisan TiO2 Pada Substrat ITO Menggunakan Metode Elektrodeposisi dan Spin Coating. JURNAL ILMU FISIKA | UNIVERSITAS ANDALAS, 8(1 SE-Riset Artikel), 17–27. https://doi.org/10.25077/jif.8.1.17-27.2016

Badan Pusat Statistik. (2022). STATISTIK KAKAO INDONESIA 2021. Jakarta: Badan Pusat Statistik. Retrieved from https://www.bps.go.id/publication/2022/11/30/be404f7a76a56887462b5187/statistik-kakao-indonesia-2021.html

Bayuseno, A. P. (2009). Analisa laju korosi pada baja untuk material kapal dengan dan tanpa perlindungan cat. Rotasi, 11(3), 32–37.

Chaudhari, H. G., & Vashi, R. T. (2016). The study of henna leaves extract as green corrosion inhibitor for mild steel in acetic acid. Journal of Fundamental and Applied Sciences, 8(2), 280–296.

Dahlan, D. (2009). Electrodeposition of Cu2O Particles by Using Electrolyte Solution Containing Glucopone as Surfactant. Jurnal Ilmu Fisika, 1(2), 18–20.

Dariva, C. G., & Galio, A. F. (2014). Corrosion inhibitors–principles, mechanisms and applications. Developments in Corrosion Protection, 16, 365–378.

Guo, L., Obot, I. B., Zheng, X., Shen, X., Qiang, Y., Kaya, S., & Kaya, C. (2017). Theoretical insight into an empirical rule about organic corrosion inhibitors containing nitrogen, oxygen, and sulfur atoms. Applied Surface Science, 406, 301–306.

Gupta, P., & Jain, G. (2014). Corrosion inhibition by Aloe barbadensis (aloe vera) extract as green inhibitor for mild steel in HNO3. IJSRR, 3(4), 72–83.

Hassan, K. H., Khadom, A. A., & Kurshed, N. H. (2016). Citrus aurantium leaves extracts as a sustainable corrosion inhibitor of mild steel in sulfuric acid. South African Journal of Chemical Engineering, 22, 1–5.

Honarvar Nazari, M., Shihab, M. S., Cao, L., Havens, E. A., & Shi, X. (2017). A peony-leaves-derived liquid corrosion inhibitor: protecting carbon steel from NaCl. Green Chemistry Letters and Reviews, 10(4), 359–379.

Ismail, A., & M Tajuddin, M. A. (2015). Banana peel as green corrosion inhibitor for stainless steel 304. In Advanced Materials Research (Vol. 1087, pp. 282–286). Trans Tech Publ.

Ituen, E., James, A., Akaranta, O., & Sun, S. (2016). Eco-friendly corrosion inhibitor from Pennisetum purpureum biomass and synergistic intensifiers for mild steel. Chinese Journal of Chemical Engineering, 24(10), 1442–1447.

Jamaluddin. (2012). Elektrodeposisi Lapisan Tipis Cu-O (Copper Oxide) Menggunakan Arus Pulsa (On-Off) dan Arus Kontinu dengan Surfaktan SDS (Sodium Dodecyl Sulphat). Universitas Andalas, Padang.

Jannah, E. F. (2007). Karakterisasi lapisan tipis alloy nife hasil elektrodeposisi pada substrat Cu dan ITO.

Mobin, M., & Rizvi, M. (2017). Polysaccharide from Plantago as a green corrosion inhibitor for carbon steel in 1 M HCl solution. Carbohydrate Polymers, 160, 172–183.

Murti, E. A., Handani, S., & Yetri, Y. (2016). Pengendalian Laju Korosi pada Baja API 5L Grade BN Menggunakan Ekstrak Daun Gambir (Uncaria gambir Roxb). Jurnal Fisika Unand, 5(2), 172–178.

Nugroho, F. (2015). Penggunaan inhibitor untuk meningkatkan ketahanan korosi pada baja karbon rendah. Jurnal Angkasa, 7(1), 151–158.

Oktaviani, Y. (2014). Sintesis Lapisan Tipis Semikonduktor dengan Bahan Dasar Tembaga (Cu) Menggunakan Chemical Bath Deposition. Jurnal Fisika Unand, 3(1).

Purnomo, A. (2015). Pengaruh Variasi Konsentrasi Inhibitor Ekstrak Kulit Buah Kakao (Theobroma

cacao) terhadap Laju Korosi Pipa Baja Karbon A53 pada Media Air Laut.

Rahmawatf, F., Wahyuningsih, S., & Handayani, N. (2008). Modifikasi Permukaan Lapis Tipis Semikonduktor Ti02 Bersubstrat Grafit dengan Elektrodeposisi Cu. Indonesian Journal of Chemistry, 8(2008).

Rodríguez Torres, A., Valladares Cisneros, M. G., & González Rodríguez, J. G. (2016). Medicago sativa as a green corrosion inhibitor for 1018 carbon steel in 0.5 M H2SO4 solution. Green Chemistry Letters and Reviews, 9(3), 143–155.

Sujatno, A., Salam, R., Bandriyana, B., & Dimyati, A. (2017). Studi Scanning Electron Microscopy (Sem) Untuk Karakterisasi Proses Oxidasi Paduan Zirkonium. In Jurnal Forum Nuklir (Vol. 9, p. 44). https://doi.org/10.17146/jfn.2015.9.1.3563

Tissos, N. P., Dahlan, D., & Yetri, Y. (2018). Synthesis of Cuprum (Cu) layer by electrodeposition method with theobroma cacao peels as corrosion protector of steel. International Journal on Advanced Science Engineering Information Technology, 8(4), 1290–1295.

Turnip, L. B., Handani, S., & Mulyadi, S. (2015). Pengaruh penambahan inhibitor ekstrak kulit buah manggis terhadap penurunan laju korosi baja ST-37. Jurnal Fisika Unand, 4(2).

Umoren, S. A., & Solomon, M. M. (2017). Synergistic corrosion inhibition effect of metal cations and mixtures of organic compounds: a review. Journal of Environmental Chemical Engineering, 5(1), 246–273.

Victoria, S. N., Prasad, R., & Manivannan, R. (2015). Psidium guajava leaf extract as green corrosion inhibitor for mild steel in phosphoric acid. Int. J. Electrochem. Sci, 10(3), 2220–2238.

Wang, H., Zhu, Y., Hu, Z., Zhang, X., Wu, S., Wang, R., & Zhu, Y. (2016). A novel electrodeposition route for fabrication of the superhydrophobic surface with unique self-cleaning, mechanical abrasion and corrosion resistance properties. Chemical Engineering Journal, 303, 37–47.

Yetri, Y. (2021). Potential Activated Carbon of Theobroma cacao L. Shell for Pool Water Purification in Politeknik Negeri Padang. Jurnal Riset Teknologi Pencegahan Pencemaran Industri, 12(1), 32–38. Retrieved from https://doi.org/10.21771/jrtppi.2021.v12.no1.p32-38

Yetri, Y., Emriadi, E., Jamarun, N., & Gunawarman, G. (2016). Effisiensi Inhibisi Korosi Baja Lunak Dalam Media Asam Dengan Inhibitor Ekstrak Kulit Buah Kakao (Theobroma Cacao). Jurnal Riset Teknologi Pencegahan Pencemaran Industri, 7(2), 67–80.

Yetri, Y., & Jamarun, N. (2015). Corrosion inhibition of environmental friendly inhibitor using Theobroma cacao peels extract on mild steel in NaCl solution. Journal of Chemical And Pharmaceutical Research, 7(5), 1083–1094.

Yetri, Y., & Jamarun, N. (2016). Corrosion Behavior of Environmental Friendly Inhibitor of Theobroma cacao Peels Extract for Mild Steel in NaCl 1.5 M. EnvironmentAsia, 9(1).

Yetri, Y., Jamarun, N., Nakai, M., & Niinomi, M. (2015). Effect Of Polar Extract Of Cocoa Peels Inhibitor On Mechanical Properties And Microstructure Of Mild Steel Exposed in Hydrocloric Acid. In Applied Mechanics and Materials (Vol. 776, pp. 193–200). Trans Tech Publ.

Zulkifli, F., Yusof, M. S. M., Isa, M. I. N., Yabuki, A., & Nik, W. B. W. (2017). Henna leaves extract as a corrosion inhibitor in acrylic resin coating. Progress in Organic Coatings, 105, 310–319.

Vol. 14 No. 2 (2023) 10-22

Jurnal Riset
Teknologi Pencegahan Pencemaran Industri

Journal homepage : https://www.jrtppi.id

Kementerian Perindustrian
REPUBLIK INDONESIA

Water Hyacinth Potential in The Pollution Impact Reduction of Coffee Agroindustry Wastewater

Elida Novita[1], **Sri Wahyuningsih**[1], **Mastuki Andika**[1], **Hendra Andiananta Pradana**[1]

[1] Department of Agriculture Engineering, Faculty of Agricultural Technology, University of Jember, Jawa Timur 68121 Indonesia.

ARTICLE INFO

Article history:
Received October 26, 2022
Received in revised form February 15, 2023
Accepted April 11, 2023
Available online November 10, 2023

Keywords :
Agroindustry
Phytoremediation
Water Quality

ABSTRACT

Coffee processing wastewater originating from the coffee agroindustry has the potential to reduce environmental quality. Water hyacinth is one of the biological agents capable of reducing pollutants in wastewater through a rhizofiltration mechanism in the phytoremediation process. The pollutant-reducing ability of water hyacinth is limited, so the replacement of water hyacinth is one of the alternatives for optimizing the phytoremediation method. This research aimed to compare the replacement time of water hyacinth to the decreased parameters, namely turbidity, Biochemicals Oxygen Demand (BOD), Chemicals Oxygen Demand (COD), ammonia, and phosphate in the treatment of coffee processing wastewater using the phytoremediation method. The research stages consisted of water hyacinth acclimatization, determination of hydraulic resistance time, water hyacinth replacement time, and analysis of wastewater pollutant reduction. The density of water hyacinth used is 30 grams / L, and the incubation time is 14 days. The results showed that replacing water hyacinth improved the quality of coffee processing wastewater. The most water hyacinth replacement was on the seventh day. The percentage of turbidity parameters, Biochemicals Oxygen Demand (BOD), Chemicals Oxygen Demand (COD), ammonia (NH_3-N), and phosphate (PO_4-P) in the treatment of coffee processing wastewater with replacement of water hyacinth sequentially is 92.02%; 81.10%; 81.05%; 76.03% and 72.40%.

1. INTRODUCTION

The wet processing method of coffee cherries is one of the techniques applied to downstream agro-industrial products. This processing will produce better coffee quality (da-Mota et al., 2020; Firdissa et al., 2022). However, the application of a wet process which includes pulping, fermentation, washing, and drying, produces wastewater which causes environmental problems such as high exposure to organic matter, odour formation, increased turbidity, and decreased pH values (Ijanu et al., 2020; Campos et al., 2021). Coffee industry wastewater has the potential to reduce aesthetics and increase the value of water turbidity in water bodies if it is channelled directly without any treatment. It is due to the high Total Suspended Solid (TSS) value of 5947.56 mg/L (Novita et al., 2021). Then, in line with this, coffee processing wastewater contains high organic matter and is indicated by the values of Biochemicals Oxygen Demand (BOD) and Chemicals Oxygen Demand (COD). The BOD and COD values of the coffee processing industrial wastewater were 120.23 – 3770 mg/L and 387.05 – 4302 mg/L (Genawaw et al., 2021; Novita et al., 2021a; Wangpoom et al., 2022). Several efforts to treat coffee processing wastewater have been studied using physical, chemical, biological or combination methods (Samuel, 2021; Zagklis & Bampos, 2022). Phytoremediation is an alternative wastewater treatment

*Correspondence author.
E-mail : elida_novita.ftp@unej.ac.id (Elida Novita)

doi : https://10.21771/jrtppi.2023.v14.no.2.p10-22

Accreditation number : (Ristekdikti) 158/E/KPT/2021

technique that is environmentally friendly, inexpensive, and easier to apply than biological and chemical methods (Materac et al., 2015; Novita et al., 2021b; Delgado-Gonzalez et al., 2021). In line with this, coffee processing wastewater is biodegradable or has a fairly high organic matter content (Rattan et al., 2015). Phytoremediation is generally used for the treatment of wastewater containing heavy metals. Suppose the phytoremediation method handles coffee processing wastewater with high organic matter content. In that case, the organic matter is expected to be a source of nutrients to support plant growth in the phytoremediation process.

Water hyacinth is a biological agent that effectively reduces pollutants in wastewater. Water hyacinth has a hyperaccumulator ability to reduce organic and inorganic materials by supplying organic and inorganic nutrients from wastewater as a growth medium (Bais et al., 2016; Crini, 2019). Water hyacinth plants can reduce organic and inorganic matter by up to 80%. In line with this, applying phytoremediation techniques using water hyacinth can reduce BOD and COD in wastewater from agricultural activities by 75-80% (Ijanu et al., 2020; Polinska et al., 2021; Novita et al., 2022). The study of agro-industrial and domestic wastewater treatment using water hyacinth in the phytoremediation techniques with constructed wetland method reduced total suspended solid, i.e. 90% (Valipour et al., 2015; Denisi et al., 2021). Water hyacinth as a biofilter media has a limit in absorbing pollutants in wastewater. The morphological stages of water hyacinth, such as root length, growth stage, density, and wastewater characteristics, influence it.

Water hyacinth plants can absorb pollutants for 7-21 days (Rezania et al., 2016; Ali et al., 2020). Another study reported that water hyacinth has the most optimum absorption of pollutants in wastewater for 7-14 days in the phytoremediation process using both batch and semi-continuous systems (Rezania et al., 2016; Novita et al., 2022). Then, after phytoremediation for 7-14 days, water hyacinth absorption of reaches saturation point, and pollutants decrease due to a decrease in the rhizofiltration mechanism, water hyacinth operational age, and the availability of organic matter and oxygen (Rezania et al., 2016; Mi et al., 2020; Peng et al., 2020; Novita et al., 2022). In general, experiments on wastewater treatment using water hyacinth in the phytoremediation process only replaced plants once the leaves turned yellow and died. Appropriate replacement of aquatic plants positively impacts the removal of pollutants in wastewater. The purpose of this research was to compare the replacement time of water hyacinth to the decreased parameters, namely turbidity, Biochemicals Oxygen Demand (BOD), Chemicals Oxygen Demand (COD), ammonia (NH_3-N), and phosphate (PO_4-P) in the treatment of coffee processing wastewater using the phytoremediation method.

2. METHODS

This research was conducted by experimenting with the wastewater treatment of the coffee agroindustry using the phytoremediation method (batch process) with water hyacinth plants. Then quantitative descriptive is a research approach used to describe the impact of water hyacinth replacement time on the phytoremediation process with a circulation system on improving the quality of coffee agroindustry wastewater.

The research was conducted from June 2015 to April 2016. Meanwhile, the research location is in the Water Quality Laboratory-Environmental Control and Conservation Engineering, Department of Agricultural Engineering, Faculty of Agricultural Technology, University of Jember, Jember Regency. Then, wastewater samples analysis was also carried out at the Environmental Engineering Laboratory, Department of Environmental Engineering, Sepuluh Nopember Institute of Technology, Surabaya. The tools used in this study consisted of a glass aquarium that functioned as a phytoremediation reactor with dimensions of 160 cm x 30 cm x 30 cm with a working volume of 80 Liters (Figure 1), water pump KD 150, table, sample bottles, digital scales, Erlenmeyer with volume namely 125 and 250 mL, oven (Memmert Brand), ruler 50 cm, temperature incubator or refrigerator (Panasonic brand), Winkler bottles with volume 125 mL and 250 mL, volumetric flasks with volume 1000 and 2000 mL, pH meter-HI 223 (Hanna Brand), spectrophotometer-HI

83099 (Hanna Brand), turbidimeter-TN-100 (Thermo Scientific Eutech Brand), COD reactor-HI 839800 (Hanna Brand), and an acclimatization pond. The materials used in this study consisted of coffee processing wastewater from coffee agroindustry in smallholder plantations in the Jember Regency and PTPN XII Kalisat Jampit Bondowoso, water hyacinth with an average root length of 20 cm, distilled water free of ions (aquadest), reagents COD high range (HR) (Hanna Brand) with concentration value detection: 200 to 15,000 mg/L, alkaline iodide azide (laboratory grade – Merck made German), sodium thiosulfate 0.025 N (laboratory grade - Merck made German), manganese sulfate 40% (laboratory grade - Merck made German), sulfuric acid 20 N (laboratory grade - Merck made German), starch indicator 5% (laboratory grade - Merck made German), reagent N (laboratory grade - Merck made German), and sodium hydroxide 1 N (laboratory grade - Merck made German).

The working principle of the phytoremediation aquarium with circulation is that coffee processing wastewater is accommodated in a plastic tub (80 L) with a hole at the bottom. Coffee processing wastewater flows from a plastic storage tank or plastic tube to a phytoremediation reactor filled with water hyacinth. In this study, the phytoremediation method used a batch system. Coffee wastewater is circulated using the help of a water pump so that coffee processing wastewater in the aquarium remains homogeneous and nutrient absorption by water hyacinth is uniform. Circulation or discharge of coffee processing wastewater in this study, considering the Hydraulic Retention Time (HRT). According to research by Rukmawati et al. (2015), The optimal hydraulic retention time (HRT) is 8 hours 31 minutes with a flow rate of 10.61 mL/s in the phytoremediation of coffee processing wastewater using water hyacinth. The smaller the debt used, the greater or longer the HRT. The longer the HRT, the higher the decrease in turbidity, COD, BOD, TDS, N and P parameters. The HRT value is calculated using equation 1 (Valipour et al., 2015; Ghosh & Sarkar, 2021). Then, discharge was used in this research is 3.47 mL/s with an HRT of 9 hours 12 minutes. At this HRT, the wastewater flows smoothly, and there is no blockage in the flow hole.

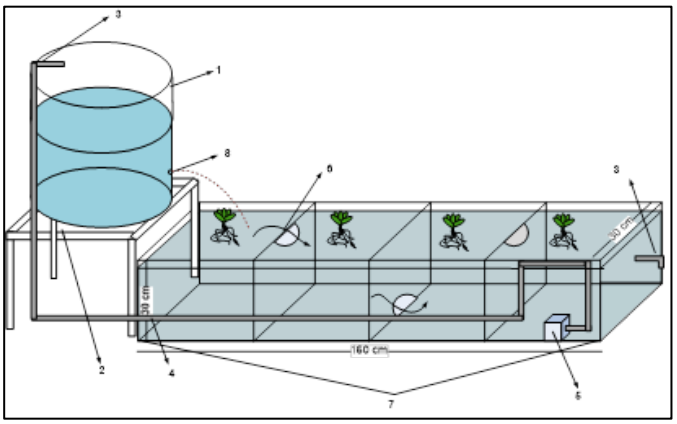

Sketch of Phytoremediation Reactor

Explanation:

1. Plastic Tube with a Volume of 80 L
2. Table
3. Elbow (1/2 inch)
4. Hose
5. Water Pump KD 105
6. Bulk head
7. Glass Aquarium
8. Flow Hole

Figure 1. Phytoremediation Reactor

$$HRT = \frac{VAT}{IFR} \quad (1)$$

Explanation:

HRT : Hydraulic Retention Time (Hours)
VAT : The volume of the Aeration Tank (L)
IF : Influent Flow Rate (L/Hours)

Table 1. Detail of Experiment

Treatment	Experiment	
	Replacement of water hyacinth (RW)	No replacement of water hyacinth (NRW)
Water Hyacinth Replacement	water hyacinth plant, more than 50% of the leaves have withered	No
Phytoremediation Duration (Days)	14	14
Daily Parameters Examination	pH and turbidity	pH and turbidity
Initial and End Parameters Examination (on day 0 and day 14)	turbidity, BOD, COD, ammonia, and phosphate	turbidity, BOD, COD, ammonia, and phosphate
Discharge (mL/s)	3.47	3.47
HRT	9 hours 12 minutes	9 hours 12 minutes

Table 2. Data Collecting Methods and Analysis of Wastewater Quality Parameters

Parameters	Analysis Methods	References	Data Collecting
pH	Electrometric	SNI 06-6989.11-2004	During 14 days (Daily Data)
Turbidity	Spectrophotometric	QI/LKA/11	During 14 days (Daily Data) and Day 1 and 14 Data
Biochemical Oxygen Demand (BOD)	Titrimetric-Winkler Method	Standard Method: APHA 5210 B-1998	Initial and End Data (Day 1 and 14 data)
Chemical Oxygen Demand (COD)	Spectrophotometric	QI/LKA/19	
Ammonia (NH_3-N)	Spectrophotometric	SNI 06-6989.30-2005	
Phosphate (PO_4-P)	Spectrophotometric	SNI 06-6989.30-2005	

Water hyacinth is obtained from a swamp area located in Jember Regency. The selected water hyacinth has a root length average of 20 cm and is in the vegetative period (not yet flowering) (Valipour, 2015). Before water hyacinth is used as a biofilter, acclimatization is carried out first. Acclimatization aims to adjust the water hyacinth conditions to have good pollutant absorption capabilities. Acclimatization is done by placing water hyacinths in the acclimatization pond for approximately 7-14 days before being used as a biofilter. The acclimatization pond with dimensions 100 cm x 20 cm x 20 cm or 40 L contains water from rainwater reservoirs and is left exposed to direct sunlight (Elizabeth et al., 2020: Hasibuan et al., 2020; Novita et al., 2022). Before the coffee processing wastewater was placed in a glass aquarium, the initial characteristics were measured. This measurement aims to identify the initial conditions of wastewater before biological treatment is carried out to determine the efficiency of the treatment method (Jones et al., 2018; Novita et al., 2022; Simanjuntak et al., 2022).

There were 2 (two) phytoremediation experiments in this study, namely the replacement of water hyacinth (RW) and no replacement of water hyacinth (NRW) (Table 1). Each experiment contained two replications. The first experiment (RW) is to replace the water hyacinth when the leaves have withered. Water hyacinth replacement occurs if more than 50% of the leaves have withered in one water hyacinth plant. The study's characteristics of wilted water hyacinth leaves were yellowing leaves and dry leaf edges. In the second experiment (NRW), without changing the water hyacinth until the treatment ends. Both treatments used the same debit or discharge. Each process is carried out for 14 days. Another study reported that water hyacinths could grow and absorb organic matter and heavy metals in wastewater within 7-15 days (Saha et al., 2017: Safauldeen et al., 2019: Ali et al., 2020). Each aquarium has the same density of water hyacinth, which is 30 grams/L with an

average root length of 20 cm. Measurement of daily parameters or measurement of parameters every day for 14 days, namely pH and turbidity. The parameters that were only measured at the beginning and end of the treatment were turbidity, BOD, COD, ammonia, and phosphate. This measurement aims to calculate the phytoremediation efficiency of coffee processing wastewater using water hyacinth. Then the measurement results will be compared with the Coffee Processing Wastewater Quality Standard, which refers to Regulation of the Minister of Environment of the Republic of Indonesia Number 5/2014 (Minister of Environment of the Republic of Indonesia, 2014).

Consideration of the performance of wastewater quality improvement using the phytoremediation method is indicated by the parameters pH, turbidity, Biochemical Oxygen Demand (BOD), Chemical Oxygen Demand (COD), ammonia (NH_3-N), and phosphate (PO_4-P). Details of the method of measuring these parameters can be seen in Table 2.

Data analysis was carried out using a quantitative descriptive approach. This approach will describe the effect of 2 experiments on reducing pollutants in coffee processing wastewater. The decrease in pollutants is identified by the percentage value of the efficiency of reducing pollutant substances in coffee processing wastewater in the coffee agroindustry. Then the equation used to evaluate the percentage of pollutant concentration can be seen in equation 2 (Jones et al., 2018; Novita et al., 2022; Simanjuntak et al., 2022).

$$PER = \frac{Co-Ci}{Ci} \times 100\% \quad (2)$$

Explanation:

PER : Percentage of Efficiency Removal (%)

Co : Initial Pollutant Concentration (mg/L)

Ci : End Pollutant Concentration (mg/L)

A comparison of experiments based on the percentage value of the efficiency of reducing pollutant concentrations is used for further discussion in selecting treatment alternatives. The statistical test used is the General Linear Model Repeated Measures or the General Linear Model (GLM) using SPSS 16.0 software (Damanik-Ambarita et al., 2016: Araromi et al., 2018). Taking the best alternative in the water hyacinth replacement experiment in the phytoremediation process based on the overall percentage reduction value such as parameters turbidity, Biochemical Oxygen Demand (BOD), Chemical Oxygen Demand (COD), ammonia (NH_3-N), dan phosphate (PO_4-P).

3. RESULT AND DISCUSSION

3.1. Characteristics of Coffee Processing Wastewater

Coffee processing wastewater from coffee agroindustry activities can pollute the environment if the content of water quality parameters in the waste does not meet the quality standards set by the government. These conditions can be seen in Table 3. Several parameters that do not meet wastewater quality are referred to Regulation of the Minister of Environment of the Republic of Indonesia Number 5/2014, namely, BOD, COD, and pH.

Table 3. Characteristics of Coffee Processing Wastewater

Parameters	Initial Value	End Value	Wastewater Quality Standard*	Units
Biochemical Oxygen Demand (BOD)	1,434 - 2,106	271 - 590	90	mg/L
Chemical Oxygen Demand (COD)	2,274.5 - 3,200	64.17 – 81.05	200	mg/L
Turbidity	424 – 523	42 – 64.88	-	NTU
pH	4.7-4.8	6.25 – 6.70	6-9	-
Ammonia (NH_3-N)	104.11-201.18	72.40 – 76.03	-	mg/L
Phosphate (PO_4-P)	10.71 - 67.65	5.91 – 8.59	-	mg/L

*Code: RW = Water Hyacinth Replacement

*Sources: Regulation of the Minister of Environment of the Republic of Indonesia Number 5/2014

The pH parameter indicates the chemical nature of the acidic or basic coffee processing wastewater. The pH value of the waste is 4.2 – 5.3 and is in the acid category, so it is corrosive (Novita et al., 2022). If coffee processing wastewater is directly discharged into the ground or water bodies, it can pollute the environment and threaten its biotic life. In line with this, based on chemical parameters in the form of initial values of BOD and COD of coffee processing wastewater, it indicates the presence of quite high organic matter. The organic matter is predicted to come from breaking down complex compounds such as carbohydrates, proteins, and fats found in coffee fruit flesh during fermentation into simpler compounds such as monosaccharides (Buck et al., 2021).

Comparing BOD and COD values can indicate organic matter characteristics in coffee processing wastewater. The ratio of BOD and COD values in coffee wastewater processing is > 0.1, then it indices that coffee processing wastewater contains high levels of easily decomposed organic matter (Novita et al., 2021a; Novita et al., 2022). Then the value of the ratio of BOD and COD of this wastewater is 0.65, so it is in the biodegradable category. Recommendations for wastewater treatment with a characteristic ratio of BOD and COD > 0.1, namely the biological method with the help of microorganisms and aquatic plants such as water hyacinth (Echhornia crassipes) (Saha et al., 2017; Novita et al., 2022).

3.2. Analysis of Turbidity Parameter

Referring to Figure 1, the phytoremediation process with water hyacinth replacement reduced the turbidity value of coffee processing wastewater with a reduction efficiency value of more than 87% for all treatments. On the seventh day, the water hyacinth had withered and reached its saturation point in both the RW and NRW treatments. Furthermore, the average decrease in turbidity values was stable in the RW treatment from day 2 to day 14.

Specifically, the percentage of efficiency of decreasing turbidity parameters in RW and NRW treatments, respectively, is 92.02% and 87.60%. Suspended particles mainly cause turbidity. In this experiment, there was no precipitation phase and particle size separation through the suspended particle filtering method. Then, circulation causes the coffee processing wastewater particles not to precipitate and return to the phytoremediation reactor and are homogenized again. It happens because of the decrease in turbidity due to the decomposition of organic compounds by a plant which is also commonly referred to as phytodegradation (Polinska et al., 2021). In line with this condition, the BOD reduction efficiency values for the RW and NRW treatments were 81.10% and 64.17%, respectively. Referring to the research results by Singh and Balomajumder (2021), Water hyacinth plants have the principle of rhizofiltration to reduce turbidity through phytoextraction, phytodegradation, phytovolatilization, rhizofiltration, and phytostabilization. It is a series of processes experienced by water hyacinths to absorb contaminants and nutrients in the coffee processing wastewater to be deposited on plant parts. The replacement of water hyacinth has an impact on reducing the amount of water hyacinth that has reached its saturation point in absorbing pollutants so that water hyacinth organs such as roots improve and the living habitat of microorganisms is better so that the absorption of organic and inorganic compounds increases.

3.3. Analysis of pH Parameter

The presence of these ions in excess causes coffee processing wastewater to be acidic because it has a low pH value. This condition is supported by the results of the examination of the initial pH value in coffee processing wastewater of 4.7-4.8, which is presented in Figure 2. Coffee processing wastewater tends to be acidic, presumably due to the reshuffling of sugar in the coffee fruit flesh during fermentation. The fermentation resulted in converting glucose into acidic compounds with the help of aerobic and anaerobic microorganisms so that the pH value would tend to be low (Cruz-Salomon et al., 2018: Ijanu et al., 2020). The results of measuring the pH value for 14 days represent that the wastewater circulation system and the application of water hyacinth in each treatment greatly influence the increase in the pH value.

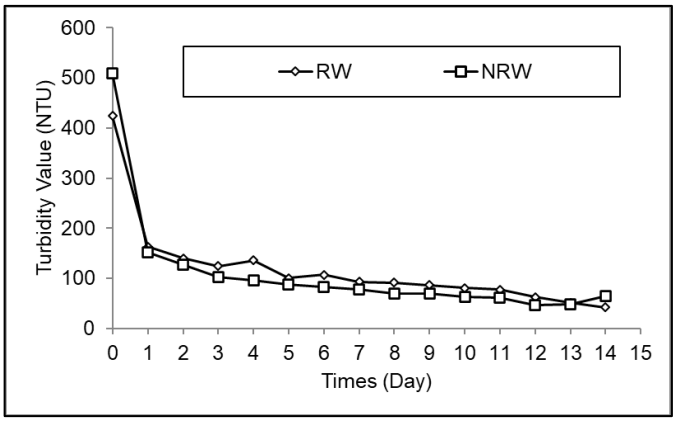

(a)

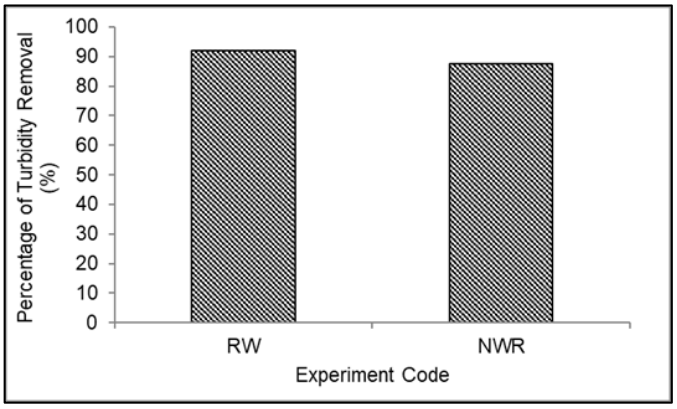

(b)

Figure 1. Data Trend of Turbidity Removal (a) Data Trend of Turbidity Parameter dan (b) Percentage of Turbidity Reduction

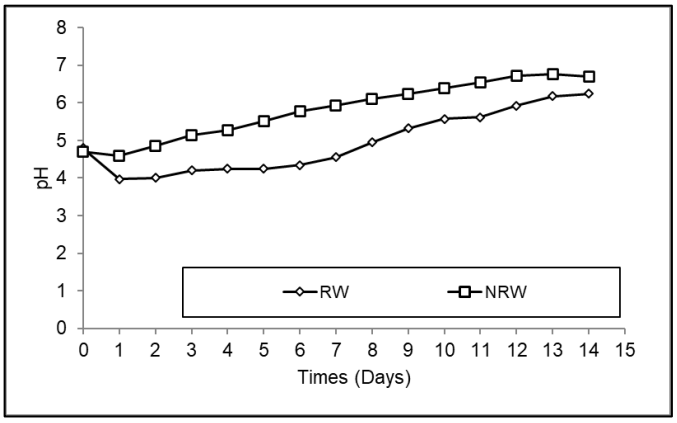

Figure 2. Fluctuation of pH Value

In the water hyacinth (RW) replacement treatment, the pH increased from the initial pH of 4.8 to day 14 of 6.3. In the treatment without replacing water hyacinth (NRW), the initial pH increased by 4.7 to 6.7. The increase in the pH of the liquid waste is due to the photosynthetic activity of water hyacinth, which requires a lot of carbon dioxide (CO_2). The process of photosynthesis is the process of taking CO_2 dissolved in water which then produces energy (glucose) and oxygen. Dissolved oxygen in water can increase the pH value. When the water hyacinth is replaced, the pH value will increase the next day because the new water hyacinth absorbs more organic matter.

3.4. Analysis of BOD and COD Parameters

Exposure to the organic matter in coffee processing wastewater can be approached by examining the BOD and COD values. Referring to Figure 3, replacing water hyacinth in the coffee agroindustry wastewater treatment contributes to an increase in the reduction of the BOD and COD values. The BOD reduction efficiency values for the RW and NRW treatments were 81.10% (271 mg/L) and 64.17% (590 mg/L), respectively. Then the COD reduction efficiency values in the RW and NRW treatments, respectively, are 81.05% (431 mg/L) and 64.18% (937 mg/L). In general, water hyacinth replacement treatment contributes to the effectiveness of remediation of exposure to the organic matter in coffee processing wastewater by more than 81.05%.

The decrease in the BOD value is the same as the decrease in the COD value caused by the periodic replacement of water hyacinth. Water hyacinth in a fresh condition is thought to increase the oxygen supply through photosynthesis and reduce organic matter as a source of nutrients. The oxygen supply during the process increases the dissolved oxygen needed by microorganisms to reduce organic matter contained in coffee processing wastewater. This phenomenon maintains the dissolved oxygen concentration to support the oxygen supply for microorganisms attached to the water hyacinth roots and in wastewater (Valipour, 2015; Novita et al., 2022). This process will oxidize compounds both easily decompose and are difficult to decompose. However, although the RW treatment has relatively high BOD and COD reduction potential, the coffee processing wastewater has not met the wastewater quality standard referred to in Regulation of the Minister of the Environment of the Republic of Indonesia

Number 5 of 2014, so secondary treatment, namely constructed wetland is needed. The comparison of the end value of BOD and COD can be seen in Table 3.

3.5. Analysis of Ammonia and Phosphate Parameters

Exposure to high macronutrients such as ammonia and phosphate can disrupt aquatic life and ecosystems. The phytoremediation method is considered appropriate for removing nutrient content. Water hyacinth plants will absorb these materials to be extracted in photosynthesis (Ali et al., 2020). This condition is in line with the study's results, which showed that the percentage reduction in ammonia and phosphate values reached more than 60%. The main cause of the decrease in ammonia content is the activity of bacteria and microorganisms such as Nitrosomonas and Nitrobacter present in water hyacinth roots which can remodel ammonia (NH_3) into nitrite (NO_2) and nitrite into nitrate (NO_3), which can be absorbed by these plants (Hasibuan et al., 2018). This process is called nitrification.

Referring to Figure 4, the percentage of ammonia parameter reduction efficiency values in the RW and NRW treatments, respectively, is 76.03% (24.96 mg/L) and 72.40% (37.63 mg/L). The water hyacinth (RW) replacement treatment was higher than the NRW treatment. It is suspected that in the RW treatment, there is still fresh water hyacinth so that the bacteria that convert ammonia into nitrite and nitrate work optimally. Under aerobic conditions or sufficient oxygen availability, Nitrosomonas and Nitrobacter bacteria can work optimally in oxidizing ammonia to nitrite and nitrate. It is different from the NRW treatment. Water hyacinth decays and even dies on the last day, resulting in anaerobic conditions (lack of oxygen). So that Nitrosomonas and Nitrobacter bacteria cannot work optimally, PE treatment can be used as an alternative in reducing the value of ammonia (NH_3). The process of nutrient conversion due to phytoremediation also occurs in phosphate.

The percentage of efficiency values for decreasing phosphate parameters in RW and NRW treatments, respectively, is 86.58% (5.91 mg/L) and 19.79% (8.59 mg/L). The availability of sufficient phosphate and the condition of water hyacinth plants that are still good affect the ability to absorb nutrients by water hyacinth. This condition will affect the efficiency of phosphate reduction. In line with this phenomenon, the RW treatment had a higher phosphate reduction efficiency value than the NRW treatment. The NRW treatment replaced water hyacinth day 14. This condition resulted in the water hyacinth reaching a saturation point to absorb pollutants and decay. The decomposition of water hyacinth can increase the phosphate value in wastewater. This condition is similar to the results of the study by Rattan et al. (2015), phytoremediation with batch method resulted in the formation of phosphate granules so that the phosphate reduction process was less than optimal. Then, the circulation method can function as a continuous stirring process and maximize the nutrient degradation process in wastewater (Valipour et al., 2015).

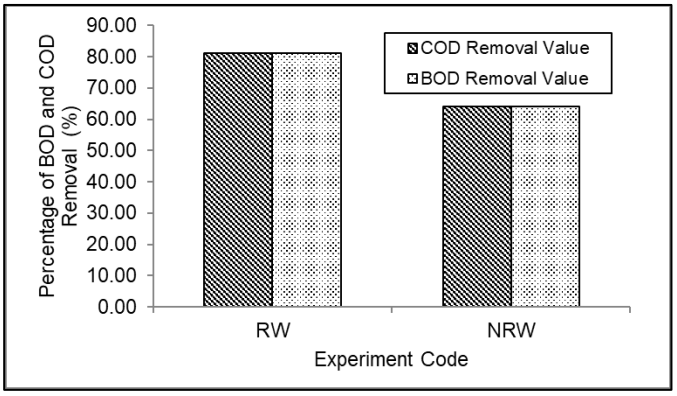

Figure 3. Percentage of BOD and COD Reduction

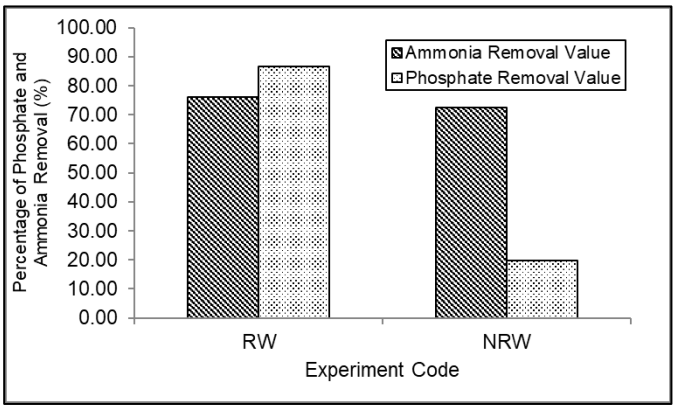

Figure 4. Percentage of Ammonia and Phosphate Reduction

Table 4. Time and Total of Water Hyacinth Replacement

Water Hyacinth Replacement Time (Day)	Number of Water Hyacinths Replacement (Stem)
1	-
2	-
3	-
4	-
5	-
6	-
7	12
8	-
9	5
10	-
11	6
12	-
13	2
14	-

3.6. Morphology Analysis Change of Water Hyachint

Water hyacinth is an aquatic plant from the kingdom Plantae and belongs to the Pontederiaceae family. Water hyacinth plants live floating in the water and have oval-shaped leaves with a tapered base and a swollen stalk. This plant can reproduce very quickly, both generatively and vegetatively. Vegetative reproduction can double in 7-14 days (Valipour et al., 2015). Water hyacinths undergo morphological changes along with the process of reducing pollutants in coffee processing wastewater. Morphological changes of water hyacinth after the phytoremediation process can be seen in Figure 5.

The roots of the water hyacinth plant change to become slimy and black. It is because the most important role in the process of absorption of organic matter is the roots. The stems of the water hyacinth plant change stem color. Initially green, it changes to yellowish and brownish. There was also a change in the leaves, which were initially green, turned yellowish and brownish withered. Leaf discoloration from green to yellow to dead water hyacinth is caused by roots absorbing contaminants in coffee processing wastewater. The cause of dead water hyacinth is due to water hyacinth carrying out the process of phytoaccumulation and phytodegradation. Phytoaccumulation is the process of plants pulling contaminants from the media so that they accumulate around plant roots. This process is known as phytoextraction, phytodegradation, phytovolatilization, rhizofiltration, and phytostabilization. Meanwhile, phytodegradation is the decomposition of contaminants by plant roots to be broken down into non-toxic organic substances.

3.7. Recommendation of Water Hyacinth Replacement Time

This research was conducted with two treatments, namely, the replacement of water hyacinth (RW) and no water hyacinth replacement (NRW). Water hyacinth is replaced when wilted water hyacinth leaves dominate one water hyacinth plant. For example, in one water hyacinth, there are eight leaves, water hyacinth replacement is carried out if at least four leaves wither. Withered leaves starting from the edges of the leaves, dry up. It is due to the inhibition of metabolism in the cells of the leaf margins, resulting in a lack of nutrients, and eventually, the cells die (Ali et al., 2020). This study replaced the withered water hyacinth with new water hyacinth.

Table 4 shows that the water hyacinth replacement treatment was carried out three times within 14-15 days (Saha et al., 2017: Safauldeen et al., 2019: Ali et al., 2020). The first water hyacinth replacement was performed on the seventh day of the RW treatment. It is because, on the seventh day, the water hyacinth has reached its saturation point. Water hyacinth plants wilt or die due to their maximum ability to absorb contaminants. After the water hyacinth reaches the saturation point in absorbing organic matter, the water hyacinth leaves wither (the edges of the leaves are dry, and the centre of the leaves is yellow). This experiment indicated that the conditions for growing water hyacinth were not fulfilled in coffee processing wastewater because it has a high enough contaminant and a low pH value, resulting in the growing conditions for water hyacinth getting worse and dying. Then, on the seventh day,

not all water hyacinths reached saturation. It is influenced by the availability of nutrients or nutrients in wastewater covering organic matter, indicating BOD and COD parameters, ammonia, and phosphate. Then, the longer the number of water hyacinth plants replaced, the less on day 14. It indicates that the quality of coffee processing wastewater is getting better.

The treatment of coffee processing wastewater has various impacts on turbidity, BOD, COD, ammonia, and phosphate parameters. Therefore, the General Linear Model statistical test method is used to generalize the results of handling coffee processing wastewater using the phytoremediation method. Generalization was carried out on the RW and NRW treatments on the efficiency value of decreasing turbidity, BOD, COD, ammonia, and phosphate parameters.

(a) (b) (c)

Figure 5. Morphology Change of Water Hyacinth (a) roots, (b) leaves, and (c) stem

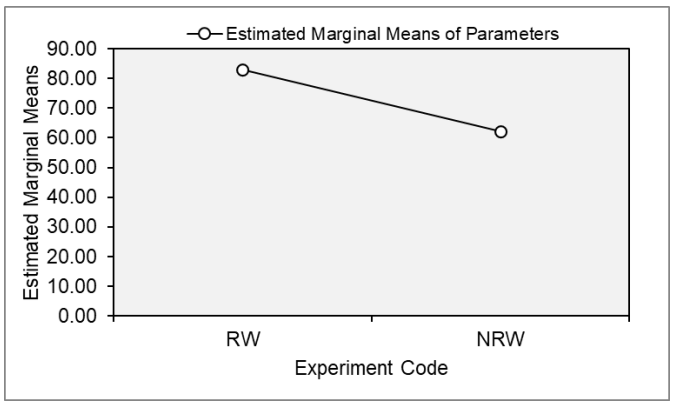

Figure 6. Graph of General Linear Model Test

Figure 6 shows that RW has an estimated marginal means value of 83.14 on the overall percentage reduction of turbidity, COD, BOD, ammonia, and phosphate. The estimated marginal means value is greater than the value in the NRW treatment. Then, the estimated marginal means for the NRW treatment is 62.20. Estimated marginal means describe the accumulated scoring for each treatment based on the parameters analyzed (Damanik-Ambarita et al., 2016: Araromi et al., 2018). Therefore, RW treatment is recommended for handling coffee agroindustry wastewater using circulation phytoremediation techniques with water hyacinth replacement. However, it is necessary to carry out further or secondary treatment so that the BOD and COD values of coffee processing wastewater still meet the quality standards in the Regulation of the Minister of the Environment of the Republic of Indonesia Number 5 of 2014.

4. CONCLUSION

The replacement of water hyacinth in phytoremediation using the circulation method in handling coffee processing wastewater has a more positive impact on improving wastewater quality than phytoremediation that does not replace water hyacinth. Then the recommendation for water hyacinth replacement is 7 days, which is the best or alternative time for processing wastewater treatment in the coffee agroindustry. It is supported by the results of statistical tests using the General Linear Model, representing that the water hyacinth replacement treatment has the highest overall value than the treatment without water hyacinth replacement. The percentage of turbidity parameters, Biochemicals Oxygen Demand (BOD), Chemicals Oxygen Demand (COD), ammonia (NH_3-N), and phosphate (PO_4-P) in the treatment of coffee processing wastewater with replacement of water hyacinth sequentially is 92.02%; 81.10%; 81.05%; 76.03% and 72.40%. Furthermore, the secondary treatment, namely filtration as a physic method or constructed wetland as combination methods for the effluent of phytoremediation applied, needs to be done considering that the BOD and COD parameters do not meet the quality standards in the Regulation of the

Minister of the Environment of the Republic of Indonesia Number 5 of 2014.

ACKNOWLEDGMENT

This work was funded by the Indonesian Ministry of Education and Culture Grant Program 2014/2015. We highly appreciate the support of all related parties who assisted us in completing this research.

REFERENCE

Ali, S., Abbas, Z., Rizwan, M., Zaheer, I. E., Yavas, I., Unay, A., Abdel-Diam, M. M., Bin-Jumah, M., Hasanuzzaman, M. & Kalderis, D. (2020). Application of Floating Aquatic Plant in Phytoremediation of Heavy Metals Polluted Water: A Review. Sustainability, 12(1927), 1-33. https://doi.org/10.3390/su12051927

Arorami, D. O., Majekomduni, O. T., Adeniran, J. A., & Salawudeen, T. O. (2018). Modeling of Activated Sludge Process for Effluent Prediction-a Comparative Using ANFIS and GLM Regression. Environment Monitoring Assessment, 190(495), 1-17. https://doi.org/10.16966/2381-5299.17

Bais, S. S., Lawrence, K. & Pandey, A. K. (2016). Phytoremediation Potential of Eichhornia crassipes (Mart.) Solms. International Environmental Agriculture Biotechnology, 1, 210-2017. https://doi.org/10.22161/ijeab/1.2.16

Buck, N., Wohlt, D., Winter, A. R. and Ortner, E. (2021). Aroma-Active Compound in Robusta Coffee Pulp Puree-Evaluation of Physicochemical and Sensory Properties. Molecules, 26(3925): 1-14. https://doi.org/10.3390/molecules26133925

Campos, R. C., Pinto, V. R. A., Melo, L. F., da Rocha, S. J. S. S. & Coibra, J. S. (2021). New Sustainable Perspectives for "Coffee Wastewater" and Other by-Products: A Critical Review. Future Food, 4(2021), 1-10. https://doi.org/10.1016/j.fufo.2021.100058

Crini, G. & Lichtfouse, E. (2019). Advantages and Disadvantages of Techniques Used for Wastewater Treatment. Environment Chemicals Letters, 17, 145-155. https://doi.org/10.1007/s10311-018-0785-9

Cruz-Salomon, A., Rios-Valdovinos, E., Pola-Alberos, F., Lagunas-Rivera, S., Meza-Gordillo, R. & Ruiz-Valdiviezo, V.M. (2018). Evaluation of Hydraulic Retention Time on Treatment of Coffee Processing Wastewater (CPWW) in EGSB Bioreactor. Sustainability, 10(83), 1-11. https://doi.org/10.3390/su10010083

da-Mota, M. C. B., Batista, N. N., Rabelo, M. H. S., Ribeiro, D. E., Borem, F. M. & Schwan, R. F. (2020). Influence of Fermentation Conditions on the Sensorial Quality of Coffee Inoculated with Yeast. Food Research International, 136(2020), 1-8. https://doi.org/10.1016/j.foodres.2020.109482

Damanik-Ambarita, M. N., Everaert, G., Fario, M. A. E., Nguyen, T. H. T., Lock, K., Musonge, P. L. S., Suhareva, N., Dominguez-Granda, L., Bennetsen, E., Boets, P. dan Goethals, P. L. M. (2016). Generalized Linier Models to Identify Key Hydromorphological and Chemical Variabel Determining the Occurrence of Macroinvertebrates in the Guayas River Basin (Equador). Water. 8(7), 297. https://doi.org/10.1007/10.3390/w8070297

Delgado-Gonzalez, C. R., Madariaga-Navarrete, A., Fernandez-Cortes, J.M., Islas-Pelcastre, M., Oza, G., Iqbal, H.M. & Sharma, A. (2021). Advances and Applications of Water Phytoremediation: A Potential Biotechnological Approach for the Treatment of Heavy Metals from Contaminated Water. International Journal of Environmental Research and Public Health, 18(5215), 1-21. https://doi.org/10.3390/ijerph18105215

Denisi, P., Biondono, N., Bombino, G., Falino, A., Zema, D. A. & Zimbone, S. M. (2021). A Combined System Using Lagoons and Constructed Wetland for Swine Wastewater Treatment. Sustainability, 13(12390), 1-14. https://doi.org/10.3390/su132212390

Zagklis, D. P. & Bampos, G. (2022). Tertiary Wastewater Treatment Technologies: A Review of Technical,

Economic, and Life Cycle Aspect. Process, 2022 (10), 2304. https://doi.org/10.3390/pr10112304

Elizabeth, J., Yuniati, R., & Wardhana, W. (2020). The Capacity of Water Hyacinth as Biofilter and Bioaccumulator based on Its Size. IOP Conferences Series: Material, Science, and Engineering, 902(012064), 1-17. https://doi.org/10.1088/1757-899X/902/1/012067

Firdissa, E., Mohammed, A., Berecha, G. & Garedew, W. (2022). Coffee Drying and Processing Method Influence Quality of Arabica Coffee Varieties (Coffee arabica L.) at Gomma I and Limmu Kossa, Southwest Ethiopia. Journal of Food Quality, 2022, 1-8.

Genanaw, W., Kanno, G. G., Derese, D., & Aregu, B. (2021). Effect of Wastewater Discharge from Coffee Processing Plant on River Water Quality, Sidagama Region, South Ethiopia. Environmental Health Insights, 15(2021). https://doi.org/10.1177/11786302211061047

Ghosh, K. & Sarkar, A. (2021). Evaluating Urban Wastewater Remediation Efficiency of the Hydroponic Vetiver System Through Predictive Modelling Using Artificial Neural Network. Environmental Technology & Innovation, 24(2021), 1-15. https://doi.org/10.1016/j.eti.2021.102007

Hasibuan, E. N., Djalalemah, A., Asmar, G. A. & Cahyonugroho, O. H. (2018). The Growth Rate and Chlorophyll Content of Water Hyacinth under Different Type of Water Sources. IOP Conferences Series: Material, Science, and Engineering, 902(012064), 1-17. https://doi.org/10.1088/1757-899X/902/1/012064

Ijanu, E. M., Kamarudin, M. A. & Norashiddin, F. A. (2020). Coffee Wastewater Treatment: a Critical Review on Current Treatment Technologies with a Proposed Alternative. Applied Water Science, 10(11), 1-11. https://doi.org/10.1007/s13201-019-1091-9

Jones, J. L., Jenkins, R. O. & Haris, P. I. (2018). Extending the Geographics Reach of the Water Hyacinth Plant in Removal of Heavy Metals from Temperature Northern Hemisphere River. Scientific Report, 8(11071), 1-15. https://doi.org/10.1038/s41598-018-29387-6

Materac, M., Wyrwicka, A., & Sobiecka, E. (2015). Phytoremediation Techniques in Wastewater Treatment. Environmental Biotechnology, 11(1), 10-13. https://doi.org/10.14799/ebms249

Mi, Z., Idrees, I., Danish, P., Ahmad, S., Ali Q., & Malik, A. (2020). Potetntial of Water Hyacinth (Eichhornia crassipes L.) for Phytoremediation of Heavy Metals from Wastewater. Biological and Chinicals Sciences Research Journal, 2020(1), 1-7. https://doi.org/10.54112/bcsrj.v2020i1.6

Minister of Environment of the Republic of Indonesia. 2014. Peraturan Menteri Lingkungan Hidup Republik Indonesia Nomor 5 Tahun 2014 tentang Baku Mutu Air Limbah. Jakarta.

Novita, E., Salim, M. B. & Pradana, H. A. (2021a). Coffee Industry Wastewater Treatment with Coagulation-Flocculation Method Using a natural Coagulant of Tamarind Seeds (Tamarindus indica L.). Jurnal Teknologi Pertanian, 22(1), 13-24. https://doi.org/10.21776/ub.jtp.2021.022.01.2

Novita, E., Wahyuningsih, S. & Adinda, C. (2021b). Studi Kelayakan Teknik dan Biaya Terhadap Alternatif Fitoremediation pada Air Limbah Pengolahan Kopi. Agrointek, 15(2), 513-520. https://doi.org/10.21107/agrointek.v15i2.9056

Novita, E., Wahyuningsih, S., Safrizal, M. R., Puspitasari, A. I. & Pradana, H. A. (2022). Kajian Perbaikan Kualitas Air Limbah Pengolahan Kopi Menggunakan Metode Fitoremediasi dengan Tanaman Eceng Gondok (Eichhornia crassipes). Jurnal Sains dan Teknologi, 11(1), 197-203. https://doi.org/10.23887/jstundiksha.v11i1.45298

Peng, H., Wang, Y., Tan, T. L. & Chen, Z. (2020). Exploring the Phytoremediation Potential of Water Hyacinth by FTIR Spectroscopy and ICP-OES for

Treatment of Heavy Metal Contaminated Water. International Journal of Phytoremediation, 22(9):939-951. https://doi.org/10.1080/15226514.2020.1774499

Polinska, W., Kotowaska, U., Kiejza, D., & Karpinska, J. (2021). Insight in to the Use Phytoremediation Processes for Removal of Organic Micropollutans from Water and Wastewater; A Review. Water, 13(2065), 1-19. https://doi.org/10.3390/w13152065

Rattan, S., Parande, A. K., Nagaraju, V. D. & Ghiwari, G. K. (2015). A Comprehensive Review on Utulization of Wastewater from Coffee Processing. Environment Science Pollution Research International, 22(9), 6461-6472. https://doi.org/10.1007/s11356-015-4079-5

Rezania, S., Din, M. F. Md., Taib, S. M., Dahalan, F. A., Songip, A. R., Singh, L. & Kamyab, H. (2016). The Efficient Role of Aquatic Plant (Water Hyacinth) in Treating Domestic Wastewater in Continuous System. International Journal of Phytoremediation, 18(7), 679-685. http://dx.doi.org/10.1080/15226514.2015.1130018

Rukmawati, B. S., Novita, E., Wahyuningsih, S. & Siswoyo, S. (2015). Circulation Effect of Coffee Wastewater Flow in Water Hyacinth Phytoremediation. The 1st Young Scientist International Conferences of Water Resources Development and Environmental Protection, Malang, Indonesia, 5-7 June 2015.

Samuel, Z. A. (2021). Treatment of Combined Coffee Processing Wastewater Using Constructed Wetland/Cyperus-ustulatus and Typha-latifolia Plants Process. Global Nest Journal, 23(3), 429-433. https://doi.org/10.30955/gnj.003688

Safauldeen, S. H., Hasan, H. A. & Abdullah, S. R. S. (2019). Phytoremediation Efficiency of Water Hyacinth for Batik Textile Effluent Treatment. Journal of Ecological Engineering, 20(9), 177-187. http://dx.doi.org/10.1080/10.12911/22998993/112492

Saha, P., Shide, O. & Sarkar, S. (2017). Phytoremediation of Industrial Mines Wastewater Using Water Hyacinth. International Journal of Phytoremediation, 19(1), 87-96. http://dx.doi.org/10.1080/15226514.2016.1216078

Singh, N. & Balomajumder, C. (2021). Phytoremediation Potential of Water Hyacinth (Echhornia crassipes) for Phenol and Cyanide Elimination from Synthetic/Simulated Wastewater. Applied Water Science, 11(144), 1-15. http://dx.doi.org/10.1007/s13201-021-01472-8

Simanjuntak, N. A. M., Zahra, N. L. & Suryawan, I. W. K. (2022). Decision Making for Biological Tofu Wastewater Treatment to Improve Quality Wastewater Treatment Plant (WWTP) using Analytical Hierarcy Process (AHP). Jurnal Riset Teknologi Pencegahan Pencemaran Industri, 13(1), 20-34.

Valipour, A., Raman, V. K. & Ahn, Y-H. (2015). Effectiveness of Domestic Wastewater Treatment Using Bio-Hedge Water Hyacinth Wetland System. Water, 7, 329-347. https://doi.org/10.3390/w7010329

Wangphoom, T., Saleepochn, T., Noophan, P. L., & Li, C-W. (2022). Effects of Caffeine and COD from Coffee Wastewater on Anaerobic Ammonium Oxidation (Anammox) Activities. Water, 14(2238), 1-14. https://doi.org/10.3390/w14142238

Vol. 14 No. 2 (2023) 23-32

Jurnal Riset
Teknologi Pencegahan Pencemaran Industri

Journal homepage : https://www.jrtppi.id

Kementerian Perindustrian
REPUBLIK INDONESIA

Removal of Ammonium and Phosphate from Synthetic Wastewater of Complex Fertilizer Industry Through Struvite Crystallization Process

Muhammad Zulfikar Luthfi*[1], Tjandra Setiadi[2], Dennis Farina Nury[3], Choerudin[4]

[1] Politeknik ATI Padang.

[2] Pusat Studi Lingkungan Hidup, Institut Teknologi Bandung.

[3] Institut Teknologi Sumatera.

[4] Institut Teknologi Nasional, Bandung.

ARTICLE INFO

Article history:
Received December 5, 2022
Received in revised form February 10, 2023
Accepted April 14, 2023
Available online November 10, 2023

Keywords :
Aeration
Complex Fertilizer Waste
Magnesium Ammonium Phosphate
Struvite
Urease Enzyme

ABSTRACT

The complex fertilizer industry produces wastewater that contributes to water pollution because it contains high organic nitrogen in the form of urea which can be hydrolyzed to ammonium using the urease enzyme and high levels of phosphate and ammonium concentrations. Struvite precipitation is an effective method for removing and recovering ammonium and phosphate from wastewater. This study aimed to determine the effect of aeration and the enzyme urease in removing ammonium and phosphate in complex fertilizer synthetic wastewater through struvite precipitation. Struvite precipitation was carried out in a batch reactor with a working volume of 0.5 L with variations in aeration rate, aeration time, and the addition of urease enzyme from Jack bean peas (*Canavalia ensiformis*). Residual ammonium and phosphate levels were analyzed, and struvite crystal formation (MAP) was determined using Scanning Electron Microscope (SEM) and X-ray diffraction (XRD). The results showed that the aeration reactor could form struvite crystals and transform the ammonium and phosphate content in the synthetic wastewater of complex fertilizers. The removal of ammonium with a molar ratio of $[Mg^{2+}] : [NH_4^+] : [PO_4^{3-}]$ 1:2:1 reached 61-77% at high aeration rates because much ammonia was released into the air. The phosphate removal reached 99%. The urease enzyme was proven to hydrolyze urea into ammonium, increase the pH value, and affect the shape of the resulting struvite crystals. The precipitate product obtained was struvite crystals, which SEM-EDX and XRD analysis confirmed.

1. INTRODUCTION

The complex fertilizer industry is an industry that produces various fertilizer products, including urea, ammonium sulfate, phosphate fertilizer, NPK, and others. In addition to producing fertilizers, the complex fertilizer industry generally produces non-fertilizer by-products such as sulfuric acid, phosphoric acid, and ammonia. However, the production of complex fertilizers produces wastewater which contributes to the pollution of water bodies because it contains high levels of phosphate and ammonium concentrations. This waste will pollute the environment if it is directly disposed of without processing (Ikhlas, 2017)

Complex fertilizer wastewater also contains high concentrations of organic nitrogen as indicated by high TKN (Total Kjeldahl Nitrogen). TKN is the sum of ammonium nitrogen and organic nitrogen. The organic nitrogen contained in the complex fertilizer waste is urea, so it is necessary to hydrolyze urea. Urea hydrolysis aims to

*Correspondence author.
E-mail : zulfikar@poltekatipdg.ac.id (Muhammad Zulfikar Luthfi)

doi : https://10.21771/jrtppi.2023.v14.no.2.p23-32

Accreditation number : (Ristekdikti) 158/E/KPT/2021

convert urea into ammonium. Urea hydrolysis is known to be carried out enzymatically using the enzyme urease from jack bean urease which works at a temperature of 25oC with a pH range of 4-9 (Fidaleo & Lavecchia, 2003). Enzymatic hydrolysis of urea occurs according to the following reaction:

$$H_2N\text{-}CO\text{-}NH_2 + 2\ H_2O \rightarrow NH_3 + NH_4^+ + HCO_3^- \quad (1)$$

This reaction produces carbamates which are unstable compounds and will decompose spontaneously into carbonic acid and ammonia. Ammonia production raises the pH during the reaction (Kabdasli et al., 2006). One method extensively studied for removing high concentrations of ammonium and phosphate from wastewater is the struvite precipitation method or Magnesium Ammonium Phosphate (MAP) (Yu et al., 2012). Struvite precipitation produces crystals with an orthorhombic structure formed from magnesium, ammonium, and phosphate in the same molar concentration.

Struvite is an ideal alternative fertilizer because it has the characteristics of an odorless, clean crystal that releases nutrients slowly to the soil and has low solubility, thus avoiding the eutrophication problems that may arise from other phosphorus fertilizers (Kataki et al., 2016). The most popular method of producing struvite from sewage is the chemical precipitation method by adding a magnesium salt and adjusting the pH to a base (Kruk et al., 2014). The reaction for the formation of struvite can be expressed in the following equation (Doyle & Parsons, 2002):

$$Mg^{2+} + NH_4^+ + PO_4^{3-} + 6\ H_2O \rightarrow MgNH_4PO_4.6H_2O \quad (2)$$

The formation of struvite crystals occurs in 3 states, namely unsaturated, metastable, and supersaturated (Ye et al., 2014). This struvite crystallization method has been widely used in various types of wastewater, such as urine wastewater (Aguado et al., 2019), (X. Liu et al., 2014), palm oil mill effluent (Ngatiman et al., 2021), swine wastewater (Cai et al., 2020), municipal sewage sludge (Zin et al., 2021), dairy wastewater (Numviyimana et al., 2020).

Several studies have shown that the struvite precipitation method can efficiently remove ammonium and phosphate from wastewater. Formation of struvite from wastewater with high ammonium and phosphate content can remove up to 90% phosphate content (Aguado et al., 2019; Chrispim et al., 2019; Xavier et al., 2014) and ammonium content up to more than 80% (Daegi Kim et al., 2017) and (Siciliano et al., 2013). Thus, complex fertilizer wastewater with high ammonium and phosphate content can be processed by forming struvite as a new product line of a slow-released fertilizer.

Recent studies have not studied how adding urease enzymes and aeration affects struvite formation from complex fertilizer wastewater. Therefore, this study aims to remove high ammonium and phosphate from complex fertilizer wastewater by forming struvite crystals. The effect of adding urease enzymes to wastewater and the presence of aeration must be done to determine the amount of struvite yield and the form of struvite obtained.

2. METHODS

This research consisted of preparing synthetic wastewater; reactor preparation; struvite precipitation operation; and the analysis stage of the residual wastewater content and the characteristics of the structural crystal deposits formed.

2.1. Preparation of Synthetic Wastewater

The wastewater used is a synthetic waste. The composition of the waste has a high level of ammonium. Ammonium chloride (NH_4Cl) was used as a source of ammonium. Monopotassium phosphate (KH_2PO_4) was used as a source of phosphate, and magnesium was added as a precipitate to form struvite (MAP). The stoichiometric $[Mg^{2+}]$: $[PO_4^{3-}]$ molar ratio to form struvite is 1:1. This wastewater also has a high content of organic nitrogen in the form of urea. This urea cannot form struvite, so it needs to be hydrolyzed to be converted into ammonium with the enzyme urease. KF was used as a source of fluoride.

In ammonium base wastewater, the ammonium contained is 7705 ppm, and there is no phosphate content. It shows that the molar ratio of $[NH_4^+]$:$[PO_4^{3-}]$ is 1:0, so adding wastewater from a phosphate base is necessary to achieve a more balanced molar ratio. Phosphate source from phosphate base wastewater contained 624 ppm ammonium and 2264 ppm phosphate.

The ammonium and phosphate base wastewater were mixed until the $[NH_4^+]$:$[PO_4^{3-}]$ did not differ much. Based on the calculation of the phosphate requirement to achieve the best $[NH_4^+]$:$[PO_4^{3-}]$ molar ratio, 0.1 L of ammonium-based wastewater and 3.9 L of phosphate-based wastewater are required to achieve a waste volume of 4 L.

The results of mixing ammonium-base wastewater and phosphate-based wastewater obtained ammonium and phosphate concentrations of 801.2 mg/L and 2207.4 mg/L with a molar ratio of $[NH_4^+]$:$[PO_4^{3-}]$ 2:1. The addition of the required amount of magnesium is adjusted to the molar ratio of PO_4^{3-} which is 1: 1. So the ratio of the molar ratio $[NH_4^+]$: $[Mg^{2+}]$: $[PO_4^{3-}]$ is 2: 1: 1.

The characteristics of the treated wastewater (mixed between ammonium- and phosphate-based wastewater) used in this study can be seen in Table 1.

2.2. Reactor Preparation

The struvite precipitation device uses a bulk reactor tube with a volume of 1 litre. Wastewater is introduced by adding magnesium according to the calculated molar ratio. The reactor was fitted with a pond pump to perform aeration instead of stirring to increase the pH. The pH value is measured periodically until the specified reaction time is complete.

The aeration rate is varied by adjusting it using a rotameter which functions as a flow meter. The pump's airflow is regulated using a valve to achieve the desired aeration rate. Perforated air stones with many holes are installed at the bottom of the reactor as aeration air holes. Increasing the pH using aeration will be faster using a lot of aerated air holes compared to fewer aerated air holes (Radev et al., 2015). The reactor struvite precipitation apparatus is shown in Figure 1.

2.3. Struvite Precipitation Operations

The experiment was initiated by adding synthetic waste into the reaction zone struvite reactor and magnesium with a predetermined molar ratio of Mg:P 1:1. Aeration is turned on to act as a mixer and pH regulator. The aeration rate was varied into 2 levels, 3.4 L/L/min and 16.6 L/L/min. The length of aeration was varied into 2 levels, 2 and 4 hours. The research was also carried out with the addition of the enzyme urease isolated from Jack bean peas. The addition of urease enzyme is expected to hydrolyze urea into ammonia. The addition of the enzyme was carried out in as much as 50 mL.

2.4. Analysis

The analysis carried out in this study included an analysis of the concentration of residual wastewater resulting from struvite precipitation and characterization of the morphology and crystallinity of the struvite precipitate formed. The analysis of residual wastewater includes the analysis of NH_4 content using the phenate method. PO4 analysis using the ascorbic acid method. F analysis with SPADNS method.

Morphological analysis of struvite deposits was carried out by Scanning Electron Microscopy (SEM) and struvite crystallinity by X-Ray Diffractometer (XRD).

Table 1. Characteristics of Mixed Wastewater

Parameters	Number	Unit
Phospate	801,2	mg/L
Ammonium	2207,4	Mg/L
Fluoride	147	mg/L
Urea	3083	mg/L

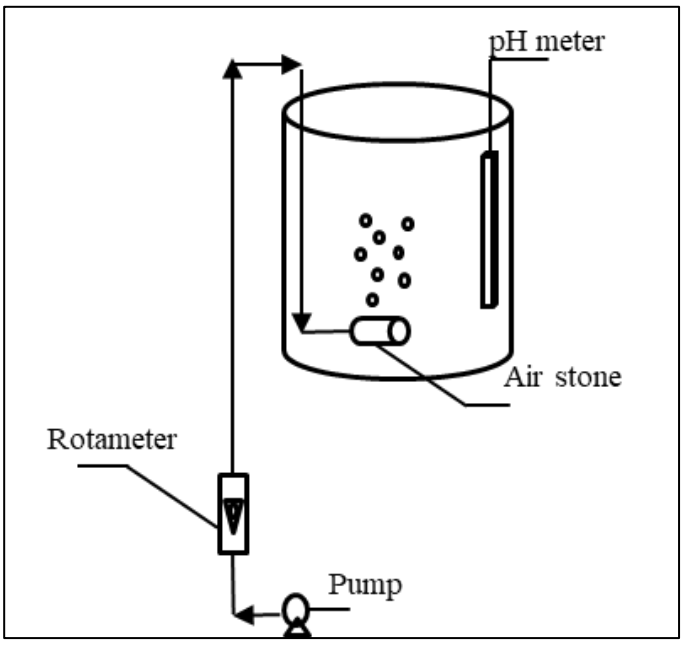

Figure 1. Reactor Struvite Precipitation

3. RESULT AND DISCUSSION

3.1. Struvite Crystals and Ammonium & Phosphate Removal

Aeration carried out in the experiment helped in the process of hydrolysis of the urease enzyme. It is also a substitute for stirring in the formation of struvite. The struvite crystal deposit formed after being observed differs based on the variations. Figure 2 shows the results of the observed struvite crystal deposition. The use of aeration with aeration for 2 hours resulted in lower struvite crystal deposits when compared to aeration for 4 hours. Aeration for 2 hours resulted in a maximum of 2.36 grams of struvite crystals, while aeration for 4 hours resulted in 2.72 grams of struvite crystals.

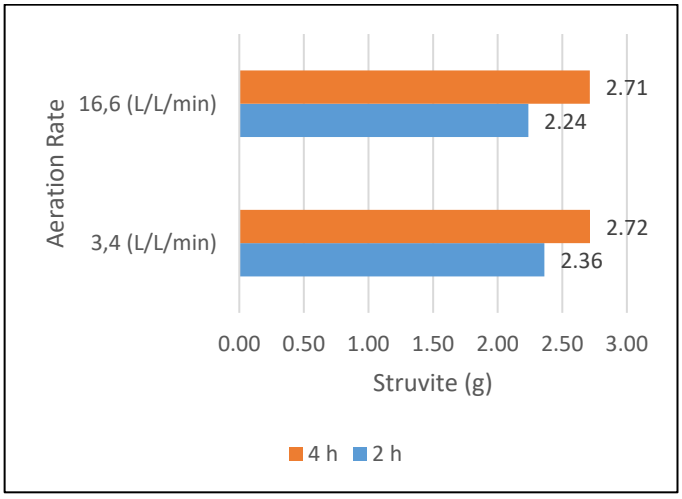

Figure 2. Aeration to Struvite Crystal Comparison

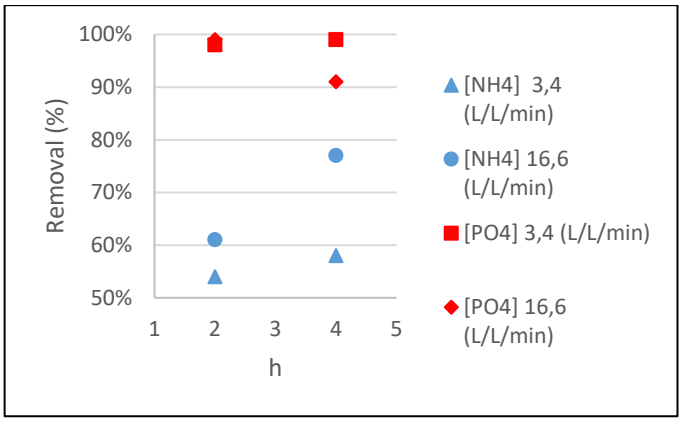

Figure 3. NH_4-N and PO_4-P Removal (%) on Aeration

The results of the struvite crystal precipitate formed are also different when compared based on the aeration rate used. At 2 hours of aeration using an aeration rate of 3.4 L/L/min, it produced a higher struvite deposit of 2.36 grams, while at an aeration rate of 16.6 L/L/min, it produced a lower struvite deposit of 2.24 grams. As for the aeration duration of 4 hours, the resulting struvite crystal deposition results were not significantly different. More prolonged aeration treatment has been shown to affect turbulence factors such as the stirring process.

The removal of ammonium (NH_4-N) and phosphate (PO_4-P) can be seen in Figure 3. Figure 3 shows the results of NH_4-N removal based on variations in aeration rate and aeration time. The use of aeration for 2 hours can remove different NH_4-N compared to 4 hours. NH_4-N removal for 2 hours ranged from 54-61%. The removal of NH_4-N for 4 hours reached 58-77%. The removal of NH_4-N with an aeration duration of 2 hours was lower than that of 4 hours.

When viewed from the variation of the aeration rate, the removal of NH_4-N also looks different. At an aeration rate of 3.4 L/L/min, NH_4-N removal for 2 hours can remove as much as 54%. While for 4 hours, it can remove as much as 58%. The difference looks overly significant. It differs from removing NH_4-N at an aeration rate of 16.6 L/L/min. Removing NH_4-N at an aeration rate of 16.6 L/L/min for 2 hours can remove NH_4-N as much as 61% and 77% for 4 hours. The result of NH_4-N removal at an aeration rate of 3.4 L/L/min was lower than the aeration rate of 16.6 L/L/min.

Figure 3 shows the results of PO_4-P removal based on variations in aeration rate and aeration time. The use of aeration for 2 hours can eliminate 99% of PO_4-P. The removal of PO_4-P with an aeration duration of 4 hours was 91-99%. The PO_4-P allowance was not significantly different. It is influenced by the amount of Mg:PO_4-P 1:1 molar ratio, so the amount of removal produced is high.

When viewed from the variation of the aeration rate used, the resulting PO_4-P removal did not show any difference. At an aeration rate of 3.4 L/L/min, 99% can be removed with an aeration period of 2 hours, as 99% removal

can be achieved with an aeration period of 4 hours. As for the aeration rate of 16.6 L/L/min, 99% of PO_4-P can be removed within 2 hours and 91% with 4 hours of aeration. In the removal results with an aeration period of 4 hours and an aeration rate of 16.6 L/L/min, there may be an error in the measurement so that it is only 91% compared to an aeration rate of 3.4 L/L/min.

The amount of PO_4-P removal in the aeration process completely formed struvite crystal deposits. The lower molar content of PO_4-P, compared to NH_4-N molars, makes the amount of PO_4-P removal high because almost all of the PO_4-P becomes struvite crystal deposits.

3.2. SEM and XRD Results

Identification of struvite was carried out by Scanning Electron Microscope (SEM) test to determine the morphological characteristics and crystal structure. Energy dispersive Xray Spectroscopy (EDX) was performed to determine the chemical components contained in the crystals. X-ray Diffraction (XRD) to identify the crystal phase. SEM analysis was performed at 1000x and 2000x magnification.

There were 3 samples analyzed; the first one was the ratio of $[Mg^{2+}]$: $[NH_4^+]$: $[PO_4^{3-}]$ 1:2:1 with 3,4 L/L/min aeration for 2 hours. This sample has a high amount of precipitation. The second sample was a sample with a ratio of $[Mg^{2+}]$: $[NH_4^+]$: $[PO_4^{3-}]$ 1:2:1 with 16.6 L/L/min aerations for 2 hours. This sample has the highest residual ammonium content. Then the third sample was a sample with a ratio of $[Mg^{2+}]$: $[NH_4^+]$: $[PO_4^{3-}]$ 1:2:1, which was aerated for 4 hours with 3.4 L/L/min and added enzymes. The results of the SEM-EDX analysis are shown in Figure 4. The results of the EDX microanalysis are shown in Figures 5 and 6.

Figure 4 (a) shows the SEM results of the sample ratio $[Mg^{2+}]$: $[NH_4^+]$: $[PO_4^{3-}]$ 1:2:1 with aeration 16,6 L/L/min for 2 hours. The results show the shape of struvite crystals that are long and tapered. The surface of the crystal also looks not rough because of the absence of impurity minerals that allow them to stick to the crystal.

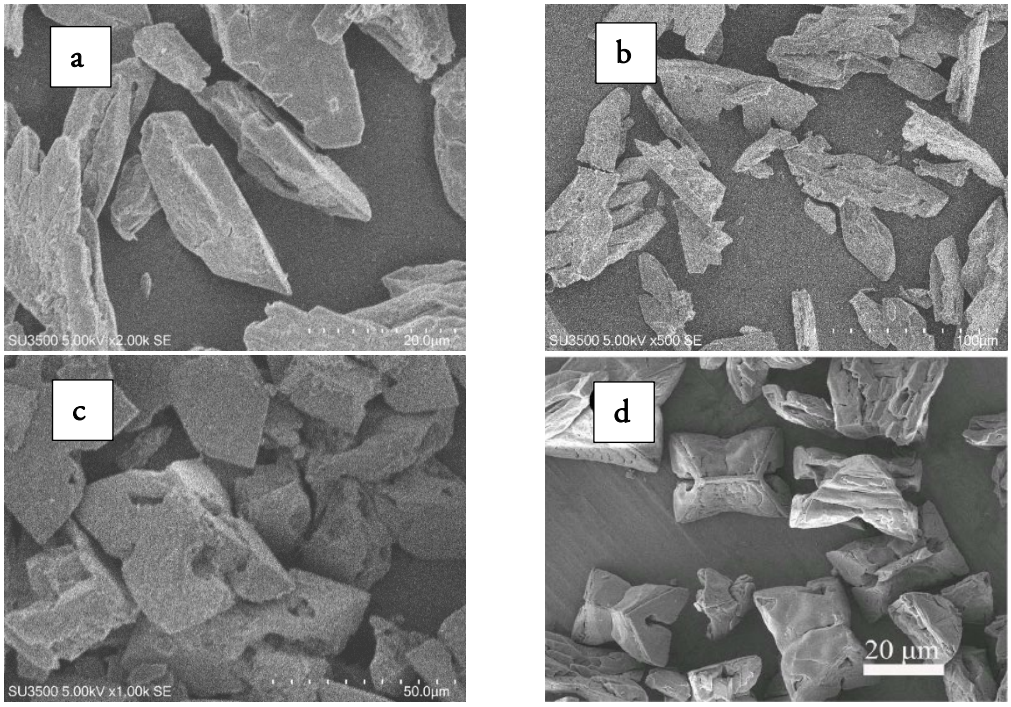

Figure 4. (a) Aeration 16,6 L/L/min for 2 hours, (b) Aeration 3,4 L/L/min for 2 hours, (c) Addition of Enzymes, (d) Biogenic Struvite Sample (Li & Zhou, 2015)

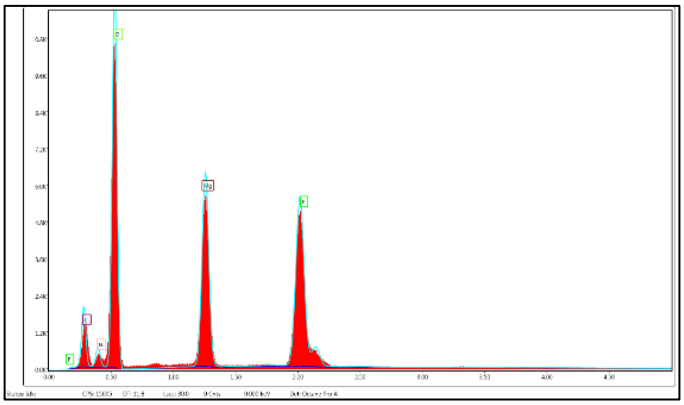

Figure 5. Microanalysis EDX $[Mg^{2+}]$: $[NH_4^+]$: $[PO_4^{3-}]$ 1:2:1

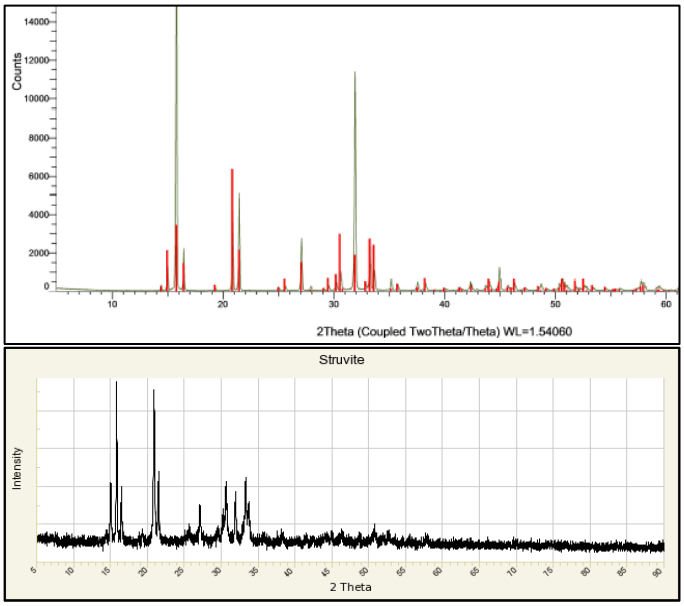

Figure 6. XRD Sample Ratio $[Mg^{2+}]$: $[NH_4^+]$: $[PO_4^{3-}]$ 1:2:1 with aeration 16,6 L/L/min for 2 hours and XRD struvite (RRUFF, 2019)

Table 2. The Chemical Component of Struvite Crystals in The Sample with The Ratio $[Mg^{2+}]$: $[NH_4^+]$: $[PO_4^{3-}]$ 1:2:1

Element	Weight %	Atomic %
C K	18.64	25.45
N K	5.81	6.8
O K	52.37	53.67
Mg K	12.53	8.45
P K	10.65	5.64

Figure 4 (b) shows the SEM results of the sample ratio $[Mg^{2+}]$: $[NH_4^+]$: $[PO_4^{3-}]$ 1:2:1 with aeration 3,4 L/L/min for 2 hours. The crystal results showed that the crystals were long and tapered, similar to those in Figure 4b. The surface of the crystal also looks not rough because of the absence of mineral impurities.

The morphology of struvite crystals can be identified based on the growth process of struvite, and their shape can vary (prism type, pyramid type, coffin-like type, needle, or feather-like type) (B. Liu et al., 2013). Pure struvite crystals with equimolar ratios will form a pointed white orthorhombic crystal structure (Daekeun Kim et al., 2009).

Different things are shown in Figure 4 (c), namely the sample with the addition of enzyme and the ratio of $[Mg^{2+}]$: $[NH_4^+]$: $[PO_4^{3-}]$ 1:2:1 with aeration of 3.4 L/L/min 4 hours. Crystals look more stacked and tapered. The different crystal forms in this sample were caused by adding enzymes to hydrolyze organic nitrogen. Recent studies have shown that the protein selectively binds to the surface of struvite crystals and produces an arrow-shaped morphology, which then evolves into an unusual X-shaped tabular structure as struvite formation progresses. It is the morphological structure of biogenic struvite (Li & Zhou, 2015). Figure 4 (d) is a picture of the morphological structure of biogenic struvite. Even so, the crystal surface on the sample looks not rough because there are no impurity minerals.

Figure 5 shows the results of EDX microanalysis of the sample ratio $[Mg^{2+}]$: $[NH_4^+]$: $[PO_4^{3-}]$ 1:2:1, and Table 2 shows the chemical components contained in struvite crystals. EDX microanalysis confirmed that the struvite formed consisted of struvite-forming compounds, namely Mg, N, and P. The percentage of chemical components and each component's mass are shown in the table. Figure 5 shows that the components that form the crystals of struvite are magnesium and phosphate, which are dominant in the absence of impurity ions.

XRD analysis required the degree of crystallinity of struvite precipitates. The XRD analysis test can be seen in Figure 6. The results of the test show that the precipitate

formed is struvite crystals when viewed from the peak point that is formed following the peak line in the literature of struvite XRD results. Although the peak line shown is higher than in the literature (RRUFF, 2019), the position of the peak line formed lies at the same theta degree.

3.3. Overall Discussion

The struvite formed from the molar ratio [Mg^{2+}] : [NH_4^+] : [PO_4^{3-}] can be predicted by modelling using the Visual Minteq 3.1 application. Visual Minteq 3.1 software can display the prediction of the amount of component concentration that is deposited at a pH value of 8.5 which is used in this study. Table 3 shows the deposited components based on the Visual Minteq 3.1 software.

Based on Table 3, the pH value data used to predict the precipitated component in Visual Minteq 3.1 Software is pH 8.5. The precipitated magnesium content reaches 98%, while the dissolved reaches 1.99%. The precipitated phosphate content reached 97.96%, while the dissolved reached 2.05%. The ammonium content, which has an excess molar ratio compared to magnesium and phosphate, impacts the amount of concentration being deposited which is lower than that of magnesium and phosphate. The deposited ammonium content is 51.27%, and the remaining 48.73% is still dissolved.

Visual Minteq 3.1 software has predicted the concentration and percentage of components that can be formed based on variations in the molar ratio [Mg^{2+}] : [NH_4^+] : [PO_4^{3-}] 1:2:1. Prediction results using visual minteq 3.1 software showed that the amount of ammonium remaining was lower than the results of the research conducted.

The results showed that the ammonium concentration removed was 54% and 61%, respectively. These results indicate that the ammonium content removed is higher than the predicted results with visual minteq 3.1 software. The results of ammonium removal that occurred in the results showed that ammonium was not only precipitated into struvite crystals but some were released into the air. A nitrogen mass balance then carries this out to determine how much ammonia is released into the air. Figure 7 shows the mass balance of nitrogen flow.

Different aeration rates affect the removal of ammonia. In Figure 7, the aeration rate of 16.6 L/L/min can release the amount of ammonia into the air up to 12.26 mmol/L. It was higher than the aeration rate of 3.4 L/L/min, which caused 7.82 mmol/L ammonia to be released into the air. The ammonium content in struvite is also different. The aeration rate of 16.6 L/L/min contains ammonium in the form of struvite up to 18.3 mmol/L, while the aeration rate of 3.4 L/L/min reaches 19.5 mmol/L.

The amount of ammonium concentration at the starting point, end point, and struvite precipitated crystals is the result of the measurements that have been made. The amount of ammonium concentration released into the air results from calculating the difference between the initial, final, and ammonium concentrations precipitated into struvite crystals. The amount of TKN, ammonium, and organic nitrogen, has decreased due to ammonium being reduced to struvite and released into the air.

Table 3. Precipitated components based on Visual Minteq 3.1 Software

Component	Total Dissolved (mol/L)	% Dissolved	Total Precipitated (mol/L)	% Precipitated
Mg^{2+}	4,62E-04	1,99	2,28E-02	98,01
NH_4^+	2,16E-03	48,73	2,28E-02	51,27
PO_4^{3-}	4,75E-04	2,05	2,28E-02	97,96

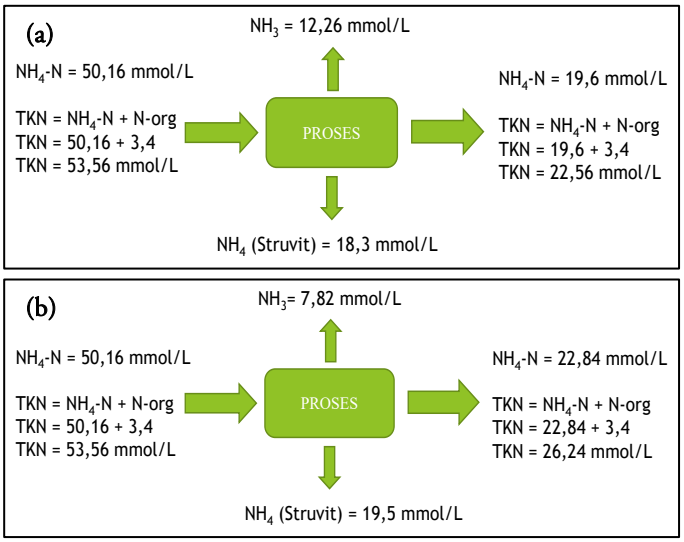

Figure 7. Total Nitrogen Balance, (a) Aeration Rate 16,6 L/L/min; (b) Aeration Rate 3,4 L/L/min

The result of enzymatic urea hydrolysis that produces ammonium has an impact on increasing the ammonium concentration to phosphate molar ratio. The increasing concentration of ammonium molar ratio did not impact increasing ammonium removal results. However, the ammonium removal efficiency will decrease further when the molar ratio of ammonium is higher than the molar ratio of phosphate and magnesium (Ikhlas & Warmadewanthi, 2017).

4. CONCLUSION

The results of this study and discussion indicate that a high aeration rate with an aeration period of 4 hours can remove up to 77% more ammonium concentration as a result of ammonia released into the air. It suggests that struvite precipitation with a higher molar ratio of ammonium than magnesium and phosphate using aeration as a mixing device is not favourable because it leads to air pollution (bad odor, etc). It differs from the prediction results using visual minteq 3.1 software which does not predict the effect of aeration. At the same time, the phosphate removal reached 99% formed into struvite. The results of SEM-EDX and XRD confirmed that the precipitate formed was struvite crystals. The addition of enzymes seemed to affect the morphology of the structures formed. It also differed from those of struvite crystals without the addition of enzymes.

ACKNOWLEDGMENT

The author is very grateful to the Bandung Institute of Technology, which has assisted in this research through facilities and funding.

REFERENCE

Aguado, D., Barat, R., Bouzas, A., Seco, A., & Ferrer, J. (2019). P-recovery in a pilot-scale struvite crystallization reactor for source separated urine systems using seawater and magnesium chloride as magnesium sources. Science of the Total Environment, 672, 88–96. https://doi.org/10.1016/j.scitotenv.2019.03.485

Cai, J., Ye, Z. L., Ye, C., Ye, X., & Chen, S. (2020). Struvite crystallization induced the discrepant transports of antibiotics and antibiotic resistance genes in phosphorus recovery from swine wastewater. Environmental Pollution, 266, 115361. https://doi.org/10.1016/j.envpol.2020.115361

Chrispim, M. C., Scholz, M., & Nolasco, M. A. (2019). Phosphorus recovery from municipal wastewater treatment: Critical review of challenges and opportunities for developing countries. Journal of Environmental Management, 248(July), 109268. https://doi.org/10.1016/j.jenvman.2019.109268

Doyle, J. D., & Parsons, S. A. (2002). Struvite formation, control and recovery. Water Research, 36(16), 3925–3940. https://doi.org/10.1016/S0043-1354(02)00126-4

Fidaleo, M., & Lavecchia, R. (2003). Kinetic study of enzymatic urea hydrolysis in the pH range 4-9. Chemical and Biochemical Engineering Quarterly, 17(4), 311–319.

Ikhlas, N. (2017). Pengaruh pH, Rasio Molar, Jenis Presipitan, dan Ion Pengganggu Dalam Recovery Amonium dan Fosfat Pada Limbah Cair PT Petrokimia Gresik dengan Metode Presipitasi Struvite, 134. Retrieved from http://repository.its.ac.id/2154/

Ikhlas, N., & Warmadewanthi. (2017). Removal of ammonium and phosphate from fertilizer industry wastewater using struvite precipitation method. Journal of Environmental and Biological Sciences, 7(2), 158–162.

Kabdasli, I., Tunay, O., Islek, C., Erdinc, E., Huskalar, S., Tatli, M. B., & Faculty, C. E. (2006). Nitrogen recovery by urea hydrolysis and struvite precipitation from anthropogenic urine. Journal of Water Science and Technology, 53, 305–312. https://doi.org/10.2166/wst.2006.433

Kataki, S., West, H., Clarke, M., & Baruah, D. C. (2016). Phosphorus recovery as struvite from farm, municipal and industrial waste: Feedstock suitability, methods and pre-treatments. Journal

of Waste Management. https://doi.org/10.1016/j.wasman.2016.01.003

Kim, Daegi, Min, K. J., Lee, K., Yu, M. S., & Park, K. Y. (2017). Effects of pH, molar ratios and pre-treatment on phosphorus recovery through struvite crystallization from effluent of anaerobically digested swine wastewater. Environmental Engineering Research, 22(1), 12–18. https://doi.org/10.4491/eer.2016.037

Kim, Daekeun, Kim, J., Ryu, H., & Lee, S. (2009). Bioresource Technology Effect of mixing on spontaneous struvite precipitation from semiconductor wastewater. Journal of Bioresource Technology, 100, 74–78. https://doi.org/10.1016/j.biortech.2008.05.024

Kruk, D. J., Elektorowicz, M., & Oleszkiewicz, J. A. (2014). Chemosphere Struvite precipitation and phosphorus removal using magnesium sacrificial anode. Journal of Chemosphere, 101, 28–33. https://doi.org/10.1016/j.chemosphere.2013.12.036

Li, H., & Zhou, G. (2015). Biomimetic synthesis of struvite with biogenic morphology and implication for pathological biomineralization. Journal of Nature. https://doi.org/10.1038/srep07718

Liu, B., Giannis, A., Zhang, J., Chang, V. W., & Wang, J. (2013). Characterization of induced struvite formation from source-separated urine using seawater and brine as magnesium sources. Journal of Chemosphere, 93(11), 2738–2747. https://doi.org/10.1016/j.chemosphere.2013.09.025

Liu, X., Hu, Z., Mu, J., Zang, H., & Liu, L. (2014). Phosphorus recovery from urine with different magnesium resources in an air-agitated reactor. Environmental Technology (United Kingdom), 35(22), 2781–2787. https://doi.org/10.1080/09593330.2014.921732

Ngatiman, M., Jami, M. S., Abu Bakar, M. R., Subramaniam, V., & Loh, S. K. (2021). Investigation of struvite crystals formed in palm oil mill effluent anaerobic digester. Journal of Heliyon.

Numviyimana, C., Warchoł, J., Izydorczyk, G., Baśladyńska, S., & Chojnacka, K. (2020). Struvite production from dairy processing wastewater: Optimizing reaction conditions and effects of foreign ions through multi-response experimental models. Journal of the Taiwan Institute of Chemical Engineers, 117, 182–189. https://doi.org/10.1016/j.jtice.2020.11.031

Radev, D., Peeva, G., & Nenov, V. (2015). pH Control during the Struvite Precipitation Process of Wastewaters. Journal of Water Resource and Protection, 07(16), 1399–1408. https://doi.org/10.4236/jwarp.2015.716113

RRUFF. (2019). Struvite R050511-RRUFF database.

Siciliano, A., Ruggiero, C., & De Rosa, S. (2013). A new integrated treatment for the reduction of organic and nitrogen loads in methanogenic landfill leachates. Process Safety and Environmental Protection, 91(4), 311–320. https://doi.org/10.1016/j.psep.2012.06.008

Xavier, L. D., Cammarota, M. C., Yokoyama, L., & Volschan, I. (2014). Study of the recovery of phosphorus from struvite precipitation in supernatant line from anaerobic digesters of sludge. Water Science and Technology, 69(7), 1546–1551. https://doi.org/10.2166/wst.2014.033

Ye, Z., Shen, Y., Ye, X., Zhang, Z., Chen, S., & Shi, J. (2014). Phosphorus recovery from wastewater by struvite crystallization : Property of aggregates. Journal of Environmental Sciences, 26(5), 991–1000. https://doi.org/10.1016/S1001-0742(13)60536-7

Yu, R., Geng, J., Ren, H., Wang, Y., & Xu, K. (2012). Combination of struvite pyrolysate recycling with mixed-base technology for removing ammonium from fertilizer wastewater. Bioresource

Technology, 124, 292–298. https://doi.org/10.1016/j.biortech.2012.08.015

Zin, M. M. T., Tiwari, D., & Kim, D. J. (2021). Recovery of ammonium and phosphate as struvite via integrated hydrolysis and incineration of sewage sludge. Journal of Water Process Engineering, 39(September). https://doi.org/10.1016/j.jwpe.2020.101697

Vol. 14 No. 2 (2023) 33-44

Jurnal Riset
Teknologi Pencegahan Pencemaran Industri

Journal homepage : https://www.jrtppi.id

Kementerian Perindustrian
REPUBLIK INDONESIA

Application of Green Retrofitting Ready Mix Concrete Plant in Indonesia to Increase Financial Benefits and Reduce Environmental Issues: A Case Study

Mohammad Kholis Ardiansyah[1], Albert Eddy Husin[1*], Mawardi Amin[1]

[1] Department of Civil Engineering, Faculty of Engineering, Universitas Mercu Buana, Jakarta 11650 , Indonesia.

ARTICLE INFO

Article history:
Received November 10, 2022
Received in revised form February 07, 2023
Accepted February 09, 2023
Available online May 02, 2023

Keywords :
FAST
Green Retrofitting
Life Cycle Cost Analysis
Ready-Mix Concrete
Value Engineering

ABSTRACT

Currently, the Indonesian government continues to encourage the realization of sustainable development. The green concept is a sustainable development trend in the construction material industry. The concrete industry plays a vital role as a supplier of concrete materials in construction, so its availability is essential. The role of concrete industry itself has a negative impact on the environment. Stakeholders increase the cost of green retrofitting so that the industry or building becomes eco-friendly. The research method was carried out using a process case study, namely, how to implement green retrofitting cost performance in the concrete industry using Value Engineering and Life Cycle Cost Analysis. Theoretically, the research results provide additional knowledge for academics; practitioners can provide problem-solving to get an overview of the implementation of the green concept in the industry regarding the flow of implementation and the benefits of savings in an environmentally friendly production process. The application of value engineering in the green retrofitting of the concrete industry has increased the cost performance of green retrofitting by 8.66% with a return of 3 years and 8 months and increased the functions and benefits of an eco-friendly and sustainable concrete industry.

1. INTRODUCTION

Today, the most important environmental problem is climate change. It is also one of the biggest problems in the whole world (Doan, Wall, Hoseini, Ghaffarianhoseini, & Naismith, 2021). According to the Environmental Performance Index (EPI) in 2022, Indonesia's ranking dropped to 164th from the previous year, 116, with an EPI Score of 28.20 out of 77.90. This rank proves that public awareness of the environment in all sectors needs to be increased. The Sustainable Development Agenda (SDGs) in 2030 declares a development shift towards sustainable development based on equality and human rights to promote social, economic, and environmental growth. Opportunities in achieving the United Nations' sustainable development goals are created by green building development (SDGs). However, instead of renovating the old structures, they create new constructions for green buildings (Hong, Ibrahim, & Loo, 2019). Green development is a crucial method to achieve sustainable development. Among the 17 SDGs, several indicators are closely related to the development of green industries, including clean water and sanitation, affordable and clean Energy, Industrial Innovation and Infrastructure, and Responsible Consumption no Production (Yuan et al., 2020).

The supply chain in the construction sector is a coordinated structure consisting of parties that contribute (directly or indirectly) to the project's overall success in producing construction products. In the world, the concrete

*Correspondence author.
E-mail : albert_eddy@mercubuana.ac.id (Albert Eddy Husin)

doi : https://10.21771/jrtppi.2023.v14.no.2.p33-44

Accreditation number : (Ristekdikti) 158/E/KPT/2021

industry or batching plant plays a vital role in the economy and development of a country because concrete is an essential material for infrastructure development (Favier, De Wolf, Scrivener, & Habert, 2018).

In Indonesia, the concrete industry and the need for concrete materials are predicted to increase according to the 2020-2024 National Medium-Term Development Plan (RPJMN). According to the Public Works and Housing Ministry, the estimation for construction materials needs, especially concrete, in the 2020-2024 fiscal year is predicted to increase by 8%. Environmental degradation, global warming, social inequality, and a shortage of natural resources are some unintended consequences of progress. The concrete industry negatively impacts the environment during its construction and production process. These impacts include waste, air dust, noise, and the excessive use of natural resources, especially water and energy. In the composition of perm3 concrete products, a material ratio of 7-15% water is required, cement 15-20%, fine aggregate 25-30%, and coarse aggregate 30-50%. The environmental impact of concrete manufacturing can be lowered by reducing the use of raw materials, reducing energy consumption, and following Best Management Practices (BMP) related to ready-mix concrete production (Kashwani, Sajwani, Ashram, & Yaaqoubi, 2014).

One proposed solution is establishing a "green" concept for industrial development that prioritizes environmental factors in its manufacturing process and operations (Susanti et al., 2017). Applying the green concept in the concrete industry in Indonesia still needs to be improved. In addition, the parameters for obtaining green concrete industry certification from related regulations still need to be added. Meanwhile, Europe and other developed countries have applied the green concrete industry concept by adopting the green Concrete Sustainability Council (CSC) concept. CSC promotes and demonstrates the concrete industry and eco-friendly products to generate the correct decisions in construction. CSC certification system in the concrete industry is applicable globally (Concrete Sustainability Council).

Some of the problems identified from the application of the concept include high green investment costs compared to conventional buildings, lack of green concepts understanding, lack of eco-friendly products on the market, and lack of financial and non-financial support from the government (Pahnael, Soekiman, & Wimala, 2020). The problems of implementing the green concept include applying energy-saving systems, lighting, conservation, and water recycling. These cause an increase in green construction costs (retrofitting costs) by 10.77% (Kim et al., 2014).

Increased costs in green projects can be handled by reducing the investment costs of waste materials. Value Engineering (VE) has vital benefits for the civil engineering construction industry, significantly saving costs and increasing project benefits. Value Engineering (VE) is a systematic review of a project, product, or process by an independent multi-disciplinary specialist team to improve performance, quality, and life-cycle costs (Berawi, 2004, as cited in Husin, 2019). VE allows the civil engineering construction industry to save costs and increase project benefits. Life Cycle Cost Analysis (LCC) in VE is value-based and helpful in determining alternatives with the lowest cost and maximum feasibility (Husin, 2015).

The effect of Value Engineering and Life Cycle Cost Analysis on the improvement of green retrofitting cost performance in the concrete industry can be examined through the correlation between the concrete industry object factors and the concept of green retrofitting. The research purposes were to determine the correlation among the most influential factors on the improvement of green retrofitting cost performance based on Value Engineering and Life Cycle Cost Analysis in the industry and provide a flow of application of the green retrofitting concept in the concrete industry to facilitate implementation so that the Indonesian concrete industry is eco-friendly and sustainable. The research results can provide additional knowledge for academics, and practitioners can provide problem-solving to get an overview of implementing the green concept in the industry.

2. METHODS

The research location was one of Indonesia's largest Indonesian concrete industries - PT. XYZ. The research was held from April to June 2022. A case study on implementing the green retrofitting concept in the concrete industry was conducted based on primary, secondary, observation, literature review, and analysis data. Showed that just half of the systematic reviews had flowcharts. For the reader to grasp the whole research review process, researchers must provide a flow chart. (Vu-ngoc et al. 2018). The concept of case study research can be seen in Figure 1.

2.1. Green Retrofit Concept in Ready-mix Concrete Industry

The green concept is the process of building a structure based on the environment and efficient resources throughout the life cycle of the building, from design, construction, operation, maintenance, renovation, and deconstruction (Ebrahim & Wayal, 2020). Concrete Sustainable Council (2022) stated that ready-mix concrete values the environment, and obtaining a Concrete Sustainable Council certificate as green in developed European countries continues. 485 Concrete industries obtained Green certification in 2021 (Concrete Sustainability Council, 2022).

Identifying and applying green concepts in the concrete industry provide a platform to address interrelated global problems through cross-sectoral methods and initiatives. It also benefits the industry participants (Susanti et asl., 2017). This rating system is a method to evaluate the quality of eco-friendly green buildings. There are categories, criteria, and benchmarks in GREENSHIP with particular points (Rahmawati, Wisnumurti, & Nugroho, 2018). CSC assessment parameters can be seen in Figure 2.

Credit criteria parameters set by CSC include Management-(M) (33 points), Environment-(E) (73 points), Social-(S) (48 points) and Economy-(B) (25 Points).

Data is obtained from the field from observations, interviews of the Green expert team and the head of the local batching plant, collecting data, visits, and self-assessment inspections. Together are then processed referring to the intended Standard rating, namely using concrete sustainable council V.2.1 parameters, then the second step is to conduct an assessment with a team of Quality Enviro Management System (QEMS), 6 experts invited to the discussion; they are 2 experts in the field of green building, 2 experts in value engineering and 1 expert in QEMS and 1 expert in industrial batching plants, experts to get the actual points obtained, from these results, the third step is then carried out to carry out an Improvement and innovation plan to get the intended rating target, namely Gold with a minimum Gold rating with a minimum point of 65% of the total standard parameter value and Pre-requisites that must be met. The highest increase in point parameters is in the environmental aspect, where the results obtained by self-assessment are 13.5 points from 73 standard points.

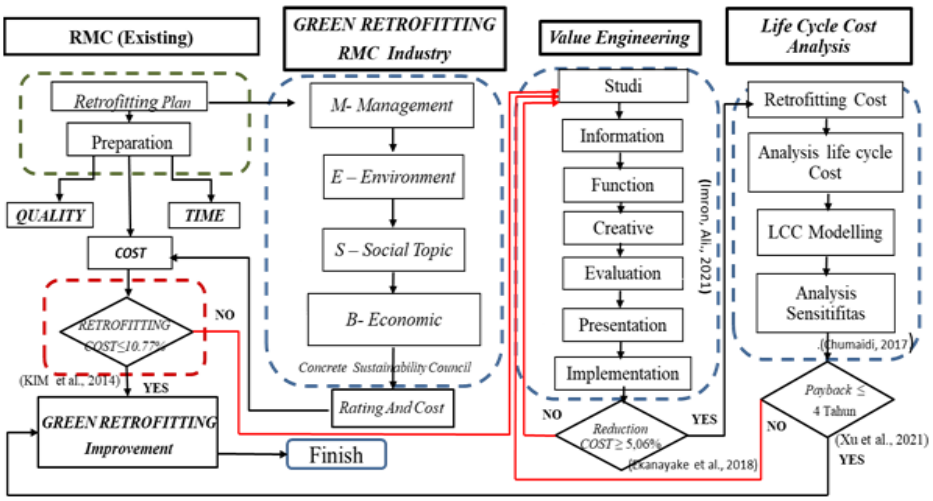

Figure 1. Flowchart of Application of the Green Retrofitting Concept with VE in the Concrete Industry to Improve Retrofitting Cost Performance

Figure 2. Rating Green RMC (Source: Concrete Sustainability Council, 2022)

2.2. Value engineering and Life Cycle Cost Analysis

In general, value engineering is a creatively organized method that aims to maximize the cost and performance of a facility or system. Over-cost checking methods are avoided so that required functions and the most affordable prices are discovered without compromising the required quality (Baghdady, 2018). The VE work plan was conducted as part of the project development. This study estimates that the creativity phase will generate original suggestions for possible projects (Berawi et al., 2015). According to Eng Karim Ragab in Planning and Project Controls Engineer SAVE International, the stages of planning Value Engineering activities include:

a. 1) Information stage, 2) function analysis stage, 3) creativity and innovation stage, 4) development stage, 5) decision analysis stage, 6) decision-making stage, 7) implementation stage, 8) recommendation stage, and 9) result (Husin, Karolina, Rahmawati, & Abdillah, 2022).
b. Functional Analysis System (FAST) Engineering Diagrams were used in Value Engineering to generate creative concepts that can be incorporated into projects (Berawi et al., 2015; Imron & Husin, 2022).

LCCA was especially useful when the project alternatives that met the performance requirements were similar, but the initial and operating costs differed. This situation requires comparison in choosing the one that maximizes cost savings (Fuller, 2006). The LCCA analytical approach assists in the discovery of the most economical option that fulfills the project objectives and contributes essential data to the overall decision-making process (Hatami & Morcous, 2016). The general steps for calculating LCC analysis were as follows:

a. Cost Breakdown Structure (CBS) – LCC Modeling without residual value -Life-cycle Cost Analysis – Sensitivity Analysis – Efficiency (Study, Correia, Samani, & Gregory, 2018).
b. Green buildings were prioritized throughout the project life cycle. It includes manufacturing materials, planning, design, construction, operation, maintenance and removal, and waste recycling (Liu, 2015).

3. RESULT AND DISCUSSION

The green industry prioritizes effectiveness and efficiency in the sustainable use of resources during production. This idea benefits society because it balances industrial development with the maintenance of environmental functions.

The independent observation and self-assessment results were a Gold rating of 127.3 (71.1%), with a planned increase in green retrofitting costs of 11.06%. The recapitulation of the self-assessment can be seen in Table 1 below:

An example of calculating points in an independent assessment is as follows:

The results obtained from the Assessment and Conformity Planning by the team are focused on Environmental Aspects and Energy and Water Efficiency parameters because they have significant points and see the need to be done innovation. The formation of an engineering team or VE team is needed to analyze the impact of the Cost increase in costs from the retrofitting plan. The data is processed and carried out studies and information to obtain the retrofitting Cost Value, namely BOQ, and make a Paretto diagram to obtain focus savings, then perform Function Analysis with FAST diagrams before and after implementation.

Table 1. Self-Assessment Recapitulation

Self-Assessment Recapitulation – CSC					
Code	Parameter	unit	Criteria CSC Standard	Assessment	Retrofitting Recognition
M	Management	Points	33	26.3	27.8
E	Environment	Points	73	13.5	41.5
S	Social	Points	48	42	42
B	Economy	Points	25	17	17
Total		Points	179	97.8	127.3
Total value		179	97.8		127.3
Percentage (min 65%)		100%	54.6%		71.1%

Table 2. Example Assessment for Item E- Environment

E- Environment					
Code	Parameter	unit	Criteria CSC Standard	Assessment	Retrofitting Recognition
E1	Life Cycle Impact	Points	6	0	0
E2	Land use	Points	5	3	5
E3	Energy & Climate	Points	22	1	12
E4	Air Quality	Points	7	2	5
E5	Water	Points	13	3	8.5
E6	Biodiversity	Points	0	0	0
E7	Secondary Materials	Points	15	2	8
E8	Transport	Points	5	2.5	3
E9	Secondary Fuels	Points	0	0	0
Total		Points	73	13.5	41.5
Percentage (min 65%)			100%	18%	57%

Bill of Quantity (BOQ) for retrofitting planning, then conducted Pareto Analysis to focus work and obtain cost performance efficiency. 80% of the total green retrofitting costs in the Pareto diagram is a budget focused on efficiency using value engineering. 83.9% at the initiation of the solar PV installation is the highest value, WWT utilization is 13.3%, Green assessment cost is 1.6%, and procurement of cover loading point is 1.2%.

The Pareto diagram in question can be seen in Figure 3

The FAST diagram existing Process and before the application of the eco-friendly concept and the VE process in the concrete industry is shown in Figure 4.

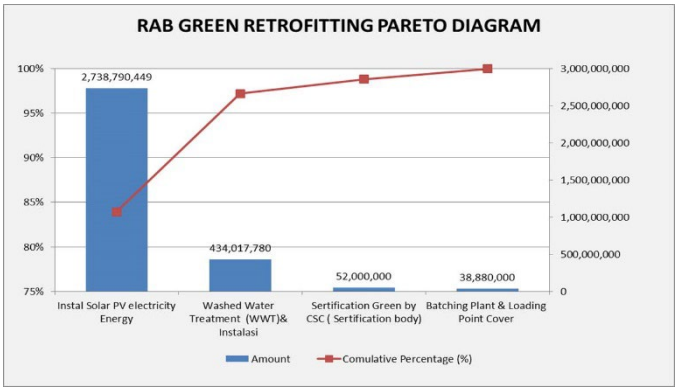

Figure 3. Pareto Diagram Information Stage

The FAST diagram existing before the retrofitting plan process is the actual condition of the concrete industry carried out the analysis. It can be seen that there needs to be an output of results with the aim of an environmentally

friendly concrete industry. The "how-why" logic model was applied to discover, categorize, develop, and choose functions that can improve project development (Berawi et al., 2015; Imron & Husin, 2022). According to the retrofitting plan focused on Energy and Water Efficiency, Additional Functions can be seen in Table 3.

All concepts for VE were refined during the evaluation stage. The material selection idea of the green concept was summarized and calculated to fulfill the objectives of Value Engineering (Imron & Husin, 2022). Each Bill of Quantity (BOQ) element was chosen without exception, and each element should show an eco-friendly function.

. Value = Function / Cost, first proposed by Miles in 1961, was later revised to Function / Resources. Even yet, because it combines quantifiable (such as cost) and immeasurable (such as function) notions, its adaption needs to be revised (Woodhead & Berawi, 2022).

The development stage aims to improve the function standard of the research topic, arrange final recommendations and implementation plans, and review technical and financial aspects for developing the chosen alternative (Bahri et al., 2018). The preparatory steps for an overall thought or opinion investigation into the initial design (PV) are developing a description of the solution, assessing the life cycle costs of the original design, and providing the proposed new design. It is the steps of the development stage (Asrul & Ozanya, 2017).

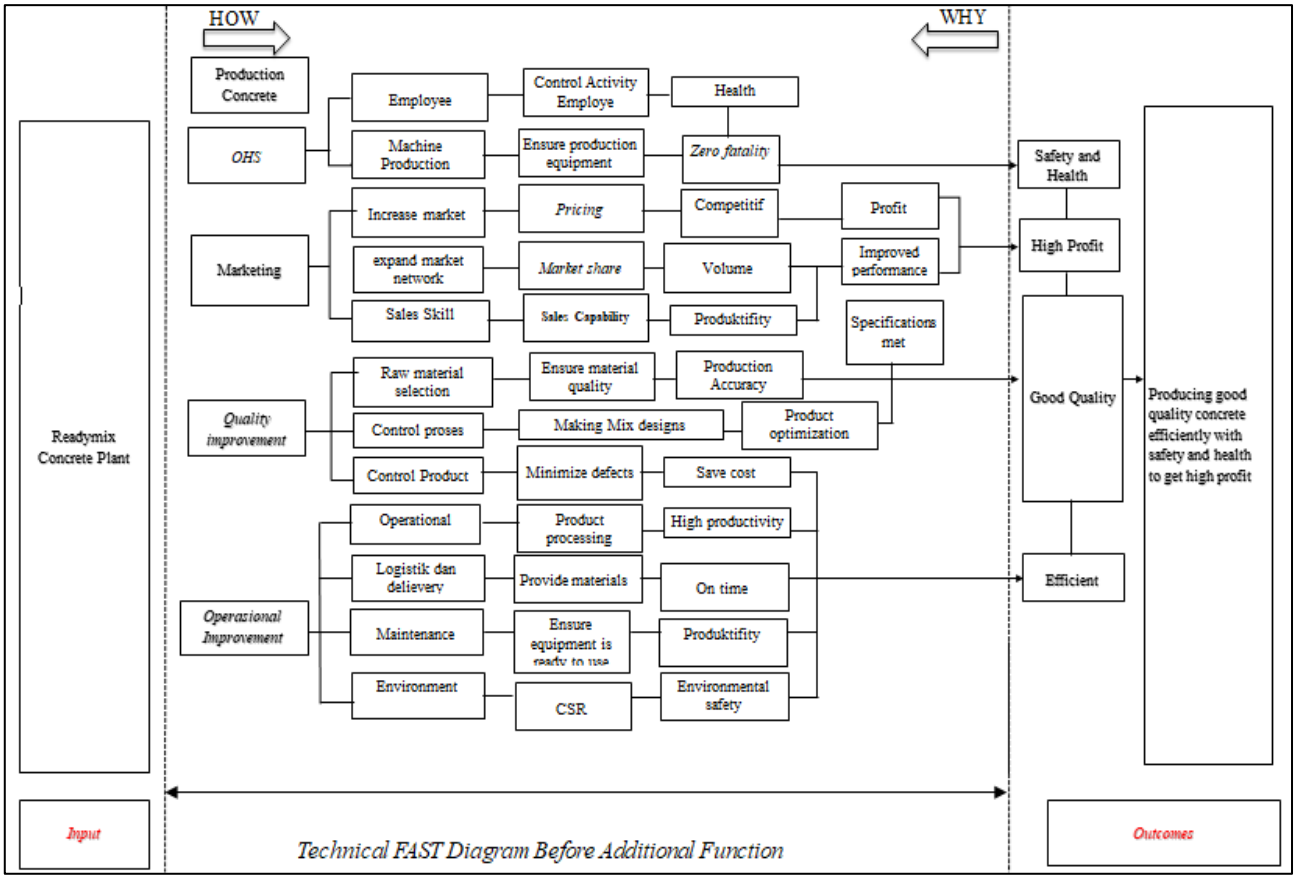

Figure 4. Concrete Industry FAST Diagram existing process and Before Additional Functions

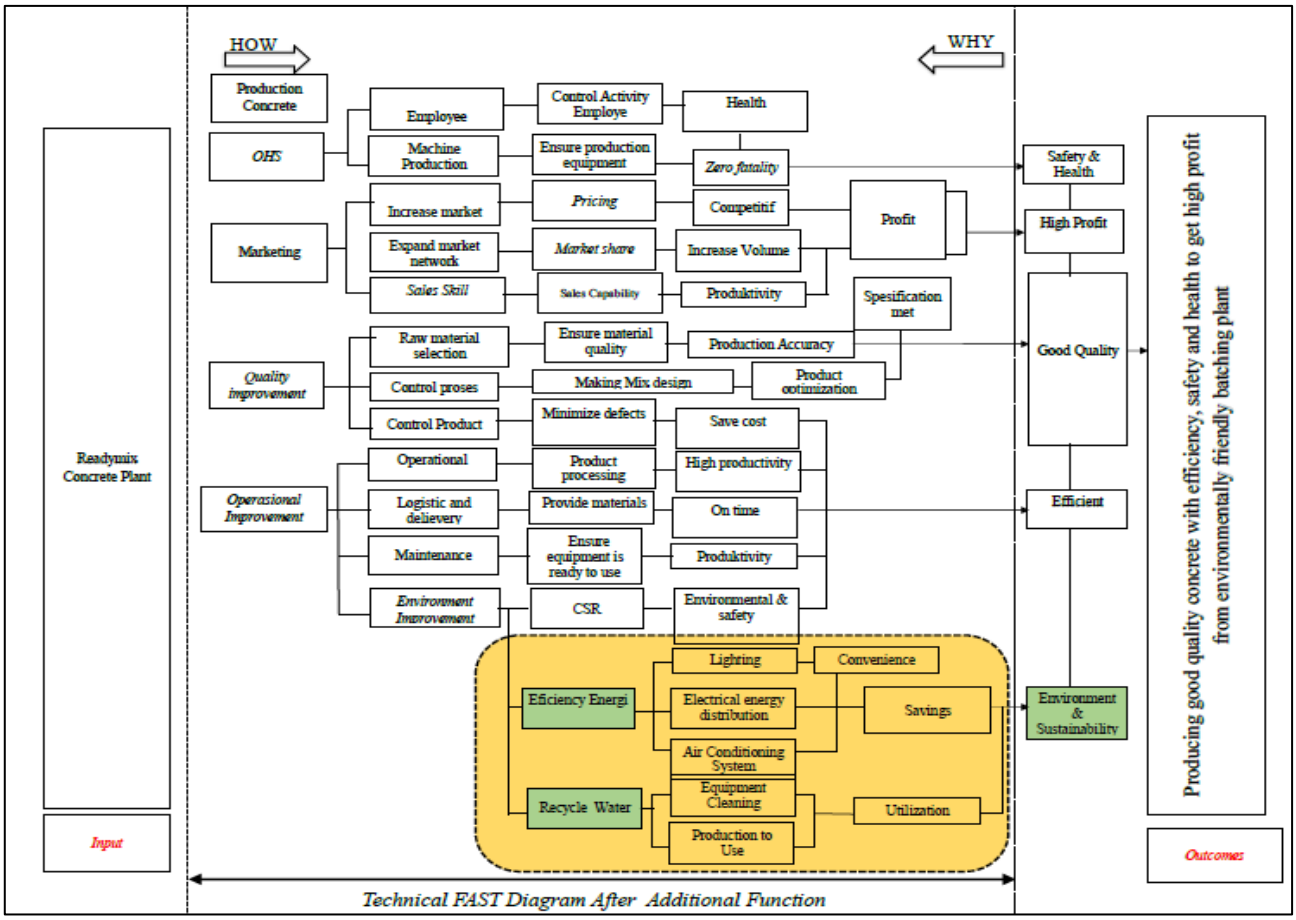

Figure 5. Concrete Industry FAST Diagram after Additional Functions (Source: Research Data Processing, 2022)

Table 3. Eco-Friendly Additional Functions in the Concrete Industry

No	*Work item*	*Analysis Function*
1	*Efficiency Energy*	*Lighting* *Electrical energy distribution* *Efficiency* *Sustainable and environmentally friendly*
No	***Work item***	***Analysis Function***
2	*Recycle Water*	*Raw material* *Production Operational Use* *Utilization and efficiency* *Sustainable and environmentally friendly*

The work items in this case study on the VE and LCCA processes were energy efficiency and recycled water to add 57% points for the environment-(E) parameter of the total 73 points.

3.1. Energy Efficiency

Energy-efficient buildings with proper design will result in lower utility invoices than conventional buildings (buildings without an energy efficiency strategy) (Gunawan, 2012). The concrete industry using PV solar energy could reduce 17,165.05 Kg CO^{2e}. If the system was started in January (rather than January 2019), it could reduce about 9% carbon footprint per month and about 205,980.6 Kg of CO2e in a year. In other words, the solar system can save production efficiency and be eco-friendly (Rasheed, 2020).

In this case study, the concept of energy efficiency using solar panels was useful to obtain more benefits and improve the function of the eco-friendly concrete industry. The roof area for solar power plants in the PT. XYZ batching plant area was as follows:

The office roof area was 15 m × 30 m = 450 m^2

The roof area of the Stockpile was 15 m × 45 m = 675 m^2

So, the total roof area was 1125 m^2. The maximum PV used was 2.38 × 1.09 = 2.59 m^2.

Maximum calculation Total Solar Module =

$$\frac{\text{Batching plant roof area } (m^2)}{\text{Module surface area } (m^2)} \quad (1)$$

Table 4. Green Retrofitting Cost Before and After VE

Component	Function		Cost Before VE (IDR)	Cost After VE (IDR))
	Verb	Noun		
Efficiency Energy	Lighting and Energy Operations	Sustainable and environmentally friendly	2.738.790.449	2.462.290.449
Water Recycle	Utilization and Savings	Sustainable and environmentally friendly	434.017.780	427.955.780
Cover Loading Point	Dust Reduction	Sustainable and environmentally friendly	38.880.000	38.880.000
Certification Green	Assessment green Lable	Sustainable	52.000.000	52.000.000
Total (IDR)			3.263.688.229	2.981.126.229
Total VE (Cost before-after) (IDR)			282.562.000	
Percentage Saving base on Value Engineering (%)			**8.66%**	

Table 5. Monetary Benefit for Efficiency Energy and Recycle water

ITEM	MONETARY BENEFIT				REMARK
	AMOUNT	UOM	VALUE/ UOM (IDR)	TOTAL (IDR)	
Saving Energy	176000	Kwh	1.142	200.946.240	40% of rate capacity 550KVA
Excess Energy for CSR	10000	Kwh	1.142	11.417.400	Cost CSR /month
Water Saving	385.61	M3	45.000	17.352.450	Target saving 50% (25% for Raw material and 25 % flashing)
Total Monetary Benefit/ Month (IDR)					**229.716.090**
Total Benefit /Year (IDR)					**2.756.593.080**

The maximum installed solar panels was 1125 m2: 2.59 m2 = 445 pcs solar panels. The installed power for the factory area was 555 KVA, a voltage of 380V, and 3 phases. The calculation used the DOD (Depth of discharge) assumption, 80% battery, and 4.5 hours PSH (Peak Sun Hours). The VE team used software to calculate the off-grid solar panel system, resulting in a minimum solar panel capacity of 151.29 KWp. If using a 550 wp Monocrystalline type of solar panel, the total solar panel was 275 pcs of solar panels < 445 maximum solar panels for the number of solar panels with a batching plant roof area. The number of batteries with a capacity of 48V 70AH was 165 pcs, and a 15KW inverter was 11 pcs. The installed generator and PLN could be allocated for other benefit values, while the generator was used to back up when the system was off during operation.

3.2. Recycle Water

The large-capacity concrete industrial wastewater provided a vivid example of this phenomenon. This waste comes from the concrete manufacturing process, industrial washing waste, and washing mixers after making concrete (Widodo, 2010). Liquid waste or wastewater is liquid waste from homes, businesses, workplaces, industries, and other public places. This waste contains components or substances that can damage human health or life and disrupt environmental sustainability (Kencanawati, 2016). The concept of utilizing and using wastewater requires specific handling. Reducing the use of clean water in the concrete industrial process can add benefits and eco-friendly functions. Wastewater treatment in the concrete industry aims to reduce wastewater pollutant parameters according to quality standard requirements or certain qualities for reuse.

The selection of Washed Water Treatment (WWT) design must be focused on the type of waste produced in the concrete industry. The main goal is to use recycled water for re-production and focus on wastewater quality and the quantity of wastewater produced for clean water efficiency. The wastewater treatment is designed based on the process's order divided into primary, secondary, and tertiary treatments. The design of the Washed Water Treatment (WWT) pond in the VE process was as follows:

Figure 6. WWT Image for Benchmark

The calculation of pipe installation was used to distribute 25% of production material to replace clean water. Then, it was also used for washing truck mixers, plant operations, and water sprinklers. The planned wastewater capacity was 95 m3. The distribution of recycled water was expected to save 50% of the use of clean water each month. In addition, the concrete industry business stakeholder will benefit. Energy efficiency and recycled industrial water provided the benefits of saving production processes. Life cycle costing is a powerful tool for quantifying costs over time due to price changes (Dwaikata & Ali, 2018).

Table 6. Feasibility Analysis of Applying Green Concept in the RMC Industry

FEASIBILITY ANALYSIS					
Information	**2022**	**2023**	**2024**	**2025**	**2026**
Net Income (IDR)	(3.400.625.114)	1.180.096.672	1.373.504.739	1.512.225.006	1.693.766.771
PV Value (IDR)	-3.400.625.114	983.413.893	953.822.735	875.130.212	816.824.253

Table 7. NPV, IRR, Return Period, and BCR Result

Criteria Investment			Value		Remark
NPV (IDR)			1.938.825.115		FEASIBLE PROJECT
IRR			39.75 %		FEASIBLE PROJECT
Payback Period	3	Year	8.6	Month	FEASIBLE PROJECT
Benefit Cost Ratio			1.63		FEASIBLE PROJECT

Investment analysis requires an analyst to examine the net present value (NPV) and internal rate of return. The analysis also required other indicators, such as return periods, to choose the suitable investment. Internal Rate of Return (IRR) and Net Present Value (NPV) was used to indicate a project's feasibility. Decision makers used the NPV approach to evaluate the investment of money today with future returns after considering value, time, and money (Weber, 2014). The calculation of the investment value for the application of the eco-friendly concept in the concrete industry can be seen in Table 6 below:

In the first year, industry players will incur high costs as initial capital to obtain the Green concept. The calculation of monetary benefits obtained each year will reduce capital costs and get benefits and benefits from implementing the Green Concept with positive value results for the NPV calculation.

The VE and LCCA calculations showed that the green concept in the industry could be applied. The rate of return in the calculation of the LCCA analysis was 3 years 8 months according to the predetermined target of < 4 years.

3. CONCLUSION

From the previous explanation, the conclusions of the application of the Green Concept for the concrete industry with the VE method are as follows:

- Regarding the flow of implementation and the benefits of saving in an environmentally friendly production process, the application of value engineering to the green retrofitting of the concrete industry has been proven to increase the cost performance of green retrofitting by 8.66% with a return of 3 years and 8 months and to increase the functions and benefits of the concrete industry which are environmentally friendly and sustainable.
- The research hypothesis is that improving the green retrofitting cost performance in the concrete industry using value engineering methods can be feasible, eco-friendly, and more profitable for the government and stakeholders in the future.

The novelty of this research is applying the green retrofitting concept for Indonesia's concrete industry with VE and adding eco-friendly functions in the concrete industry process to incentivize the government to provide benefits for industries that implement the green concept.

ACKNOWLEDGEMENT

Thanks to PT.Solusi Bangun Indonesia (Semen Indonesia Group), who have facilitated this research

REFERENCES

Asrul, N., & Ozanya, R. (2017). Penerapan Metode Value Engineering Pada Proyek Pembangunan Asrama Putera Yayasan Tapuz Kota Pariaman, 3, 29–38. https://doi.org/10.21063/SPI3.1017.29-38

Baghdady, A. M. (2018). Enhancing Optimization and sustainability of Ready Mixed Concrete through Value Engineering Approach ., (February). https://doi.org/10.13140/RG.2.2.13487.64166

Bahri, K., Indryani, R., Sipil, D. T., Sipil, F. T., Teknologi, I., Definisi, A., & Rekayasa, K. (2018). Penerapan Rekayasa Nilai (Value Engineering) Pekerjaan Arsitektural Pada Proyek Pembangunan Transmart Carrefour Padang, 7(1), 3–7.

Berawi, M. A., Berawi, A. R. B., Prajitno, I. S., Nahry, Miraj, P., Abdurachman, Y., … Ivan, A. (2015). Developing conceptual design of high speed railways using value engineering method: Creating optimum project benefits. International Journal of Technology, 6(4), 670–679. https://doi.org/10.14716/ijtech.v6i4.1743

Concrete Sustainability Council. (2022). Concrete Sustainability Council. Retrieved from http://www.concretesustainabilitycouncil.org/

Doan, D. T., Wall, H., Hoseini, A. G., Ghaffarianhoseini, A., & Naismith, N. (2021). Green Building Practice in the New Zealand Construction Industry: Drivers and Limitations. International Journal of Technology, 12(5), 946–955. https://doi.org/10.14716/ijtech.v12i5.5209

Dwaikata, L. N., & Ali, K. N. (2018). Author ' s Accepted Manuscript Green Buildings Life Cycle Cost Analysis and Life Cycle Budget Development :

Practical Applications Reference : Journal of Building Engineering. https://doi.org/10.1016/j.jobe.2018.03.015

Ebrahim, A., & Wayal, A. S. (2020). ICRRM 2019 – System Reliability, Quality Control, Safety, Maintenance and Management. ICRRM 2019 – System Reliability, Quality Control, Safety, Maintenance and Management. Springer Singapore. https://doi.org/10.1007/978-981-13-8507-0

Favier, A., De Wolf, C., Scrivener, K., & Habert, G. (2018). A sustainable future for the European Cement and Concrete Industry Technology assessment for full decarbonisation of the industry by 2050. BRISK Binary Robust Invariant Scalable Keypoints, 12–19.

Fuller, S. (2006). WBDG : Life-Cycle Cost Analysis (LCCA) Life-Cycle Cost Analysis (LCCA) WBDG : Life-Cycle Cost Analysis (LCCA). Whole Building Design Guide, (Lcc), 1–11.

Gunawan, B. dkk. (2012). Buku Pedoman Energi Efisiensi untuk Desain Bangunan Gedung di Indonesia.

Hatami, A., & Morcous, G. (2016). Deterministic and Probabilistic Life-cycle Cost Assessment: Applications to Nebraska Bridges. Journal of Performance of Constructed Facilities, 30(2). https://doi.org/10.1061/(asce)cf.1943-5509.0000772

Hong, W. T., Ibrahim, K., & Loo, S. C. (2019). Urging green retrofits of building facades in the tropics: A review and research agenda. International Journal of Technology, 10(6), 1140–1149. https://doi.org/10.14716/ijtech.v10i6.3627

Husin, A. E. (2015). Model Aliansi Strategis Dalam Kemitraan Pemerintah dan Swasta Pada Mega Proyek Infrastruktur Berbasis Value Engineering Untuk Meningkatkan Nilai Kelayakan Proyek, 1–337.

Husin, A. E. (2019). Implementation Value Engineering In Diaphragm Wall at High Rise Building, 8(1), 16–23.

Husin, A. E., Karolina, T., Rahmawati, D. I., & Abdillah, C. F. (2022). Increasing Value of Façade at Green Hotel Building Based on Value Engineering. The Open Civil Engineering Journal, 15(1), 398–405. https://doi.org/10.2174/1874149502115010398

Imron, A., & Husin, A. E. (2022). Value Engineering and Life-cycle Cost Analysis to Improve Cost Performance in Green Hospital Project Value engineering and life-cycle cost analysis to improve cost performance in green hospital project, (December 2021). https://doi.org/10.24425/ace.2021.138514

Kashwani, G., Sajwani, A., Ashram, M. Al, & Yaaqoubi, R. Al. (2014). Evaluation of Environmental Requirements for Sustainable Ready-Mix Concrete Production in Abu Dhabi Emirate, (March), 333–339.

Kencanawati, C. I. P. K. (2016). Sistem Pengelolaan Air Limbah dan Sampah. Sistem Pengolahan Air LImbah, (7473), 1–55.

Kim, J., Ph, D., Asce, M., Greene, M., Kim, S., & Ph, D. (2014). Cost Comparative Analysis of a New Green Building Code for Residential Project Development, 1–10. https://doi.org/10.1061/(ASCE)CO.1943-7862.0000833.

Liu, H. (2015). Evaluating construction cost of green building based on life-cycle cost analysis: An empirical analysis from Nanjing, China. International Journal of Smart Home, 9(12), 299–306. https://doi.org/10.14257/ijsh.2015.9.12.30

Pahnael, J., Soekiman, A., & Wimala, M. (2020). Penerapan Kebijakan Insentif Green Building di Kota Bandung (Green Building Incentive Policy in Bandung). J.Infras, 6(1), 1–13.

Rahmawati, A., Wisnumurti, W., & Nugroho, A. M. (2018). Pengaruh Penerapan Green Retrofit Terhadap Life Cycle Cost pada Bangunan Gedung. Rekayasa Sipil, 12(1), 64–70. https://doi.org/10.21776/ub.rekayasasipil/2018.012.01.9

Rasheed, Z. A. (2020). Conversion of Ready-mix Concrete Energy to Solar PV.

Study, C., Correia, N., Samani, P., & Gregory, J. (2018). Life-cycle Cost Analysis of Prefabricated Composite and Masonry Buildings : Comparative Study, 24(1), 1–11. https://doi.org/10.1061/(ASCE)AE.1943-5568.0000288.

Susanti, H. D., Arfamaini, R., Sylvia, M., Vianne, A., D, Y. H., D, H. L., … Aryanta, I. R. (2017). No 主観的健康感を中心とした在宅高齢者における 健康関連指標に関する共分散構造分析 Title. Jurnal Keperawatan. Universitas Muhammadya Malang, 4(1), 724-732.

Vu-ngoc, H., Elawady, S. S., Mehyar, G. M., Abdelhamid, H., Mattar, O. M., Halhouli, O., … Hirayama, K. (2018). Quality of flow diagram in systematic review and / or meta-analysis, 1–16.

Weber, T. A. (2014). On the (non-) equivalence of IRR and NPV, 52, 25–39. https://doi.org/10.1016/j.jmateco.2014.03.006

Widodo, S. (2010). Pemanfaatan air limbah produksi beton, VI(1), 1–10.

Woodhead, R., & Berawi, M. A. (2022). Evolution of Value Engineering to Automate Invention in Complex Technological Systems. International Journal of Technology, 13(1), 80–91. https://doi.org/10.14716/ijtech.v13i1.4984

Yuan, Q., Yang, D., Yang, F., Luken, R., Saieed, A., & Wang, K. (2020). Green industry development in China: An index based assessment from perspectives of both current performance and historical effort. Journal of Cleaner Production, 250(November). https://doi.org/10.1016/j.jclepro.2019.119457

Vol. 14 No. 2 (2023) 45-53

Jurnal Riset
Teknologi Pencegahan Pencemaran Industri

Journal homepage : https://www.jrtppi.id

Kementerian Perindustrian
REPUBLIK INDONESIA

Easy Preparation of Zinc Molybdate Photocatalyst ($ZnMoO_4$) and Its Application for Degradation of Methylene Blue

Ridla Bakri*[1], Rika Firmansyah[1], Yoki Yulizar[1]

[1] Department of Chemistry, Universitas Indonesia.

ARTICLE INFO

Article history:
Received January 11, 2023
Received in revised form January 20, 2023
Accepted April 26, 2023
Available online November 10, 2023

Keywords :
Methylene Blue
Organic Pollutant
Photocatalyst
Zinc Molybdate

ABSTRACT

Using photocatalyst is one way to overcome the problem of dye waste in water. Hazardous chemicals are commonly used in the manufacture of photocatalysts. In this research, $ZnMoO_4$ was prepared through an environmentally friendly and cost-effective synthesis. $ZnMoO_4$ was synthesized using peppermint leaf extract. The alkaloid content of the leaf extract was hydrolysed to form hydroxy ions. Subsequently, the hydroxyl ions were subjected to a hydrothermal process, resulting in the formation of $ZnMoO_4$. The functional groups, crystalline structure and morphology of $ZnMoO_4$ were characterised using fourier transform infrared (FTIR), X-ray diffraction (XRD), field emission scanning electron microscopy (FE-SEM), and transmission electron microscopy (TEM). The band gap energy was investigated through UV-Vis diffuse reflectance spectroscopy (UV-Vis DRS). The photocatalytic activity of $ZnMoO_4$ was tested against the organic pollutant methylene blue under visible light irradiation and its degradation products were analysed with a UV-Vis spectrophotometer at a wavelength of 664 nm. After 80 minutes of irradiation, the photocatalytic process of $ZnMoO_4$ degraded 99% of methylene blue. The excellent photodegradation performance suggests that the transition activity of electron currents from the valence band to the conduction band on $ZnMoO_4$ is occurring effectively.

1. INTRODUCTION

Methylene blue (MB) is commonly used in the textile, paper and paint industries (Pham et al., 2021; Riwayati, Fikriyyah, & Suwardiyono, 2019; Simi & Azeeza, 2010). The presence of methylene blue in water is a pollutant that is harmful to humans (Ken Gillman, 2011; Radoor, Karayil, Jayakumar, Parameswaranpillai, & Siengchin, 2021). Photocatalysis is one of the treatment methods for dye wastewater (Sagadevan et al., 2022; Sirirerkratana, Kemacheevakul, & Chuangchote, 2019). The basis of photocatalysis is the use of light to excite electrons to form photogenerated electron-hole pairs and initiate redox reactions on the surface of the photocatalyst (Low, Yu, Jaroniec, Wageh, & Al-Ghamdi, 2017). Metal oxide semiconductors with a wide band gap act as photocatalysts under UV light, while metal oxides with a narrow band gap adsorb visible light (Astuti, Listyani, Suyati, & Darmawan, 2021; Meng et al., 2017; Widiyandari, Ketut Umiati, & Dwi Herdianti, 2018). Sunlight with a high visible light content can be used as a photocatalytic light source (Liebel, Kaur, Ruvolo, Kollias, & Southall, 2012; Wang et al., 2018). Therefore, narrow bandgap semiconductors are needed to optimise the use of visible light from sunlight.

$ZnMoO_4$ is a non-toxic oxidation metal commonly used as anode material (Fei et al., 2017; Zhang, Feng, Liu, & Guo, 2019), catalyst (Petrović et al., 2021), anti-bacterial (Mardare, Tanasic, Rathner, Müller, & Hassel, 2016), and

*Correspondence author.
E-mail : ridla.bakri@sci.ui.ac.id (Ridla Bakri)

doi : https://10.21771/jrtppi.2023.v14.no.2.p45-53

Accreditation number : (Ristekdikti) 158/E/KPT/2021

anti-corrosion (Xing, Xu, Wang, & Hu, 2019) as well as photocatalyst (Chen, Zhang, Yang, Yang, & Sun, 2021; Yan et al., 2019). β-$ZnMoO_4$ has a monoclinic phase system with Zn and Mo atomic bonds attached to 6 oxygen atoms and can adsorb visible light. It is a metastable material that transforms into α-$ZnMoO_4$ at high temperatures (Ait Ahsaine et al., 2016). The production of $ZnMoO_4$ usually uses chemicals such as NaOH base, which are harmful to the environment (Lv, Tong, Zhang, Su, & Wang, 2011).

Indonesia is renowned for its rich biodiversity and vast plant species, which hold immense potential in the development of green synthesis methods. The development of green synthesis methods in this research aims to reduce the use of hazardous and toxic materials. In this paper, fabrication of $ZnMoO_4$ was carried out by green synthesis using peppermint leaves extract. Peppermint contains secondary metabolites such as flavonoids, tannins, saponins and alkaloids. (Fialová et al., 2014; Puspitasari, Mareta, & Thalib, 2021). The content of alkaloids can replace the use of the starting NaOH material, while flavonoids, tannins, and saponins can be used as capping agents that can maintain the formation of nanoparticles so that they are stable to form nanoparticles (Weldegebrieal, 2020; Yulizar, Apriandanu, & Ashna, 2020; Yulizar, Bakri, Apriandanu, & Hidayat, 2018).

2. MATERIAL AND METHODS

2.1. $ZnMoO_4$ Synthesis

To obtain secondary metabolites in peppermint leaves, dry and clean leaves were macerated with methanol in a ratio of 1:5 (g/v). The filtrate was added with n-hexane in a ratio of 1:1 (v/v) and then separated. The resulting solution of the methanol fraction was concentrated to thickening using a vacuum rotary evaporator. The viscous liquid is dissolved in water as peppermint extract (PE) and stored in the refrigerator.

Stirred for 10 minutes with 5 mL of $(NH_4)_6Mo_7O_{24}.4H_2O$ and $Zn(NO_3)_2.4H_2O$ at a ratio of 0.15 mmol and 1.05 mmol, respectively. Into the mixture then added 1 mL of peppermint extract (PE) and stirred it for 30 minutes. The stirred mixture was placed in a 25-mL Teflon autoclave chamber and then heated in an oven at 160°C for 6 hours. Cool the autoclave to room temperature. The precipitate formed was washed with distilled water and methanol three times each and then heated at 80°C for 3 hours until a light grey powder was formed.

2.2. Material Characteristics

To prove that the synthesized catalyst is $ZnMoO_4$, the catalyst was characterized using various instruments. X-ray diffraction (XRD) Shimadzu 2700 was used to analyse the structure of the nanoparticles, the Fourier Transform Infrared (FTIR) Shimadzu Prestige 21 was used to determine functional groups, DRS UV-vis Spectrophotometer Agilent Technologies Carry 60 was used to test band gap, field emission - scanning electron microscopy spectroscopy (FESEM-EDX) JEOL JIB-4610F and Transmission Electron Microscope (TEM) - Tecnai 200 kV D2360 was used to see the morphology and atomic composition.

2.3. Photocatalytic Activity of $ZnMoO_4$

8 mg ZnMoO4 powder were added to 50 mL of 1x10-5 M methylene blue (MB) solution with constant stirring under visible light (125 W lamp, λ 420 nm, Philips) for 80 minutes. The degradation of the MB solution that occurred was measured using an Agilent Cary 100 UV-Vis Spectrophotometer at a wavelength of 664 nm. The calculation of the percentage degradation of MB is done by the equation:

$$\%\ degratation = \frac{A_0 - A_t}{A_0} \times 100\%$$

where A_0 is the initial concentration of MB dye and A_t is the residual concentration of MB.

3. RESULT AND DISCUSSION

3.1. Characterization Material

A phytochemical screening of peppermint leaves extract was carried out based on a previous study by Dwi, Anam, & Kusrini (2016). Table shows the result of the phytochemical test. It revealed the presence of secondary metabolites in methanol fractions such as alkaloids, flavonoids, tannins, and saponins. The phytochemical

results of the n-hexane fraction did not contain secondary metabolites of alkaloids, flavonoids, tannins, and saponins. This indicates that the secondary metabolites used are polar.

FTIR tests were also performed to determine the functional groups in the peppermint extract. The results of the FTIR test can be seen in Figure 1(a). The presence of a spectrum at wave number 1643 cm-1 indicates the presence of the NH functional group, which indicates alkaloids in the sample. A wide peak with a maximum peak at a wavelength 3331 cm-1 indicates the presence of a hydroxy functional group (-OH), which is part of the flavonoids, tannins, and saponins.

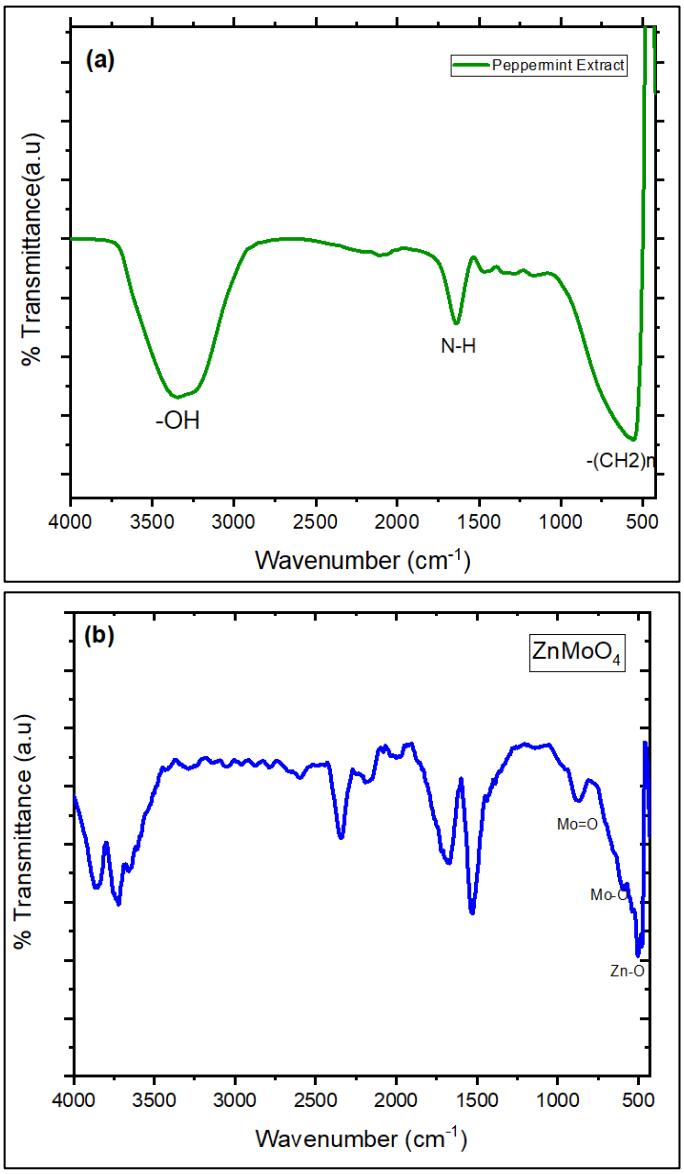

Figure 1. FTIR Spectra of (a) Peppermint Extract and (b) $ZnMoO_4$

Table 1. Result of Phytochemical Test

Metabolic Secondary	n-Hexane Fraction	Methanol fraction
Alkaloid	-	+
Flavonoid	-	+
Tannin	-	+
Saponin	-	+

FTIR spectra in Figure 1(b) show the presence of ZnO bonds at 489 cm^{-1} (Bharathi, Sivakumar, Udayabhaskar, Takebe, & Karthikeyan, 2014), as well as Mo-O bonds at 609 and 882 cm^{-1} (Reddy, Vickraman, & Justin, 2018). The presence of wave numbers at 1500-4000 indicate the presence of organic compounds derived from residual secondary metabolites still bound to ZnMoO4. Spectra in the 1500-2000 ranges are regional triple bonds for C=N, C=C and C=O; 2000-2500 ranges are regional triple bonds for C≡C and C≡N while 2500-4000 are regional single bonds for the C-H group and O-H (Nandiyanto, Oktiani, & Ragadhita, 2019).

The alkaloid compounds in the leaf extract will be hydrolysed in water to form OH- bases, which will react with metal ions Zn^{2+} and $(Mo_7O_{24})^{6-}$ to form hydroxy compounds. By the pressure in the hydrothermal process these hydroxy compounds will form metal oxide $ZnMoO_4$. Meanwhile, the presence of other secondary metabolites such as flavonoids, saponins, and tannins, act as a capping agent that maintains the stability of particle formation. The reaction between alkaloids and metal ions is shown in the following reactions:

$$Zn(NO_3)_2.4H_2O_{(s)} \rightarrow Zn^{2+}{}_{(aq)} + 2NO_3^-{}_{(aq)} + 4H_2O_{(l)} \quad (1)$$

$$(NH_4)6Mo_7O_{24}.4H_2O_{(s)} \rightarrow 6NH_4^+{}_{(aq)} + Mo_7O_{24}^{6-}{}_{(aq)} + 4H_2O_{(l)} \quad (2)$$

$$R_2\text{-}N\text{-}CH_{3\,(aq)} + H_2O_{(l)} \rightleftharpoons R_2\text{-}N{+}H\text{-}CH_{3\,(aq)} + OH^-{}_{(aq)} \quad (3)$$

$$7\ Zn^{2+}{}_{(aq)} + Mo_7O_{24}^{6-}{}_{(aq)} + OH^-{}_{(aq)} \rightarrow 7\ ZnMoO_{4(s)} + 4\ H_2O_{(l)} \quad (4)$$

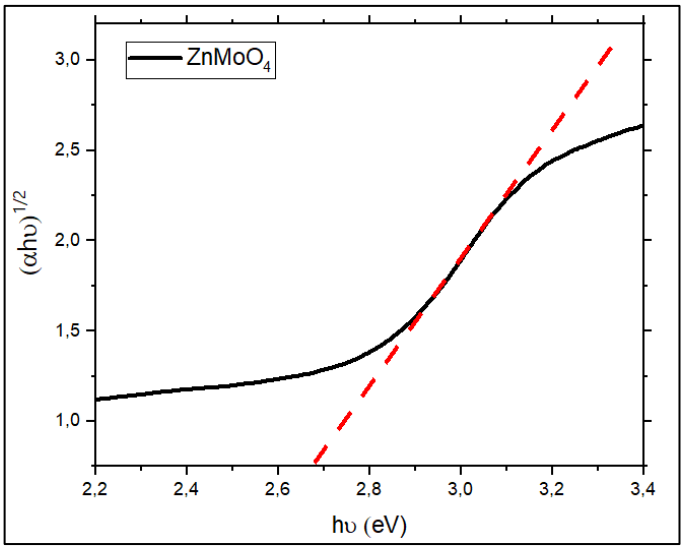

Figure 2. Bandgap Energy of $ZnMoO_4$

The estimated bandgap energy of ZnMoO4 was determined using the Tauc Plot equation as follows:

$$\alpha h\upsilon = A(h\upsilon - Eg)^{1/2}$$

where α is absorption coefficient, h is Planck's constant, υ is the frequency of light, Eg is energy bandgap, and A is a constant number. By plotting $(\alpha h\upsilon)^{1/2}$ and hυ into a graph, and extrapolating $(\alpha h\upsilon)^{1/2} = 0$ linearly, one can estimate the energy value Eg of the bandgap. As shown in Figure 2, the energy of the bandgap of $ZnMoO_4$ is 2.67 eV. This result shows that the electrons of $ZnMoO_4$ are easily excited by visible light (Jiang et al., 2014; Lv et al., 2011).

The diffraction patterns of $ZnMoO_4$, shown in Figure 3, were analysed by XRD. In the $ZnMoO_4$ diffraction pattern with a value of 2θ is 18.64; 24.16; 30.24; 30.96; 36.01; 36.35; 38.10; 40.99; 44.32; 48.56; 49.96; 51.31;53.63; 53.96; 54.78. Meanwhile, those indexed on PDF2 00-016-0310 have a value of 2θ which corresponds to the Miller index (100), (110), (-111), (020), (021), (120), (200), (210), (-112), (022), (220), (130), (-221), (202), and (-131) and has a monoclinic phase form.

FE-SEM EDX analysis was used to investigate the morphology and elemental composition of $ZnMoO_4$. Figure 4(a-b) depicts the morphology of $ZnMoO_4$ at different magnifications, resulting in non-uniform agglomerated flakes. EDX mapping analysis of $ZnMoO_4$ is shown in Figure 4(c-d). The mapping results show that the elements Zn, Mo, and O are distributed evenly. The results of the EDX elemental composition calculation are shown in Figure 4(e), where the atomic compositions of Zn, Mo, and O are 17%, 14%, and 69%, respectively. This corresponds to the original mole number of the synthesis with a mole ratio of 1:1:4 for $ZnMoO_4$. The results of TEM are shown in Figure 5. The SEM and TEM images show a variety of particle sizes with relatively the same shape, namely flakes. This indicates that the formation of $ZnMoO_4$ has been successfully synthesised.

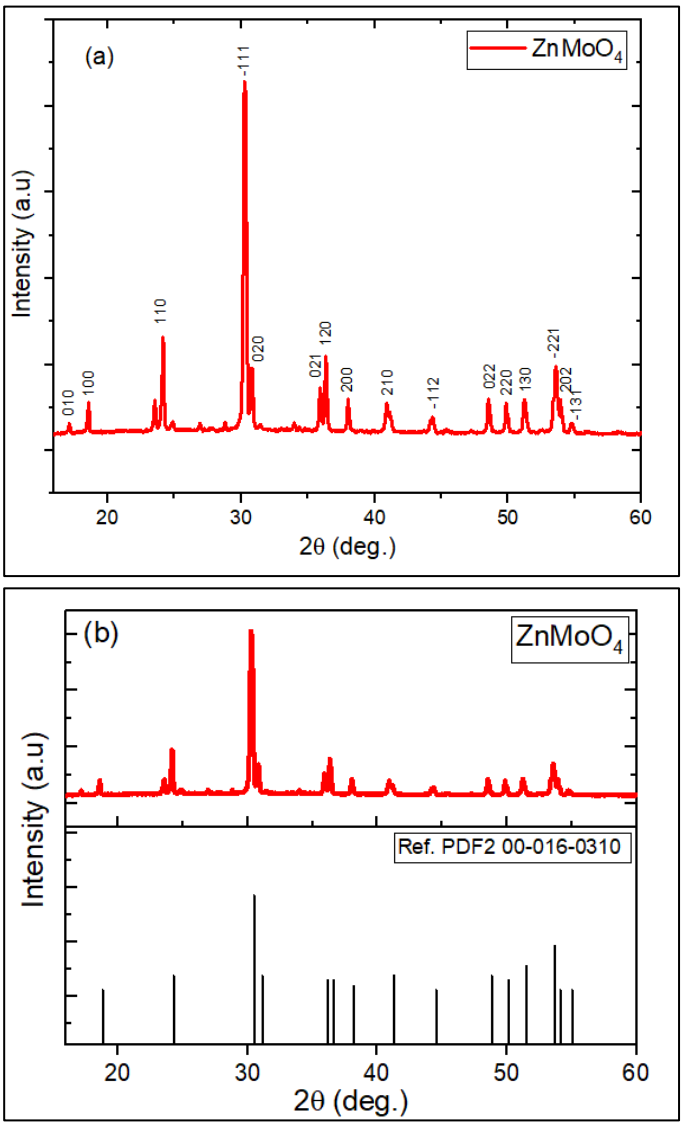

Figure 3. XRD Pattern of (a) $ZnMoO_4$ (b) $ZnMoO_4$ dan Index Miller (b) $ZnMoO_4$ and Ref. PDF2 00-016-0310

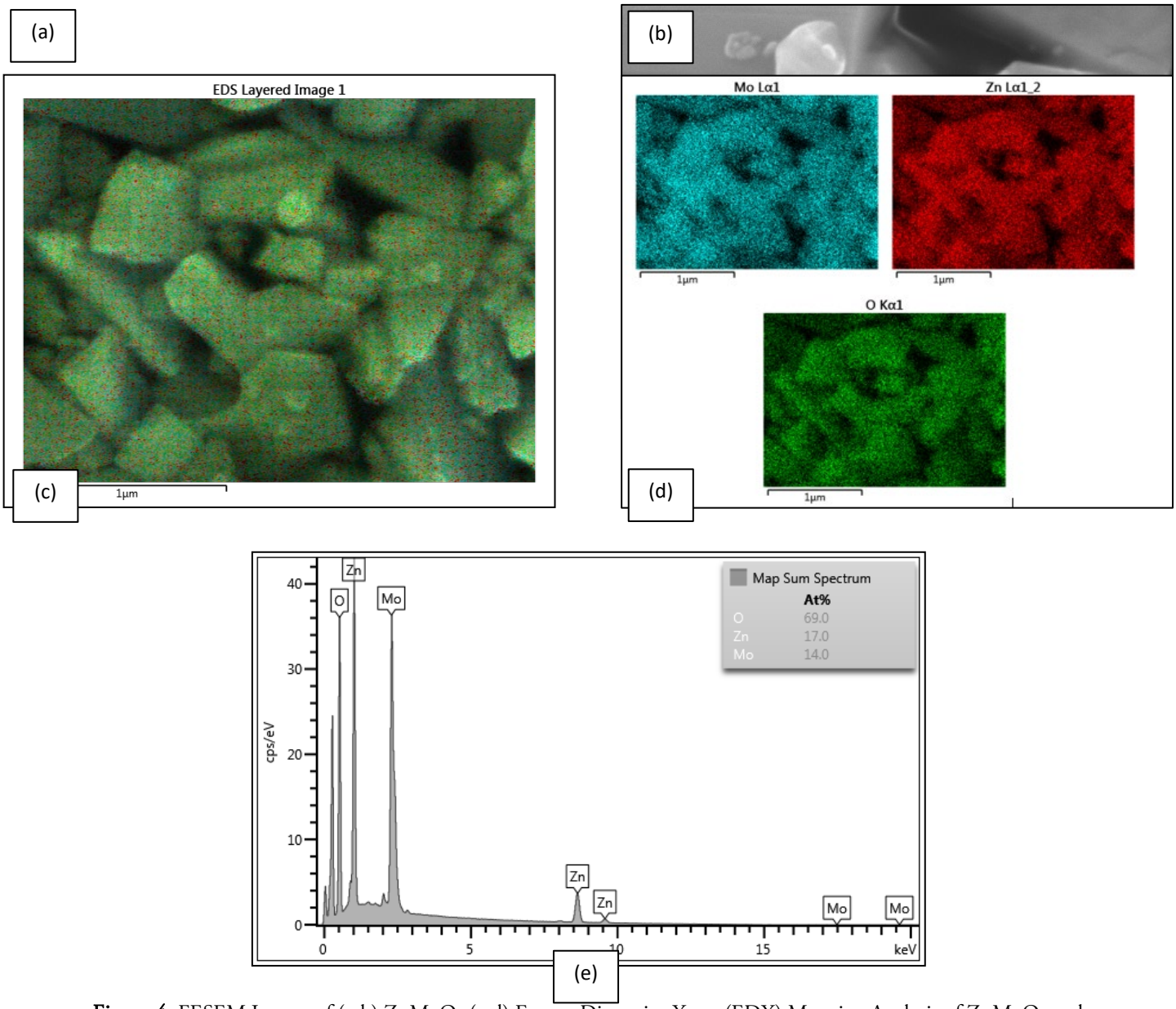

Figure 4. FESEM Images of (a-b) $ZnMoO_4$ (c-d) Energy Dispersive X-ray (EDX) Mapping Analysis of $ZnMoO_4$ and (e) EDX Spectrum of $ZnMoO_4$

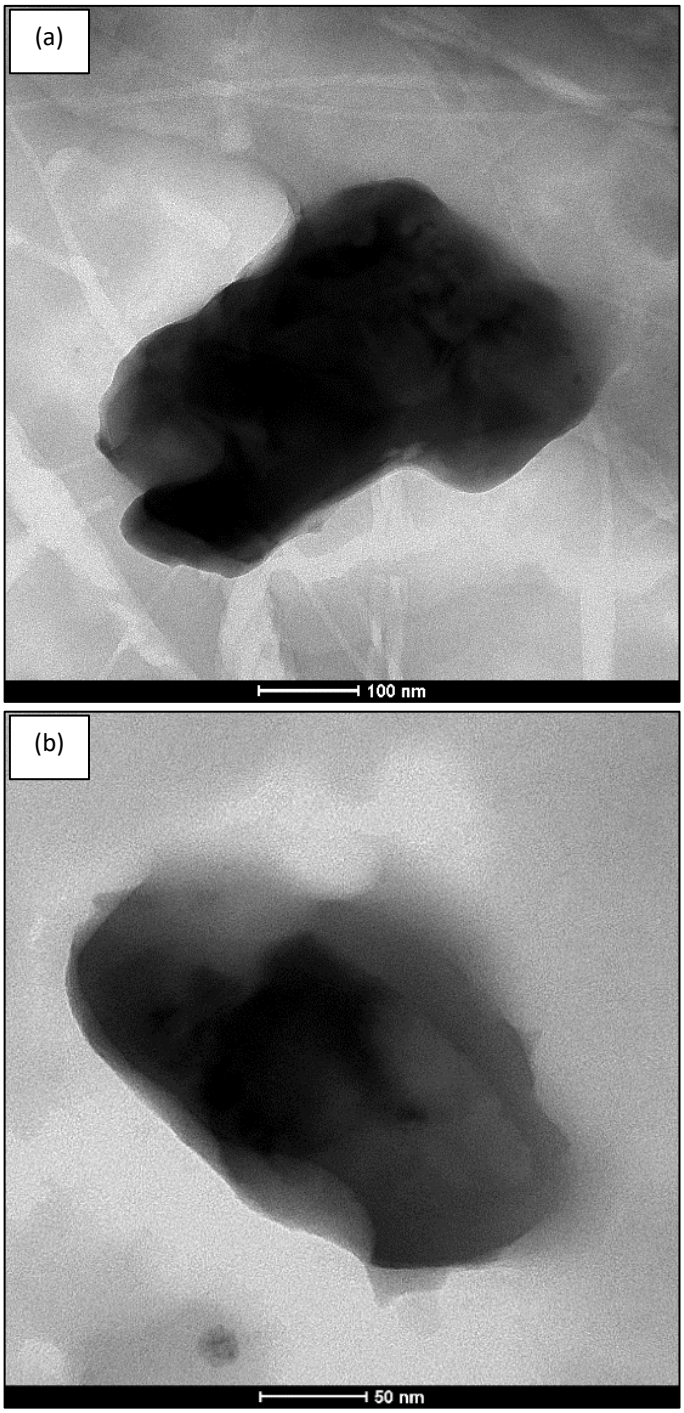

Figure 5. TEM Images of $ZnMoO_4$ (a) 100 nm scale (b) 50 nm scale

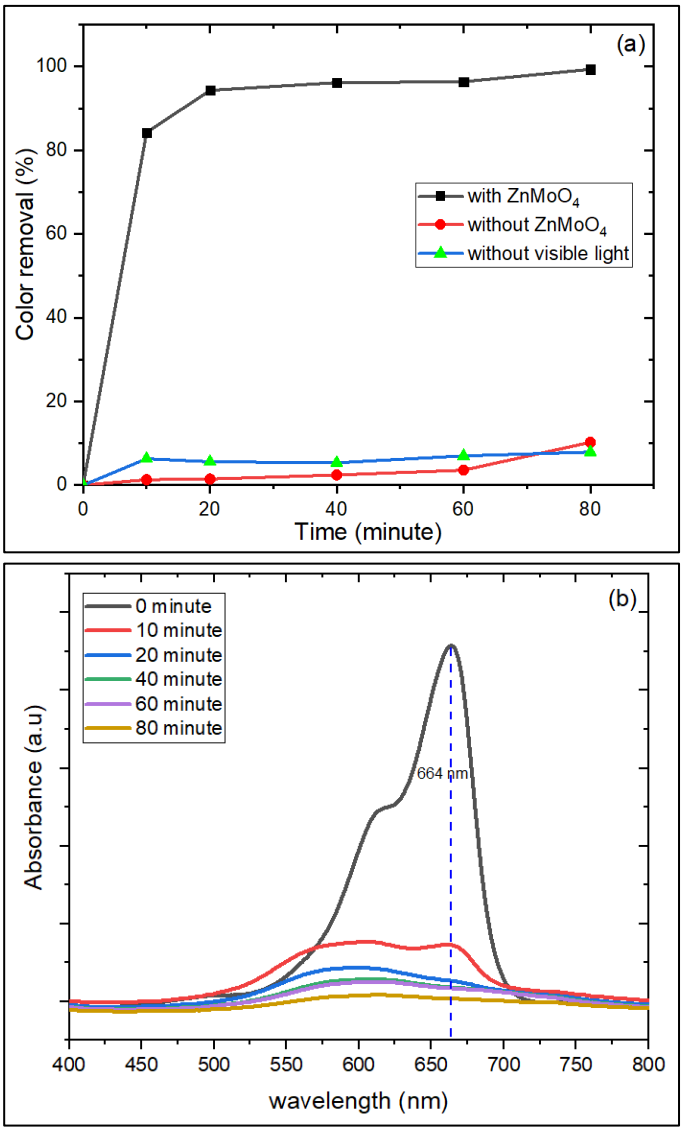

Figure 6. (a) % Degradation of Methylene Blue (MB) (b) Spectra Spectrophotometric Uv-Vis of MB Degradation by $ZnMoO_4$

3.2. Performance of Photocatalytic Degradation

A photocatalytic test was performed on irradiated MB under visible light. Figure 6(a) shows the degradation of methylene blue (MB) by $ZnMoO_4$ under visible light reaches 99.3%, whereas degradation of MB without $ZnMoO_4$ is only 10.4% and the degradation in the absence of visible light is about 7.90%. The process without visible light indicates the presence of dye adsorption by the catalyst. This adsorption process is relatively small compared to the degradation of dyes, that reaches 99%. Therefore, the degradation of MB is affected by the photocatalytic process. Photocatalysis is triggered by visible light, that is adsorbed

by $ZnMoO_4$ and excites electrons. This photogeneration process produces electron (-) in the conduction band (ecb^-) and holes (+) in the valence band (hvb^+). The electrons react with O_2 to form superoxide radicals ($O_2\bullet^-$), meanwhile, the holes in the valence band react with OH^- / H_2O to form hydroxy radicals (•OH). These hydroxy radicals, along with the superoxide radicals ($O_2\bullet^-$) produced by the electrons in the conduction band, react with MB to degrade it into H_2O and CO_2. Figure 6(b) is the uv vis spectrophotometer spectra of MB degradation by $ZnMoO_4$ catalyst for 80 min. From the figure it can be seen the absorbance decrease at a maximum wavelength of 664 nm. This decrease is due to the photocatalytic process which degrades MB into simpler compounds. The reaction:

$$ZnMoO_4 + h\upsilon \rightarrow ZnMoO_4\,(ecb^- + h\upsilon b^+) \quad (5)$$

$$h\upsilon b^+ + OH^- \rightarrow \bullet OH \quad (6)$$

$$ecb^- + O_2 \rightarrow O_2\bullet^- \quad (7)$$

$$O_2\bullet^- + H_2O \rightarrow HO_2\bullet + OH^- \quad (8)$$

$$HO_2\bullet + HO_2\bullet \rightarrow H_2O_2 + O_2 \quad (9)$$

$$H_2O_2 + O_2\bullet^- \rightarrow \bullet OH + OH^- + O_2 \quad (10)$$

$$\bullet OH + O_2\bullet^- + MB \rightarrow CO_2^- + H_2O \quad (11)$$

4. CONCLUSION

The facile preparation of $ZnMoO_4$ photocatalyst has been successfully synthesized by using environmentally friendly natural materials. The synthesis of $ZnMoO_4$ by green synthesis has a morphology in the form of flakes and the shape of the phase system formed is monoclinic. The bandgap of $ZnMoO_4$ is 2.67 eV, which makes it active as a photocatalyst under visible light. Photodegradation of methylene blue by $ZnMoO_4$ under visible light showed very good results, with the colour degradation rate reaching 99%.

ACKNOWLEDGMENT

Financial support for this research comes from LPDP Indonesia.

REFERENCE

Ait Ahsaine, H., Zbair, M., Ezahri, M., Benlhachemi, A., Bakiz, B., Guinneton, F., & Gavarri, J. R. (2016). Structural and Temperature-dependent vibrational analyses of the non-centrosymmetric ZnMoO4 molybdate. Journal of Materials and Environmental Science, 7(9), 3076-3083.

Astuti, Y., Listyani, B. M., Suyati, L., & Darmawan, A. (2021). Bismuth oxide prepared by sol-gel method: Variation of physicochemical characteristics and photocatalytic activity due to difference in calcination temperature. Indonesian Journal of Chemistry, 21(1), 108-117.https://doi.org/10.22146/ijc.53144

Bharathi, V., Sivakumar, M., Udayabhaskar, R., Takebe, H., & Karthikeyan, B. (2014). Optical, structural, enhanced local vibrational and fluorescence properties in K-doped ZnO nanostructures. Applied Physics A: Materials Science and Processing, 116(1), 395-401. https://doi.org/10.1007/s00339-013-8139-8

Chen, P., Zhang, Z., Yang, S., Yang, Y., & Sun, Y. (2021). Synthesis of BiOCl/ZnMoO4 heterojunction with oxygen vacancy for enhanced photocatalytic activity. Journal of Materials Science: Materials in Electronics, 32(18), 23189-23205. https://doi.org/10.1007/s10854-021-06805-6

Dwi, J., Anam, K., & Kusrini, D. (2016). Penentuan Total Kadar Fenol dari Daun Kersen Segar, Kering dan Rontok (Muntingia calabura L.) serta Uji Aktivitas Antioksidan dengan Metode DPPH. Jurnal Kimia Sains Dan Aplikasi, 19(1), 15-20 https://doi.org/10.14710/jksa.19.1.15-20

Fei, J., Sun, Q., Li, J., Cui, Y., Huang, J., Hui, W., & Hu, H. (2017). Synthesis and electrochemical performance of α-ZnMoO4 nanoparticles as anode material for lithium ion batteries. Materials Letters, 198(3), 4-7. https://doi.org/10.1016/j.matlet.2017.03.160

Fialová, S., Tekel'ová, D., Švajdlenka, E., Potúček, P., Jakubová, K., & Grančai, D. (2014). The variability of secondary metabolites in Mentha × piperita cv. "Perpeta" during the development of inflorescence. Acta Facultatis Pharmaceuticae

Universitatis Comenianae, 61(2), 21-25. https://doi.org/10.2478/afpuc-2014-0012

Jiang, Y. R., Lee, W. W., Chen, K. T., Wang, M. C., Chang, K. H., & Chen, C. C. (2014). Hydrothermal synthesis of β-ZnMoO4 crystals and their photocatalytic degradation of Victoria Blue R and phenol. Journal of the Taiwan Institute of Chemical Engineers, 45(1), 207-218.https://doi.org/10.1016/j.jtice.2013.05.007

Ken Gillman, P. (2011). Review: CNS toxicity involving methylene blue: The exemplar for understanding and predicting drug interactions that precipitate serotonin toxicity. Journal of Psychopharmacology, 25(3), 429-436. https://doi.org/10.1177/0269881109359098

Liebel, F., Kaur, S., Ruvolo, E., Kollias, N., & Southall, M. D. (2012). Irradiation of skin with visible light induces reactive oxygen species and matrix-degrading enzymes. Journal of Investigative Dermatology, 132(7), 1901-1907. https://doi.org/10.1038/jid.2011.476

Low, J., Yu, J., Jaroniec, M., Wageh, S., & Al-Ghamdi, A. A. (2017). Heterojunction Photocatalysts. Advanced Materials, 29(20), 1-20. https://doi.org/10.1002/adma.201601694

Lv, L., Tong, W., Zhang, Y., Su, Y., & Wang, X. (2011). Metastable monoclinic ZnMoO 4: Hydrothermal synthesis, optical properties and photocatalytic performance. Journal of Nanoscience and Nanotechnology, 11(11), 9506-9512. https://doi.org/10.1166/jnn.2011.5269

Mardare, C. C., Tanasic, D., Rathner, A., Müller, N., & Hassel, A. W. (2016). Growth inhibition of Escherichia coli by zinc molybdate with different crystalline structures. Physica Status Solidi (A) Applications and Materials Science, 213(6), 1471-1478. https://doi.org/10.1002/pssa.201532786

Meng, X., Hao, M., Shi, J., Cao, Z., He, W., Gao, Y., … Li, Z. (2017). Novel CuO/Bi2WO6 heterojunction with enhanced visible light photoactivity. Advanced Powder Technology, 28(12), 3247-3256. https://doi.org/10.1016/j.apt.2017.09.036

Nandiyanto, A. B. D., Oktiani, R., & Ragadhita, R. (2019). How to read and interpret ftir spectroscope of organic material. Indonesian Journal of Science and Technology, 4(1), 97-118. https://doi.org/10.17509/ijost.v4i1.15806

Petrović, M., Rančev, S., Velinov, N., Radović Vučić, M., Antonijević, M., Nikolić, G., & Bojić, A. (2021). Triclinic ZnMoO4 catalyst for atmospheric pressure non-thermal pulsating corona plasma degradation of reactive dye; role of the catalyst in plasma degradation process. Separation and Purification Technology, 269(April). https://doi.org/10.1016/j.seppur.2021.118748

Pham, H. L., Nguyen, V. D., Nguyen, V. K., Le, T. H. P., Ta, N. B., Pham, D. C.,Dang, V. T. (2021). Rational design of magnetically separable core/shell Fe3O4/ZnO heterostructures for enhanced visible-light photodegradation performance. RSC Advances, 11(36), 22317-22326. https://doi.org/10.1039/D1RA03468E

Puspitasari, L., Mareta, S., & Thalib, A. (2021). Karakterisasi Senyawa Kimia Daun Mint (Mentha sp.) dengan Metode FTIR dan Kemometrik. Sainstech Farma, 14(1), 5-11. Retrieved from https://ejournal.istn.ac.id/index.php/saintechfarma/article/view/931

Radoor, S., Karayil, J., Jayakumar, A., Parameswaranpillai, J., & Siengchin, S. (2021). Release of toxic methylene blue from water by mesoporous silicalite-1: characterization, kinetics and isotherm studies. Applied Water Science, 11(7), 1-12. https://doi.org/10.1007/s13201-021-01435-z

Reddy, B. J., Vickraman, P., & Justin, A. S. (2018). Investigation of novel zinc molybdate-graphene nanocomposite for supercapacitor applications. Applied Physics A: Materials Science and

Processing, 124(6), 1-9. https://doi.org/10.1007/s00339-018-1793-0

Riwayati, I., Fikriyyah, N., & Suwardiyono, S. (2019). ADSORPSI ZAT WARNA METHYLENE BLUE MENGGUNAKAN ABU ALANG-ALANG (Imperata cylindrica) TERAKTIVASI ASAM SULFAT. Jurnal Inovasi Teknik Kimia, 4(2), 6-11. https://doi.org/10.31942/inteka.v4i2.3016

Sagadevan, S., Fatimah, I., Egbosiub, T. C., Alshahateet, S. F., Lett, J. A., Weldegebrieal, G. K., … Johan, M. R. (2022). Photocatalytic Efficiency of Titanium Dioxide for Dyes and Heavy Metals Removal from Wastewater. Bulletin of Chemical Reaction Engineering & Catalysis, 17(2), 430-450. https://doi.org/10.9767/bcrec.17.2.13948.430-450

Simi, A., & Azeeza, V. (2010). Removal of methylene blue dye using low cost adsorbent. Asian Journal of Chemistry, 22(6), 4371-4376.

Sirirerkratana, K., Kemacheevakul, P., & Chuangchote, S. (2019). Color removal from wastewater by photocatalytic process using titanium dioxide-coated glass, ceramic tile, and stainless steel sheets. Journal of Cleaner Production, 215, 123-130. https://doi.org/10.1016/j.jclepro.2019.01.037

Wang, J. C., Lou, H. H., Xu, Z. H., Cui, C. X., Li, Z. J., Jiang, K., … Shi, W. (2018). Natural sunlight driven highly efficient photocatalysis for simultaneous degradation of rhodamine B and methyl orange using I/C codoped TiO2 photocatalyst. Journal of Hazardous Materials, 360, 356-363. https://doi.org/10.1016/j.jhazmat.2018.08.008

Weldegebrieal, G. K. (2020). Synthesis method, antibacterial and photocatalytic activity of ZnO nanoparticles for azo dyes in wastewater treatment: A review. Inorganic Chemistry Communications, 120(July), 108140. https://doi.org/10.1016/j.inoche.2020.108140

Widiyandari, H., Ketut Umiati, N. A., & Dwi Herdianti, R. (2018). Synthesis and photocatalytic property of Zinc Oxide (ZnO) fine particle using flame spray pyrolysis method. Journal of Physics: Conference Series, 1025(1). https://doi.org/10.1088/1742-6596/1025/1/012004

Xing, X., Xu, X., Wang, J., & Hu, W. (2019). Preparation and inhibition behavior of ZnMoO4/reduced graphene oxide composite for Q235 steel in NaCl solution. Applied Surface Science, 479(February), 835-846. https://doi.org/10.1016/j.apsusc.2019.02.149

Yan, Q., Wang, P., Guo, Y., Chen, Y., Si, Y., & Zhang, M. (2019). Constructing a novel hierarchical ZnMoO4/BiOI heterojunction for efficient photocatalytic degradation of tetracycline. Journal of Materials Science: Materials in Electronics, 30(20), 19069-19076. https://doi.org/10.1007/s10854-019-02264-2

Yulizar, Y., Apriandanu, D. O. B., & Ashna, R. I. (2020). La2CuO4-decorated ZnO nanoparticles with improved photocatalytic activity for malachite green degradation. Chemical Physics Letters, 755(June). https://doi.org/10.1016/j.cplett.2020.137749

Yulizar, Y., Bakri, R., Apriandanu, D. O. B., & Hidayat, T. (2018). ZnO/CuO nanocomposite prepared in one-pot green synthesis using seed bark extract of Theobroma cacao. Nano-Structures and Nano-Objects, 16, 300-305. https://doi.org/10.1016/j.nanoso.2018.09.003

Zhang, Z., Feng, C., Liu, J., & Guo, Z. (2019). Synthesis of ZnMoO4 with different polymorphas anode materials for lithium-ion batteries application. Journal of Materials Science: Materials in Electronics, 30(22), 20213-20220. https://doi.org/10.1007/s10854-019-02405-7